

# MORPHOMETRIC METHODS FOR SIMULATION OF WATER FLOW

CENTRALE LANDBOUWCATALOGUS



0000 0547 2127

40951

BIBLIOTHEEK  
LANDBOUWUNIVERSITEIT  
WAGENINGEN

Promotor: Dr. Ir. J. Bouma  
hoogleraar in de bodeminventarisatie en landevaluatie,  
speciaal gericht op de (sub)tropen

NNO8201, 1683

H.W.G. Booltink

# **Morphometric methods for simulation of water flow**

## **Proefschrift**

ter verkrijging van de graad van doctor  
in de landbouw- en milieuwetenschappen  
op gezag van de rector magnificus,  
dr. C.M. Karssen,  
in het openbaar te verdedigen  
op vrijdag 22 oktober 1993  
des namiddags te half twee in de Aula  
van de Landbouwuniversiteit te Wageningen

15n 506990

Aan mijn ouders  
voor Marga, Jules en Diede

CIP-GEGEVENS KONINKLIJKE BIBLIOTHEEK, DEN HAAG

Booltink, H.W.G.

Morphometric methods for simulation of water flow / H.W.G.

Booltink. - [S.l. : s.n.]. - I11.

Thesis Wageningen. - With ref. - With summary in Dutch.

ISBN 90-5485-171-6

Subject headings: water flow / soil structure

Printed in the Netherlands by Grafisch service Centrum van de  
Landbouwwuniversiteit Wageningen

## STELLINGEN

1. Het gebruik van simulatiemodellen, voor de beschrijving van water- en stoftransport, gebaseerd op Darcy stroming in een mobile en immobile fase is in gestructureerde bodems slechts zelden een realiteit.  
*Van Genuchten, M. Th., and P.J. Wieringa. 1976. Mass transfer in sorbing porous media, I. Analytical solutions. Soil Sci. Soc. Am. J. 40:473-480.*  
*Dit proefschrift*
2. In gestructureerde bodems zijn "suction cups" voor de bemonstering van bodemvocht, door de grote concentratie gradienten op korte afstand, een onjuiste bemonsterings techniek.  
*Dit proefschrift*
3. De gescheiden kwalitatieve beschrijving van bodemstructuur, vanuit bodemfysisch en bodemmorfolologisch oogpunt, kan zowel fysisch als morfologisch worden gekwantificeerd door middel van stratificatie van macroporieren naar ruimtelijke orientatie en fractale dimensies van watervoerende macroporieren.  
*Butler, B.E. and G.D.Hubble. 1977. Morphological properties. In: Russel, J.S. and E.L. Green (eds.) Soil factors in crop production in a semi-arid environment pp. 9-32.*  
*Dit proefschrift*
4. Zonder het gebruik van bodemmorfologische karakteristieken kunnen water- en stoftransport in gestructureerde bodems niet adequaat worden beschreven.  
*Dit proefschrift*
5. Overschrijdingskansen, berekend met behulp van Monte-Carlo simulaties, zeggen vaak meer over de spreiding in invoergegevens dan over de realisatie kans van de simulatie resultaten.  
*Dit proefschrift*
6. De verzadigde waterdoorlatendheid van een bodem dient, door het ontbreken van Darcy stroming in macroporieren, te worden gedefinieerd als de minimale water doorlatendheid waarbij de bodemmatrix nog net is verzadigd.  
*Bouma, J. 1982. Measuring the hydraulic conductivity of soil horizons with continuous macropores. Soil Sci. Soc. Am. J. 46:438-441*  
*Dit proefschrift*
7. Het samenvoegen van verfijnde, complexe gewasgroei modellen met robuuste, simpele bodemfysische dan wel bodemchemische modellen leidt vrijwel automatisch tot de conclusie dat de gewasparameters de grootste gevoeligheid vertonen.  
*Singh, G., D.M. Brown, and A.G. Barr. 1993. Modelling soil water status for irrigation scheduling in potatoes. I. Description and sensitivity analysis. Agricultural Water Management, 23: 329-341.*
8. Eénzijdige importbeperkingen van tropisch hardhout door de Westerse wereld zal de ontbossing in de Derde wereld slechts bevorderen.

9. Het tot op heden door de Landbouwwuniversiteit gevoerde personeelsbeleid laat zich nog het best vergelijken met een cholesterolrijk dieet.
10. De verkeersveiligheid in Nederland is meer gebaat bij een vermindering van het aantal verkeersregels dan bij een uitbreiding hiervan.
11. Het indienen van manuscripten bij vaktijdschriften dient zoveel mogelijk te worden vermeden.
12. Door het negeren van ijsgang op de rivieren als oorzaak van vele dijkdoorbraken in Nederland geeft Rijkswaterstaat, bij de verzwaring van deze rivierdijken, eerder blijik van koud-watervrees dan van hoog-watervrees.

## Dankwoord

Alhoewel op de omslag van dit proefschrift slechts één naam prijkt, zou het nooit tot stand hebben kunnen komen zonder de steun van een groot aantal mensen. Hen wil ik dan ook bedanken voor hun, vaak onbaatzuchtige, inzet.

Op de eerste plaats wil ik mijn ouders bedanken voor de stimulering tijdens mijn studie en de vrijheid die zij mij hebben geven om mijn ambities te volgen.

Mijn promotor Prof. Dr. J. Bouma wil ik hartelijk bedanken voor de goede en creatieve suggesties en het kritisch doorlezen van de concepten. "Johan, dank voor je inspirerende en enthousiaste belangstelling en voor de juiste dosering spanning en ontspanning tijdens het onderzoek".

Peter Finke en Hugo Denier van der Gon dank ik voor de prettige samenwerking en goede sfeer op kamer 121: "zonder jullie nuchtere kijk op tal van, hier niet nader te noemen, levensbeschouwelijke zaken zouden de werkdagen aanzienlijk saaier zijn geweest".

I would like to address special thanks to Ryusuke Hatano, from Hokkaido University Japan, for a pleasant and fruitfull cooperation and for introducing fractal theory to me.

りゅうすけ、あなたがいなければこのろんぶんはこうはならなかったでしょう。

Igor Staritsky wil ik danken voor zijn steun bij de grote en vele kleine computer problemen. Piet Peters voor het uitvoeren van de talloze bodemfysische analyses en de assistentie tijdens het veldwerk. Tini van Mensvoort voor de prettige samenwerking en de besmetting met het tropen virus. Alfred Stein dank ik voor zijn statistische aviezen.

Wouter de Boer, Mirjam Hack-ten Broeke, Hans Jansen en Jan Kragt, werkzaam bij het Staring Centrum, dank ik voor de collegiale manier waarop wij hebben samengewerkt binnen de verschillende, gezamenlijke projecten. Bij het PAGV wil ik Andrea Landman, Huib Hengstdijk en Joop Alblas danken voor het ter beschikkingstellen van meetgegevens en proefveld resultaten. De heren Nieuwland en Rops van de proefboerderij "De Kandelaar" dank ik voor de mogelijkheid om bijna 4 jaar veldonderzoek op de Kandelaar te kunnen doen.

I am indebted to Dr. R.J. Wagenet and Dr. J. Hutson from Cornell University USA, for provinding copies, updates and manuals of LEACHM.

I would like to thank Daniel Giménez, now working at Minnesota University USA, for carrying out the experiments with the crust infiltrometer.

Berry Geerligs en Wim van Hof van de Fotolocatie Binnenhaven wil ik danken voor hun goede fotografische adviezen en voor het tolereren van kleigrond en

methyleen blauw naast hun kostbare foto apparatuur. I am grateful to Mr. T. Ito (Hokkaido University Japan) for analyzing, in record time, 150 images with methylene-blue staining patterns.

Peter Janssen van het Centrum voor Wiskundige Methoden van het RIVM wil ik bedanken voor zijn ondersteuning bij het gebruik van de UNCSAM en RORASC software.

Special thanks are due to the European Community projects "Nitrate in Soils and "Wastes". Without these financial supports this research would never have been possible.

Naast de mensen, hierboven genoemd, zijn er velen met name op de vakgroep Bodemkunde en Geologie die aan dit onderzoek hebben bijgedragen, hen wil ik bedanken zonder ze met name te noemen.

Het slot accoord van een muziekstuk wordt het best onthouden; deze is dan ook voor jullie: Marga, Jules en Diede bedankt.



# CONTENTS

Chapter 1	General introduction	3
Chapter 2	A suction crust infiltrometer for measuring hydraulic conductivity of unsaturated soil near saturation	15
Chapter 3	Physical and morphological characterization of bypass flow in a well-structured clay soil	25
Chapter 4	Sensitivity analysis on processes affecting bypass flow	45
Chapter 5	Using fractal dimensions of stained flow patterns in a clay soil to predict bypass flow	65
Chapter 6	Measurement and simulation of bypass flow in a structured clay soil: a physico-morphological approach	81
Chapter 7	Field monitoring of nitrate leaching and bypass flow in a structured clay soil	107
Chapter 8	Distributed modelling of bypass flow on field scale in a heavy textured clay soil	129
Chapter 9	General conclusions	159
	Abstract	163
	Samenvatting	165
	Curriculum vitae	169

# CHAPTER 1

## GENERAL INTRODUCTION

## GENERAL INTRODUCTION

### Bypass flow

The occurrence of large cracks and channels in soils (macropores) has a major impact on water and solute movement. Observation of rapid vertical movement of free water along macropores in unsaturated soils was already reported in drainage studies at Rothamsted (U.K.) by Lawes et al. (1882).

Beven and Germann (1982) defined macropore or bypass flow as: "the flow of water through a system of large pores that allows fast flow velocities and bypasses the soil matrix". Since water flow within macropores can follow different flow modes such as film-flow (Germann, 1987), it cannot be described accurately by Richards' equation (Richards, 1931) which is based on Darcian flow theory. These theories were developed for ideal homogeneous isotropic flow systems (e.g. Taylor, 1953; Klute, 1973), as pointed out by White (1985). A clear definition of a macropore is difficult to give. Beven and Germann (1982) summarized literature and concluded that macropore sizes varied in a wide range between 30 to 3000  $\mu\text{m}$ . The effects of macropore systems on water and solute transport are highly variable and cannot be characterised by pore-sizes only, as reported by Beven and Germann (1982). A functional characterization is therefore required (Bouma, 1981). Germann and Beven (1981) quantified macroporosity from conductivity measurements at lower suctions. This type of data, however, does not provide any information on functioning of macropores in terms of conducting and absorbing water. To describe preferential flow pathways dye tracers are a useful tool. Anderson and Bouma (1973), and Bouma and Dekker (1978) used methylene blue to characterize contact areas between bypass flow water and macropore walls. Van Ommen et al. (1985) used the anionic tracer iodide, to visualize absorption of water during an infiltration experiment.

Although dye tracers provide good possibilities for characterizing flow patterns in structured soils, so far only little effort has been made to use this kind of information as input for simulation models describing bypass flow and related processes.

Edwards et al. (1979) used a two-dimensional model which simulates the flow patterns of water infiltrating into the surface of a soil column. Effects of macropores were simulated by means of a cylindrical hole from which water moved away radially and vertically. A system of uniformly distributed channels with different widths and depths was used by Beven and Clark (1986) to simulate infiltration into a homogeneous soil matrix containing macropores.

Chen and Wagenet (1992) simulated water and solute transport by combining Darcian flow for transport in the soil matrix with the Hagen-Poiseuille and Chezy-Manning equations for water transport in macropores. Hatano and Sakuma (1991) designed a combined capacity-bypass flow model to simulate transport of water and solutes in an aggregated soil. In their approach soil structure was simulated by plate-like elements which reflected contact areas and exchange capacities of water and solutes. The interchange between the mobile and immobile phase occurred in an additional mixing phase.

Two-region models describing convective dispersive transport in a mobile and immobile phase were used by e.g. Van Genuchten and Wieringa (1976), De Smedt et al. (1986) and Vanclooster et al. (1992). The use of this type of models in structured soils is, however, limited, since nonideal flow modes, such as film-flow along macropore walls, cannot be described accurately by means of convective dispersive flow. Especially in moderate climates, with relative low rain intensities, these nonideal flow modes are common.

Germann and Beven (1985) and Germann (1990) simulated bypass flow using kinematic wave theory in combination with a sinkterm for water absorption. In their approach the soil matrix and macropores are considered as one domain in which water is transported as a kinematic pulse.

All these models have in common that real soil structure, defined as the physical constitution of a soil material, as expressed by the size, shape and arrangements of the elementary particles and voids (Booltink et al., 1993), is not considered. Bronswijk (1988) calculated macropore sizes by means of swelling and shrinkage characteristics measured on structure elements in the laboratory. In his approach, excess water on the soil surface during a rain event was immediately transported to the ground water without interaction with the surrounding soil. Jarvis and Leeds-Harrison (1987, 1990) developed a model which calculates water balances in two-domains, a soil matrix and macropore domain. Soil structure was represented by means of cube-shaped soil aggregates and transport

of water through the macropores was calculated using an empirical tortuosity factor. Interaction between soil aggregates and macropore water was a function of aggregate sorptivity. No water flow was modeled within the aggregates. Hoogmoed and Bouma (1980) developed a model based on measured soil morphological characteristics, describing surface storage and lateral absorption of water along macropore-walls and drainage. Although this model is based on morphological observations it does not include the effects of tortuous water transport through macropores. The model is only capable of calculating bypass flow in small soil columns with strict boundary conditions.

### Soil morphology and bypass flow

Within soil survey, soil structure is usually described in qualitative terms such as: "weak subangular blocky" (e.g. Soil Survey Staff, 1975). Although these terms describe soil structure conscientiously, they can hardly be used for calculations or model-simulation purposes. A more quantitative approach was followed by e.g. Jongerius et al. (1972) Murphy et al. (1977) and Bullock and Murphy (1980). In these studies (macro) pore spaces were visualized or measured and expressed in terms of pore size distributions. Bouma et al. (1977) and Ringrose-Voase and Bullock (1984) developed a technique for measuring macropores in undisturbed soil, using methylene blue staining patterns. They stratified macropores according to Brewer (1964) in categories of channels, vughs and planar voids and discussed functional physical properties of different types of macropores. This, however, still in descriptive, qualitative terms. Moran et al. (1989) and McBratney et al. (1990) used fluorescent dye tracers in combination with digital binary image production to interpret soil macropore structure.

Several studies focused on combined application of soil physical characteristics and morphological features. Bullock and Thomasson (1979) used image analysis of thin sections to calculate macroporosity. Total macroporosity, however, is not a very relevant property in relation with water flow processes such as bypass flow, since very few macropores, contributing only little to total macroporosity, dominate transport of water and solutes (Bouma et al., 1977).

Spaans et al. (1990) measured changes of hydraulic conductivities in a Costa Rican soil before and after clearing of tropical rainforest. In this study differences in hydraulic conductivity were illustrated with micromorphometric

analyses of thin sections. The effects of tillage on soil morphology and porosity were investigated by Shipitalo and Protz (1987). These studies, however, have in common that soil structure was used to illustrate effects of soil structure on physical properties rather than link morphology to soil physical properties in quantitative terms.

Bouma (1981) suggested to functionally characterize bypass flow by means of dye traces in combination with macromorphometric techniques. This approach was followed by Kooistra et al. (1987) who combined soil morphological measurements with computer simulations on moisture deficits. In this study the effects of horizontal planar voids on upward unsaturated flow of water were stressed. Van Stiphout et al. (1987) demonstrated, in a field study, the occurrence of bypass flow and infiltration of water from noncontinuous macropores. This subsurface infiltration process was called "internal catchment". In structured soils the use of morphometric data in combination with soil physical characteristics is particularly relevant. Fractal theory seems to be a promising tool in characterizing macropore systems, since size and shape of different combinations of functional macropores can be quantified and coupled to soil physical characteristics. Bartoli et al. (1991) used fractal dimensions to characterize soil structure, Crawford et al. (1993) used fractal theory to explain diffusion processes in heterogenous soils. Hatano et al. (1992) linked fractal dimensions of stained flow patterns with Brenner numbers for chloride breakthrough in various volcanic soils.

### Research objectives

In this study emphasis was given to combined research of bypass flow in relation to morphology of water-conducting macropores in a structured clay soil. The main questions to be answered were: (i) what soil physical methods can be used to measure and quantify the effects of bypass flow and, (ii) how can soil structure be quantified in a way that it takes into account bypass flow phenomena and expresses morphological data in a form to be used in simulation models?

To achieve these objectives, laboratory experiments were carried out to further develop and improve soil physical measurement techniques. Data from these experiments were used to define concepts for physico-morphological processes

of bypass flow. Next these concepts were tested in relative simple numerical simulation models.

Another part of this study dealt with automated monitoring of bypass flow at the "Kandelaar" experimental farm in Eastern Flevoland in the Netherlands. Field scale modelling was carried out in the clay soils occurring there to test the derived laboratory concepts with field measured data.

### Outline of the thesis

In CHAPTER 2 (Booltink et al., 1991) the crust test for measuring unsaturated hydraulic conductivity (Hillel and Gardner, 1969, 1970; Bouma et al., 1971, Spaans et al., 1990) was modified into a more operational suction crust infiltrometer. Similar to the suction infiltrometer (Perroux and White, 1988) a negative pressure head is applied to the crust, by varying the level of the Mariotte feeder burette. The effects of macropores on the hydraulic conductivity near saturation are illustrated by series of measurements in a structured heavy clay soil.

CHAPTER 3 (Booltink and Bouma, 1991) describes the combined use of soil physical and morphological methods to characterize bypass flow. Flow processes were measured in large undisturbed soil cores. The field method for measuring bypass flow described by Bouma et al. (1981) was utilized with automated outflow registration combined with 102 automated small tensiometers, installed at three depths in the columns. Methylene-blue stained flow patterns, associated with bypass flow, were morphologically characterized in terms of circumference, area, and number of stained pores. Time series of tensiometer reactions were characterized and linked with methylene blue staining patterns.

A sensitivity analysis on processes affecting bypass flow was carried out in CHAPTER 4 (Booltink and Bouma, 1993). This study showed the relative impact of different soil types on soil hydrological processes affected by rain intensity, initial pressure head of the soil water, surface storage of water, contact area of bypass water and soil on macropore walls, and hydraulic properties of the soil matrix. The sensitivity analysis was carried out using a simulation model developed by Hoogmoed and Bouma (1980). Simulated mass balances and relative sensitivity of different parameters are discussed.

In CHAPTER 5 (Hatano and Bootink, 1992) soil structure was quantified using fractal dimensions of methylene-blue stained, water conducting macropores.

Hatano et al. (1992) used similar morphological techniques to derive Brenner numbers for chloride breakthrough. The combination of fractal dimensions and methylene-blue stained volumes was used to predict total amounts of bypass flow from large soil cylinders during heavy artificial rainstorms.

The quantification of soil structure by means of fractal dimensions of stained flow patterns was further developed in CHAPTER 6 (Booltink and Hatano, 1993). Tortuosity of water pathways and contact area associated with bypass flow are important soil morphological parameters in explaining water absorption during bypass flow. Macropore geometry, expressed as fractal dimensions, was used to calculate the propagation speed of the water front in macropores during bypass flow under different initial soil conditions and various rain intensities. Methylene blue staining patterns were stratified in terms of vertical cracks and horizontal pedfaces of structure elements (Bouma et al., 1977). The developed pedotransfer function for calculating macropore flow velocity and the morphological stratification of stained flow patterns were used as input parameters in a Darcian flow simulation model extended with modules describing bypass flow and lateral absorption of bypass flow water along macropore walls (Hoogmoed and Bouma, 1980). The model was used to simulate bypass flow in 15 large soil columns.

In CHAPTER 7 (Booltink, 1993a) long-term monitoring of bypass flow and soil mineral nitrogen contents, at the "Kandelaar" experimental farm was used to investigate bypass flow and related nitrate leaching. Time series of drain discharges and related nitrate and chloride concentrations were compared with mineral nitrogen profiles in order to derive the origin of the leached nitrate in the soil profile. The effect of a catchcrop, sown directly after slurry application, on nitrate leaching was stressed. Use of tensiometers and suction cups for collecting soil solutions in structured soils are critically discussed.

CHAPTER 8 (Booltink, 1993b) describes the field scale simulation of bypass flow and the comparison with measured data. For this, the one dimensional water and solute transport model LEACHM (Wagenet and Hutson, 1989) was extended with a module describing bypass flow and tortuous water transport according to concepts described in chapter 6. A Monte-Carlo analysis was performed to calibrate the model and to investigate the sensitivity and uncertainty of the various model parameters. The model was validated using data from another winter season at the "Kandelaar" experimental farm.



## REFERENCES

- Anderson, J.L. and J. Bouma. 1973. Relationships between saturated hydraulic conductivity and morphometric data of an argillic horizon. *Soil Sci. Soc. Am. Proc.* 37:408-413.
- Bartoli, F., R. Philippy, M. Doirisse, S. Niquet, and M. Dubuit. 1991. Structure and self-similarity in silty and sandy soils: the fractal approach. *J. of Soil Sci.* 42:167-185.
- Beven, K., and R.T. Clark. 1986. On the variation of infiltration into a homogeneous soil matrix containing a population of macropores. *Water Resour. Res.* 22:383-388.
- Beven, K., and P.F. Germann. 1982. Macropores and water flow in soils. *Water Resour. Res.* 18:1311-1325.
- Booltink, H.W.G. 1993a. Field monitoring of nitrate leaching and waterflow in a structured heavy clay soil. Submitted to: *Agriculture, Ecosystems & Environment*.
- Booltink, H.W.G. 1993b. Distributed modelling of bypass flow on field scale in a heavy textured clay soil. Submitted to *Water Resour. Res.*
- Booltink, H.W.G., and J. Bouma. 1991. Physical and morphological characterization of bypass flow in a well-structured clay soil. *Soil Sci. Soc. Am. J.* 55:1249-1254.
- Booltink, H.W.G., and J. Bouma. 1993. A sensitivity analysis on processes affecting bypass flow. *Hydr. Proc.* 7:33-43.
- Booltink, H.W.G., R. Hatano, and J. Bouma. 1993. Measurement and simulation of bypass flow in a structured clay soil: a physico-morphological approach. Accepted for publication in *J. Hydrol.*
- Booltink, H.W.G., J. Bouma, and D. Giménez. 1991. A suction crust infiltrometer for measuring hydraulic conductivity of unsaturated soil near saturation. *Soil Sci. Soc. Am. J.* 55:566-568.
- Bouma, J. 1981. Soil Morphology and preferential flow along macropores. *Agric. Water Manag.* 3:235-250.
- Bouma, J., and L.W. Dekker. 1978. A case study on infiltration into dry clay soil. I Morphological observations. *Geoderma* 20:27-40.
- Bouma, J., L.W. Dekker, and C.J. Muilwijk, 1981. A field method for measuring short-circuiting in clay soils. *J. Hydrol.* 52:347-354.
- Bouma, J., D. I. Hillel, F. D. Hole, and C. R. Amerman. 1971. Field measurement of unsaturated hydraulic conductivity by infiltration through artificial crusts. *Soil Sci. Soc. Am. Proc.* 35:362-364.
- Bouma, J. A. Jongerius, O. Boersma, A. de Jager, and D. Schoonderbeek. 1977. The function of different types of macropores during saturated flow through four swelling soil horizons. *Soil Sci. Soc. Am. J.*, 41:9945-950.
- Brewer, R. 1964. *Fabric and Mineral analysis of soils.* John Wiley and Sons, New York.
- Bronswijk, J.J.B. 1988. Modelling of waterbalance, cracking and subsidence of clay soils. *J. Hydrol.* 97:199-212.
- Bullock, P. and A.J. Thomasson. 1979. Rothamsted studies of soil structure II. Measurement and characterization of macroporosity by image analysis and comparison with data from water retention measurements. *J. of Soil Sci.* 30:391-413.
- Bullock, P., C.P., Murphy. 1980. Towards the quantification of soil structure. *Journal of Microscopy* 120:317-328.

- Chen, C. and R.J. Wagenet. 1992. Simulation of water and chemicals in macropore soils. Part I. Representation of the equivalent macropore influence and its effect on soil water flow. *J. Hydr.* 130:105-126.
- Crawford., J.W., K.R., Ritz, and I. Young. 1993. Quantification of fungal morphology, gaseous transport and microbial dynamics in soil. An integrated frame work utilising fractal geometry. *Geoderma*, 56:157-172.
- De Smedt, F., F. Wauters, and J. Sevilla. 1986. Study of tracer movement through unsaturated sand. *Geoderma* 38:223-236.
- Edwards, W.M., R.R. van der Ploeg, and W. Ehles. 1979. A numerical study of the effects of noncapillary-sized pores upon infiltration. *Soil Sci. Soc. Am. J.* 43:851-856.
- Germann, P.F. 1990. Preferential flow and the generation of runoff. 1. Boundary flow theory. *Water Resour. Res.* 26:3055-3063.
- Germann, P.F. 1987. The three modes of water flow through a vertical pipe. *Soil Sci.* 144:153-154.
- Germann, P.F., and K. Beven. 1981. Water flow in soil macropores an experimental approach. *J. Soil Sci.* 32:1-13.
- Germann, P.F., and K. Beven. 1985. Kinematic wave approximation to infiltration into soils with sorbing macropores. *Water Resour. Res.* 21:990-996.
- Hatano, R., and H.W.G. Booltink. 1992. Using fractal dimensions of stained flow patterns in a clay soil to predict bypass flow. *J. Hydrol.* 135:121-131.
- Hatano, R. and T. Sakuma. 1991. A plate model for solute transport through aggregated soil columns. I. Theoretical descriptions. *Geoderma* 550:13-23.
- Hatano, R., N., Kawamura, J. Ikeda, and T. Sakuma. 1992. Evaluation of the effect of the morphological features of flow paths on solute transport by using fractal dimensions of methylene blue staining pattern. *Geoderma*, 53:31-44.
- Hillel, D. I., and W. R. Gardner. 1969. Steady infiltration into crust-topped profiles. *Soil Sci.* 107:137-142.
- Hillel, D. I., and W. R. Gardner. 1970. Measurement of unsaturated conductivity and diffusivity by infiltration through an impeding layer. *Soil Sci.* 109:149-153.
- Hoogmoed, W.B., and J. Bouma. 1980. A simulation model for predicting infiltration into a cracked clay soil. *Soil Sci. Soc. Am. J.* 44:458-461.
- Jarvis, N.J., and P.B. Leeds-Harrison. 1987. Modelling water movement in drained clay soil. I. description of the model, sample output and sensitivity analysis. *J. Soil Sci.*, 38:487-498.
- Jarvis, N.J., and P.B. Leeds-Harrison. 1990. Field test of a water balance model of cracking clay soils. *J. Hydrol.* 112:203-218.
- Jongerius, A., D. Schoonderbeek, A., Jager and S. Kowalinski. 1972. Electro-optical soil porosity investigations by means of a Quantimet B equipment. *Geoderma* 7:177-198.
- Klute, A. 1973. Soil water flow theory and its application in field situations. p.9-31. In R.R. Bruce et al. (ed.), *Field soil water regime*, SSSA Spec. Publ. 5. SSSA, Madison, W.I.
- Kooistra, M.J., R. Miedema, J.H.M. Wösten, J. Versluis, and J. Bouma. 1987. The effect of subsoil cracking on moisture deficits of pleistocene and holocene fluvial clay soils in the Netherlands. *J. of Soil Sci.* 38:553-563.

- Lawes, J.B., J.H. Gilbert, and R. Warington. 1882. *On the amount and composition of the rain and drainage water collected at Rothamsted*, Williams, Clowes and Sons Ltd., London. U.K.
- McBratney, A.B., and C.J. Moran. 1990. A rapid method for soil macropore structure. II Stereo logical model, statistical analysis and interpretation. *Soil Sci. Soc. Am J.* 54:509-515.
- Moran, C.J., A.B. McBratney, and A.J. Koppi. 1989. A rapid analysis method for soil pore structure. I Specimen preparation and digital binary image production. *Soil Sci. Soc. Am. J.* 53:921-928.
- Murphy, C.P., P. Bullock and R.H. Turner. 1977. The measurement and characterization of voids in soil thin sections by image analysis. I principles and techniques. *Journal of soil science.*
- Perroux, K. M., and I. White. 1988. Design for disc permeameters. *Soil Sci. Soc. Am. J.* 52:1205-1215.
- Richards, L.A. 1931. Capillary conduction of liquids through porous mediums. *Physics*, 1:318-333.
- Ringrose-Voase, A.J., and P. Bullock. 1984. The automatic recognition and measurement of soil pore types by images analysis and computer programs. *J. of Soil Sci.* 35:673-684.
- Shipitalo, M.J., and R. Protz. 1987. Comparison of morphology and porosity of a soil under conventional and zero tillage. *Can. J. Soil Sci.* 67:445-456.
- Soil Survey Staff. 1975. *Soil Taxonomy; a basic system of classification for making and interpreting soil surveys.* Agr. Handb. no. 436, SCS-USDA. Government Printing Office, Washington DC.
- Spaans, E. J. A., J. Bouma, A. L. E. Lansu, and W. G. Wielemaker. 1990. Measuring soil hydraulic properties after clearing of tropical rain forest in a Costa Rican soil. *Trop. Agric. Vol. 67. No. 1.* 61-65.
- Taylor, G.L. 1953. Dispersion of soluble matter in solvent flowing slowly through a tube. *Proc. Roy. Soc.* 219:186-203.
- Vanclooster, M., H. Vereecken, J. Diels, F. Huysman, W. Verstraete, and J. Feyen. 1992. Effect of mobile and immobile water in predicting nitrogen leaching from cropped soil. *Modelling Geo-Biosphere Processes.* 1:23-40.
- Van Genuchten, M. Th., and P.J. Wierenga. 1976. Mass transfer studies in sorbing porous media. I. Analytical solutions. *Soil Sci. Soc. Am. J.* 40:473-480.
- Van Ommen, H.C., L.W. Dekker, R. Dijkma, J. Hulshof, and W.H. van der Molen. 1988. A new technique for evaluating the presence of preferential flow paths in nonstructured soils. *Soil Sci. Soc. Am. J.* 52:1192-1194.
- Van Stiphout, T.P.J., H.A.J. van Lanen, O.H. Boersma, and J. Bouma. 1987. The effect of bypass flow and internal catchment of rain on the water regime in a clay loam grassland soil. *J. Hydrol.* 95:1-11.
- Wagenet, R.J. and J.L. Hutson. 1989. Leaching Estimation and Chemistry Model: A process-based model of water and solute movement, transformations, plant uptake and chemical reactions in the unsaturated zone. Continuum Water Resources Institute. Cornell University, NY.
- White, R.E. 1985. The influence of macropores on the transport of dissolved and suspended matter through the soil. *Adv. Soil Sci.* 3:95-121.

## CHAPTER 2

# A SUCTION CRUST INFILTROMETER FOR MEASURING HYDRAULIC CONDUCTIVITY OF UNSATURATED SOIL NEAR SATURATION

Published in: *Soil Science Society of America Journal*  
volume 55 page 566-568 (1991)

# A SUCTION CRUST INFILTROMETER FOR MEASURING HYDRAULIC CONDUCTIVITY OF UNSATURATED SOIL NEAR SATURATION

**H.W.G. Booltink, J. Bouma and D. Giménez**

*Departement of Soil Science and Geology, Agricultural University, P.O. Box 37, 6700 AA Wageningen, The Netherlands.*

## ABSTRACT

The laborious crust test, used to measure unsaturated hydraulic conductivity, was modified into a more operational suction crust infiltrometer. By varying the level of the mariotte tube inside the feeder-burette, different negative pressure heads can be imposed on a soil sample. Unit gradient during the measurement was ensured by adjusting the water level in the draining column under the sample. Only one crust has to be produced, which leads to less disturbances and significant savings of time. Perfect contact between crust and soil surface makes the crust infiltrometer particularly suitable for measurements in structured soils with macropores.

## INTRODUCTION

Hydraulic conductivity data are necessary to run deterministic simulation models for soil water movement. Many measurement methods have been developed (e.g., Klute, 1986). Recently, a suction infiltrometer was developed which was applied successfully in sandy soils (Perroux and White, 1988). Some problems have, however, been encountered when applied in well structured clay soils with macropores.

In that case poor contact between membrane and soil is likely to produce variable, unreproducible results that cannot be improved by the suggested application of a layer of sand between membrane and soil (Perroux and White, 1988), because sand may move into the the macropores and contact between the membrane and the loose sand can easily be disturbed.

In addition, problems have been reported with the membrane itself, which may exhibit hydrophobic features.

For several years, the crust test has been used to measure  $K_{\text{unsat}}$  values by combining fluxes at unit gradient through a crust, with corresponding negative subcrust pressure heads. The original theory was presented by Hillel and Gardner (1969, 1970). A field test, using crusts composed of sand and clay, was extensively applied in Wisconsin (Bouma et al., 1971). Later the crust material was replaced by gypsum (Bouma and Denning, 1972) and quick-setting cement (Bouma et al., 1983, Spaans et al., 1990).

One operational problem of the crust test was the necessity to replace crusts so as to obtain different fluxes and pressure heads. Replacement was laborious and often involved disturbances. Perfect and stable contact between crust and soil, however, was and is one attractive feature of the method. In this study we explore the feasibility of obtaining a range of  $K_{\text{unsat}}$  values by using only one crust and by manipulating the height of the zero-pressure level in the mariotte device of the infiltrometer. Thus, different rates of steady infiltration of water can be obtained with corresponding negative subcrust pressure heads.

## **MATERIALS AND METHODS**

### **Soil**

Measurements were made in the  $C_1$  horizon (depth 15 to 35 cm below soil surface) of a very fine, mixed, mesic Typic Fluvaquent (Soil survey Staff 1975). The soil had a strongly developed prismatic structure and contained 50% clay and continuous macropores (cracks). Samples were taken in P.V.C. cylinders with a diameter and length of 20 cm. The inside of the cylinder, with sharpened lower edges, was covered with grease to make sampling easier and to prevent flow of water along the cylinder walls. During transport to the laboratory samples were covered with plastic caps to prevent excessive evaporation and

loss of material. In the laboratory the samples were slowly saturated by means of a raising water level in a plastic container. The samples were left to saturate for at least 2 days.

### Equipment and Procedure

Saturated hydraulic conductivity ( $K_{sat}$ ) was measured by placing the cylinders with saturated soil samples on a perforated disk, covered with a non-restrictive cloth to prevent loss of material, and placed on a funnel (Fig. 1).

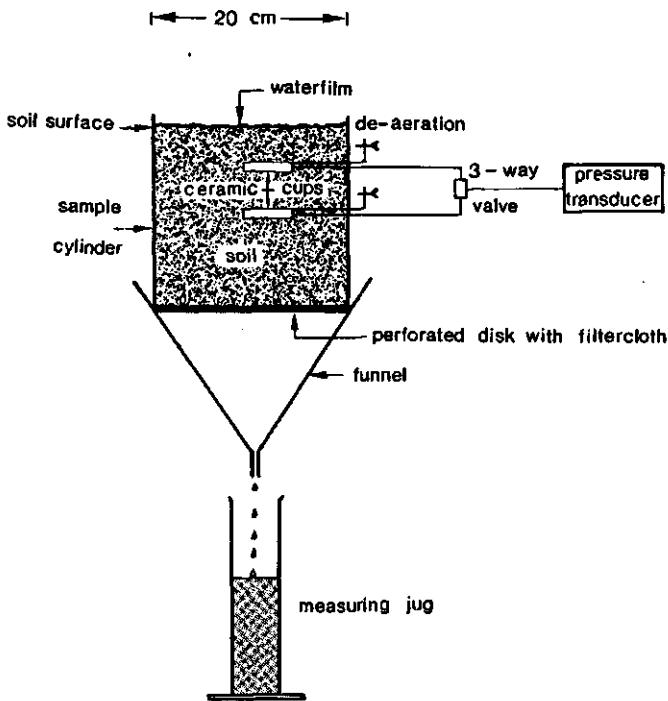


*Figure 1* Schematic diagram of the laboratory assembly to measure saturated hydraulic conductivity.

Two tensiometers were installed at 5 and 10 cm below the soil surface. The "natural" surface structure was carefully exposed without smearing the macropores. After leveling the sample in the cylinder, it was placed on the

funnel and water was shallowly ponded on top. Outflow fluxes were registered until fluxes were constant for at least one hour and pressures were zero.

Next, samples were placed on 50 cm long P.V.C. cylinders, with the same diameter as the cylinder, filled with medium textured sand.

Crusts were made of mixtures of dry, well sorted quartz sand (table 1) and 10 % (by weight) quick setting hydraulic cement (CEBAR, manufactured by Metzger Alblasterdam Netherlands). Sand and cement were mixed thoroughly before and after adding about 10 % (by weight) water. Using more water causes inhomogeneous crusts due to separation of sand and cement, and does not allow hardening.

*Tabel 1 Particle size distribution quartz sand*

Fraction ( $\mu\text{m}$ )	Distribution (% w/w)
< 53	0.2
53 - 75	0.6
75 - 105	4.0
105 - 150	38.9
150 - 210	42.7
210 - 300	12.6
300 - 420	0.9
> 420	0.1

The mixture was evenly applied on the soil surface and compressed to ensure good contact between crust and soil surface. The surface of the crust was flattened to a thickness of 1 cm, thinner crusts become relatively more sensitive to small differences in thickness and little inhomogenities.

After hardening, which takes up to 15 minutes, a perspex cap (Poly Methyl Methacrylate, manufactured by I.C.I England) was glued on top of the cylinder and water was put immediately on top of the crust. Air was removed by the airvent (Fig. 2).



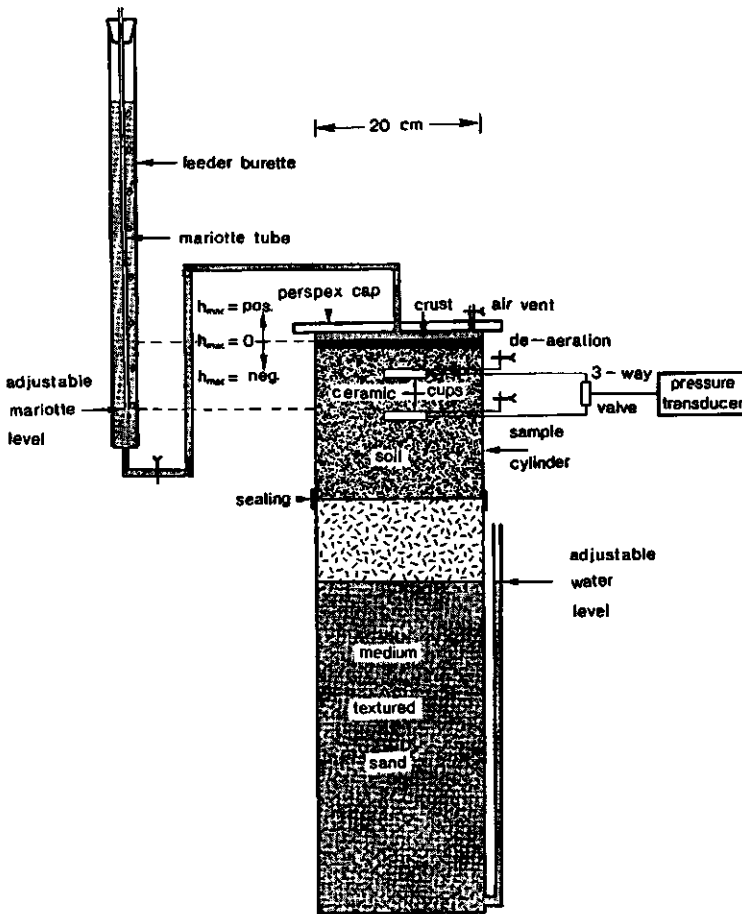


**Figure 2** Schematic diagram of the suction crust infiltrometer as used in the laboratory set-up.

Hydraulic pressure to be applied on top of the crust can be manipulated by changing the level of the mariotte tube, inside the feeder burette, relatively to the level of the crust. This is achieved by moving the feeder-burette up and down along a vertical stand (Fig. 2)

In the conventional crust method, the crust ensures steady fluxes of water into the underlying soil, which correspond with constant pressure heads at unit gradient in the underlying soil. If a negative pressure head is applied to the crust

by moving the mariotte device down, as proposed here, ( $h_{mar}$  is negative in Fig. 2.), conductivities are defined by the measured flux at a given pressure head of unit gradient. Pressure heads are measured with transducers.

To ensure unit gradient in the soil sample during measurement, the water level in the sand column below the sample is adjusted by using an overflow device. Thus, unit gradient flow is created for each experiment.

## RESULTS AND DISCUSSION

A measured hydraulic conductivity curve for the Typic Fluvaquent is presented in Fig. 3.

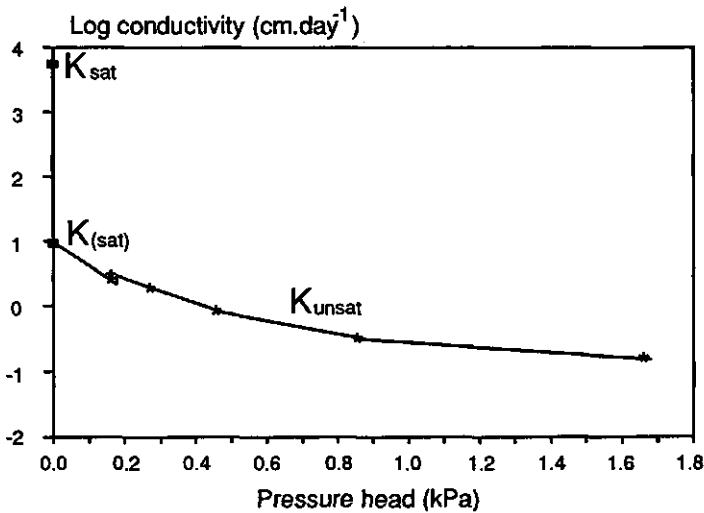


Figure 3 Conductivity curve for the Typic Fluvaquent as measured with the suction crust infiltrometer.

Fluxes and pressure heads were measured when unit hydraulic gradient was established. Fluxes ranged from  $5500 \text{ cm.day}^{-1}$  at saturation to  $0.01 \text{ cm.day}^{-1}$  at  $h = -17 \text{ cm}$ . The  $K_{sat}$  value was obtained by ponding a free standing soil sample in P.V.C. cylinder (e.g., Fig. 1). When measured in situ  $K_{sat}$  values would probably have been lower due to discontinuous macropores (Lauren et al. 1988).

The suction crust infiltrometer is particularly suitable to express the effects of macropores on  $K$ , as can be illustrated with data presented in Fig. 3. Macropores can be completely filled with water, and when they are vertically continuous, very high fluxes are obtained. With a crust, saturated conditions may still be measured in terms of zero pressures, but fluxes are strongly reduced because macropores are not completely filled with water anymore. This results in a wide range of saturated conductivities, varying from  $5500 \text{ cm.day}^{-1}$  to  $10 \text{ cm.day}^{-1}$ . This effect was earlier demonstrated by Bouma (1982) who suggested use of the  $K_{(sat)}$  notation for such conditions.

The method was convenient to use. Values were obtained rapidly because fluxes near saturation are relatively high and equilibrium conditions are reached rapidly. When fluxes become very low, the inaccuracy of measurement increases. We advise not to work with pressure heads lower than  $-30 \text{ cm}$ . The crust is produced only once, and this is a major improvement over the former procedure which required preparation of a serie of different crusts. Crusts, as prepared according to the described procedure, were, structurally stable, quite homogeneous and had perfect contact with the soil. This is better than adding sand to the soil surface which is structurally unstable and tends to flow into macropores. Contact between the membrane and loose sand can be more easily disturbed than the contact between crust and soil. Even a thin layer of sand has a major effect on infiltration characteristics in soils with macropores, as was demonstrated by Bouma et al. (1983). Use of the sand column with an adjustable free water level, was quite effective to realize unit-gradient flow.

Finally, the method can also be used in the field, using a field infiltrometer and a carved out column of soil. Here the pressure of the lower boundary can not be adjusted. This version of the method has been described elsewhere, except for the aspect of pressure manipulation (Bouma and Denning, 1972; Spaans et al. 1990). Generally, field application is preferred, but available funds do not always allow time-consuming field work and we have found that the laboratory method, described here, can yield satisfactory results when samples are taken carefully.

## ACKNOWLEDGEMENT

This study was funded by the European Community-project: "Nitrate in Soils" (EV4V.0098-NL).

## REFERENCES

- Bouma, J., D. I. Hillel, F. D. Hole, and C. R. Amerman. 1971. Field measurement of unsaturated hydraulic conductivity by infiltration through artificial crusts. *Soil Sci. Soc. Am. Proc.* 35:362-364.
- Bouma, J., and J. L. Denning. 1972. Field measurement of unsaturated hydraulic conductivity by infiltration through gypsum crusts. *Soil Sci. Soc. A. Proc.* 36:846-847.
- Bouma, J. 1982. Measuring the hydraulic conductivity of soil horizons with continous macropores. *Soil Sci. Soc. Am. J.* 46:438-441.
- Bouma, J., C. F. M. Belmans and L. W. Dekker. 1982. Water infiltration and redistribution in a silt loam subsoil with vertical worm channels. *Soil Sci. Soc. Am. J.* 46 (5) 917-921.
- Bouma, J., C. Belmans, L. W. Dekker, and W. J. M. Jeurissen. 1983. Assessing the suitability of soils with macropores for subsurface liquidwaste disposal. *J. Environ. Qual.* 12:305-311.
- Hillel, D. I., and W. R. Gardner. 1969. Steady infiltration into crust-topped profiles. *Soil Sci.* 107:137-142.
- Hillel, D. I., and W. R. Gardner. 1970. Measurement of unsaturated conductivity and diffusivity by infiltration through an impeding layer. *Soil Sci.* 109:149-153.
- Klute, A.(ed.). 1986, Second Edition. *Methods of soil analysis Part 1. Physical and Mineralogical methods.* Am. Soc. Agronomy, Monograph 9, Madison Usa.
- Lauren, J. G., R. J. Wagenet, J. Bouma, and J. H. M. Wosten. 1988. Variability of saturated hydraulic conductivity in a glassaquic hapludalf with macropores. *Soil Sci.* 145:20-28.
- Perroux, K. M., and I. White. 1988. Design for disc permeameters. *Soil Sci. Soc. Am. J.* 52:1205-1215.
- Soil Survey Staff. 1975. *Soil Taxonomy.* US. Dept. Agric. Handbook 436. Washington D.C.
- Spaans, E. J. A., J. Bouma, A. L. E. Lansu, and W. G. Wielemaker. 1990. Measuring soil hydraulic properties after clearing of tropical rain forest in a Costa Rican soil. *Trop. Agric.* Vol. 67. No. 1. 61-65.

## **CHAPTER 3**

# **PHYSICAL AND MORPHOLOGICAL CHARACTERIZATION OF BYPASS FLOW IN A WELL-STRUCTURED CLAY SOIL**

Published in: *Soil Science Society of America Journal*  
volume 55 page 1249-1254 (1991)

# PHYSICAL AND MORPHOLOGICAL CHARACTERIZATION OF BYPASS FLOW IN A WELL-STRUCTURED CLAY SOIL

H.W.G. Booltink and J. Bouma

*Departement of Soil Science and Geology, Agricultural University, P.O. Box 37, 6700 AA Wageningen, The Netherlands.*

## ABSTRACT

Bypass flow governs solute movement in well-structured clay soils. Combined use of physical and morphological methods was made in this study to better characterize the proces. Flow processes in five 200-mm long undisturbed cores of 200-mm diameter were monitored at 11-min intervals by using 102 small transducer tensiometers, divided among five samples and installed at three depths. Flow patterns along macropores were stained with methylene blue. Twenty five tensiometers in or within a distance of a few millimeters of stained macropores reacted very quickly when 10 mm of simulated rain was applied at an intensity of  $13 \text{ mm.h}^{-1}$ , and showed a drying pattern after the end of the simulated rainfall. Forty-three tensiometers inside peds reacted more slowly and showed continued wetting after the end of the simulated rainfall indicating internal catchment of water in the bottom of discontinuous macropores followed by redistribution of water. Internal catchment increased with depth in the samples, as indicated by both physical and morphological data. Using tensiometer measurements as a point-count it is estimated that 33 % of the soil volume was in close contact with continuous macropores while 42 % was influenced by the effects of internal catchment. An average of  $5.2 \text{ mm} \pm 0.96 \text{ mm}$  of the applied 10 mm water left the cores through bypass flow, while an estimated average of  $3.3 \text{ mm} \pm 0.96 \text{ mm}$  contributed to internal catchment. The

observed patterns of water movement illustrate the inadequacy of the concept of mobile/immobile water.

## INTRODUCTION

Rapid vertical movement of free water along macropores in unsaturated clay soils has often been observed (Lawes et al., 1882; White, 1985) but cannot be characterized by flow theory based on Richards' equation (e.g., Klute, 1973). Beven and Germann (1982) defined macropore or bypass flow as "the flow of water through a system of large pores that allows fast flow velocities and bypasses the unsaturated soil matrix." Different deterministic and stochastic procedures can be followed to characterize bypass flow (e.g., Valocchi, 1990; Andreini and Steenhuis, 1990; Kung, 1990; White, 1985). The effects of non-capillary-sized pores upon infiltration was studied by Edwards et al. (1979). We have focused attention on a deterministic approach using both physical and morphological techniques.

Flow patterns associated with bypass flow were morphologically characterized as a function of application rate and applied quantity of water by Bouma and Dekker (1978) using methylene blue tracers. Their study showed that stains occurred in small vertical bands on ped faces, occupying only about 2 % or less of the potentially available vertical contact area of the peds. Based on this work, Hoogmoed and Bouma (1980) developed a deterministic model that predicted vertical flow of water into the soil surface and into continuous cracks, including horizontal infiltration into the soil matrix. Their model calculations were validated by outflow measurements from soil columns but not by physical measurements inside the soil. Bouma et al. (1981) introduced a field test to measure bypass flow in large, undisturbed dry or moist soil cores. This method considered outflow as a fraction of inflow only and did not characterize flow processes inside the cores either. Van Stiphout et al. (1987) demonstrated, in a field study, the occurrence of bypass flow and infiltration of water from noncontinuous macropores inside the soil. Water infiltrated from the bottom of discontinuous cracks at 60-cm depth and from discontinuous worm channels at 120-cm depth. This subsurface infiltration process was called "internal catchment". Continuity of macropores was studied with dyes, but the effect of

the number of macropores was not considered. Bouma et al. (1982) monitored infiltration of water into a macroporous soil using different-size tensiometers. They found that measured pressure heads for large cups (8 by 2 cm) showed little variation and indicated short periods of saturation during infiltration. Small cups (0.5 by 0.5 cm), however, showed considerable variation and did not indicate saturation. This was explained by a morphological analysis, which showed that large cups intercepted water-conducting macropores while small cups did not. Sizes of tensiometer cups to be selected for monitoring should, therefore, be a function of the type of soil structure and the spacing of macropores.

The study reported here was made to characterize flow processes, including vertical and lateral infiltration and internal catchment, during bypass flow in pedal clay soils. Pressure heads in the soil were measured with a large number of small tensiometers, using transducer technology, which was also applied to obtain a continuous record of bypass flow. Staining techniques were used to quantify flow patterns along macropores, which were related to physical data.

## MATERIAL AND METHODS

### Soil

Soil samples were taken in steel cylinders (200-mm diameter by 200-mm long), at five randomly chosen locations within a field, at The Kandelaar experimental farm in Eastern Flevoland in the Netherlands. Sampling was carried out by slightly pressing the cylinders into the soil and carving out the surrounding soil in order to reduce soil disturbances during sampling. The cylinders had sharpened lower edges and inside surfaces were covered with grease. The soil was a mixed, mesic Hydric Fluvaquent (Soil Survey Staff, 1975), with the following horizons: A<sub>p</sub> (0-30 cm), clay (42 % clay) with a moderate, medium angular blocky structure and an abrupt wavy boundary to; 2C (30 - 70 cm), clay loam (40 % clay), strong, very coarse prismatic structure; 3C (70 - 103 cm), silty clay loam (30 % clay), strong, very coarse prismatic structure; and 4BC<sub>6</sub> (103 - 120 cm), sand, single grain. The dominant type of macropores were interpedal planar voids.



Before sampling, a field experiment using iodide tracers (Van Ommen et al., 1988) was carried out to determine which soil layer governed bypass flow. An iodide solution was ponded on top of the soil surface (area  $\approx 1 \text{ m}^2$ ) and the surface was covered with plastic sheets. After 2 d the soil was systematically peeled off in layers of 15 cm, until the groundwater was reached at a depth of 90 cm below the surface. Each layer was sprinkled with potato starch and bleaching liquor, which oxidizes iodide into iodine. Iodine gives a purple color to potato starch. Purple stains and outlines of peds were drawn on transparent sheets and were analyzed in the laboratory.

The most restrictive layer to flow occurred between 15 and 35 cm below the soil surface, this layer was therefore sampled. Natural aggregates (peds) in the layer ranged in size from 30 to 50  $\text{cm}^3$ . This implies that 120 to 200 peds were present in a single sample, which should be adequate for the sample to be representative (Lauren et al., 1988).

### Physical Methods

In order to approximate the soil physical field conditions, the cylinders with soil were placed in the laboratory, on large polyvinyl chloride columns filled with medium textured sand and having a constant groundwater level at 100-cm depth, which corresponds with the average groundwater level during bypass flow under field conditions, as was measured with a datalogger. The initial moisture content for the five samples varied from 0.42 to 0.48  $\text{m}^3 \cdot \text{m}^{-3}$ .

Seven small tensiometer cups were installed at each of the three depths (25, 65, and 125 mm) in each core. Tensiometer cups were 10 mm long and 5 mm in diameter, and were installed at randomly chosen distances from the core wall, through prebored holes in the steel cylinder. Installation was carried out at a slightly upward angle to prevent water flow towards the cups (Fig. 1). In order to prevent disturbances during installation, a 4.5 mm diameter auger was used. By using an auger with a diameter a little smaller than the diameter of the cup, good contact between cup and soil was ensured and disturbances of the soil were minimized.

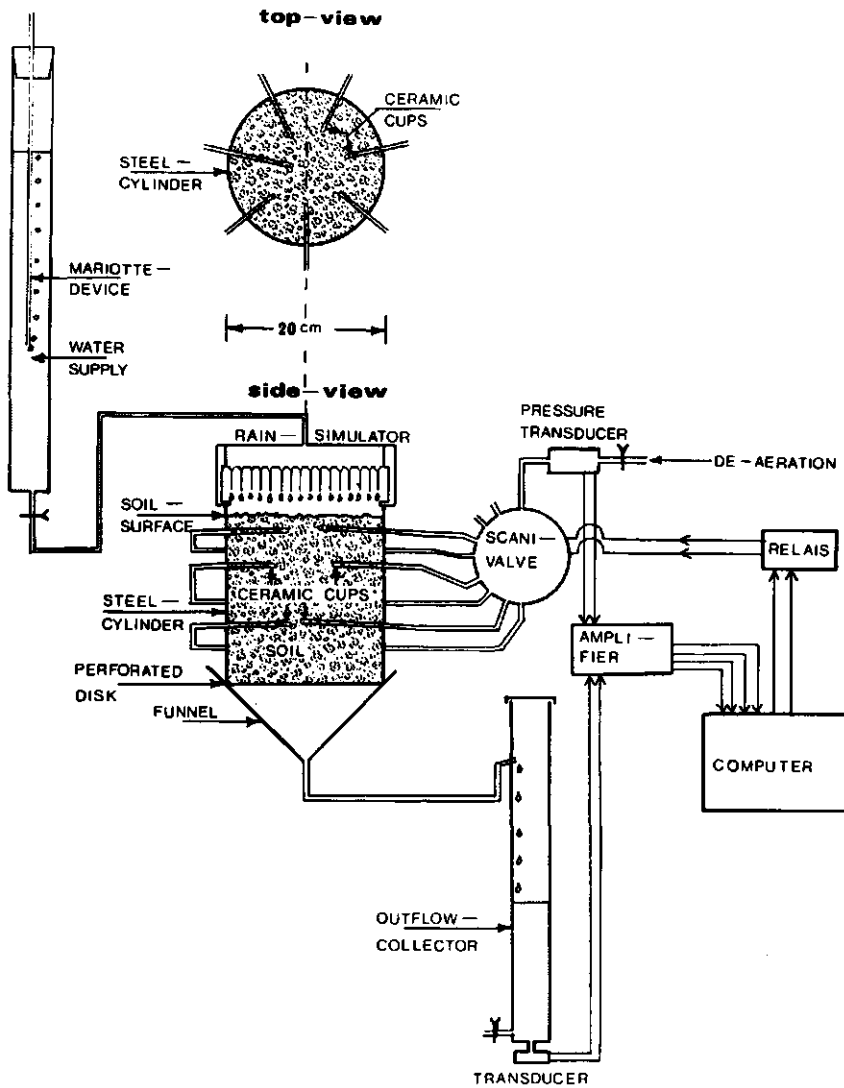


Figure 1 Laboratory set up for measuring bypass flow

The cylinders with soil were placed on a funnel (Fig. 1) and cups were left for equilibration for at least 16 h before the experiment was started. Every 30 s, a

computer-controlled Scanivalve (Scanivalve Corp., San Diego, CA) connected a tensiometer cup with the pressure transducer. In this way every cup was sampled once every 11 min. Response time of the cups in water was  $< 5$  s. Rain intensity was controlled by means of a mariotte device (Fig. 1). For all experiments, a shower of 10 mm of rain was applied with an intensity of  $13 \text{ mm}\cdot\text{h}^{-1}$ . In the Netherlands, such a rain storm has a probability of occurrence of once in two yr (Buishands and Velds, 1980). The shower caused nearly immediate ponding on top of the sample (saturated hydraulic conductivity [ $K_{\text{sat}}$ ] of the soil matrix was  $48 \text{ mm}\cdot\text{d}^{-1}$ ). The bottom of the sample was covered with a perforated plate and the sample was placed on a funnel. Outflow, which always had a blue color, was measured in a collector equipped with a differential pressure transducer in the bottom. This transducer was read every 30 s by the computer.

### Morphological Methods

At the start of the experiment, the exposed upper surface of the sample was dusted with methylene blue powder (dissolving the methylene in the rain water caused plugging of the rain simulator). Rainfall simulation was started after a period of about 45 min, in which the automatic registration equipment was tested. Ten mm of precipitation, which dissolved the methylene blue, was added and the rain simulator was stopped. Scanning of outflow and of the tensiometers was continued for several hours, until changes in measured pressure heads were small.

After termination of the experiment, the sample was peeled off in layers to depths of 15, 25, 45, 65, 90, 110, 125, and 160 mm below the top, and for every layer a cross section of the methylene blue patterns was drawn on transparent sheets. When tensiometers were present in a layer, their position was also indicated on the sheets. The grease, applied to minimize disturbances during sampling, created a thin hydrophobic layer along the wall of the sample, which prevented water flow along the wall of the sample cylinder. This unwelcome short-circuiting was not noticed during peeling off.

The observed patterns were digitized using software of a geographical information system. Surface area, length of contour, and number of stains were determined for each level. Total surface area examined per sample per layer was  $31\,416 \text{ mm}^2$ .

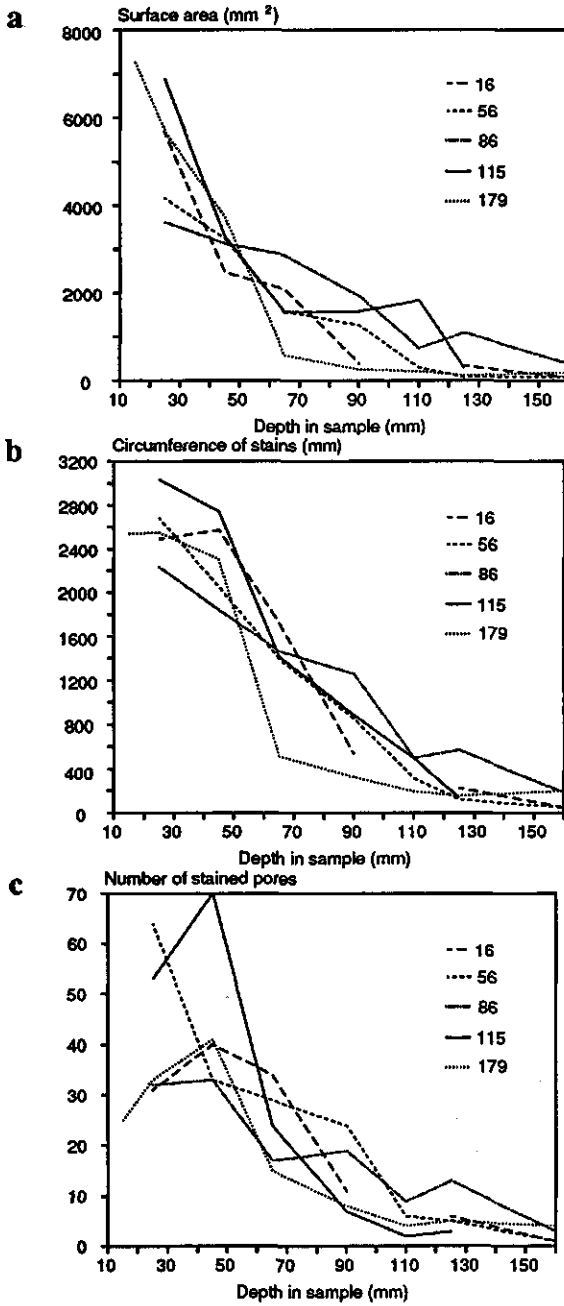


**Figure 2** Surface area (a) circumference (b) and number (c) of blue stained macropores for the five samples. The numbers in the figures are core sample numbers.

## RESULTS AND DISCUSSION

### Morphological Data

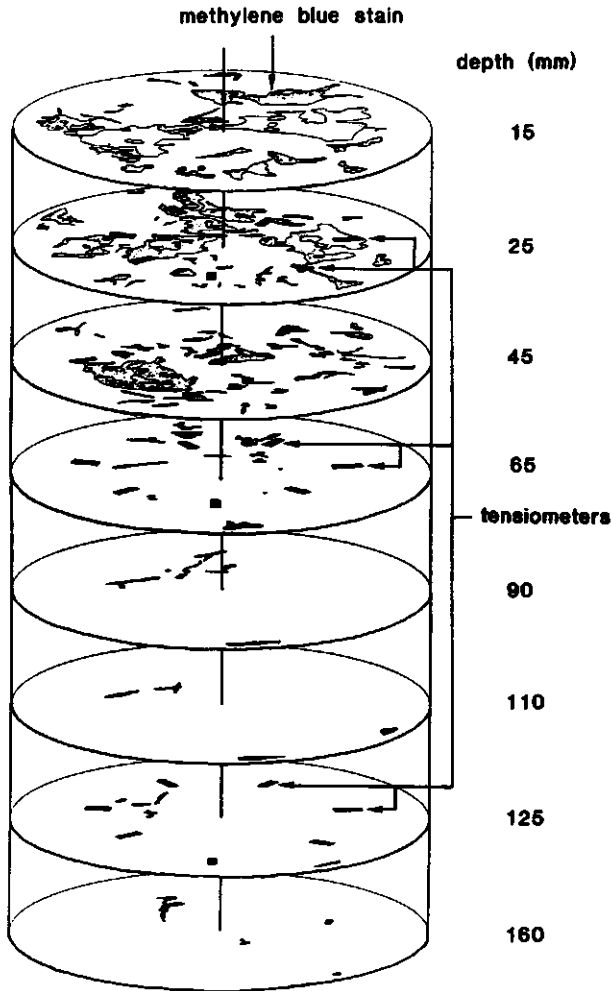
Figure 2 shows the results of the methylene blue dye tracing for all five cores. A rapid decline of blue colored surface area to a depth of 65 mm is perceptible for most samples; below 65 mm, the area decreased gradually (Fig. 2a). The perimeter of the blue stained area stayed rather constant to 45- mm depth for 3 samples, after which it decreased rapidly (Fig. 2b). From 10 mm downwards, only small changes occurred. The two other samples showed a gradual decrease to a depth of 125 mm. The number of colored stains first increased or stayed constant in 4 samples to a depth of 45 mm, and then decreased until it became rather constant at a depth of 110 mm below the soil surface (Fig. 2c). The presence of an increasing number of pores with depth to 45 mm is explained by the fact that the few large blue stains in the top layer divided in more small ones, as is indicated by the nearly equal perimeter of the stains at depths from 0 to 45 mm.

Figure 3 shows a three-dimensional reconstruction of the staining pattern for Sample 179. Positions of tensiometers are indicated at depths of 25, 65, and 125 mm. The sharp decrease of surface area, perimeter and number of stained pores is clearly visible at 65 mm depth.

### Physical Data

The soil water pressure head measurements for Sample 179 are shown in Fig. 4. The rainfall period is indicated by a bar, starting at 45 min and ending after  $\approx$  85 min. For the 25-mm depth, two types of tensiometer reactions can be distinguished: one very fast one, starting shortly after application begins and going to a saturated condition (e.g., T1, T2, T3, T5, and T6), the second showing a rather slow increase of pressure head, which continued long after simulated rainfall had stopped (e.g., T4). This second type indicates redistribution of water in the sample and expresses, therefore, the hydraulic effects of internal catchment. The fast-reacting cups, on the contrary, showed the opposite behavior. Pressure heads became more negative once simulated rainfall had stopped because free water disappeared from the vertically continuous macropore and the measured pressure head returned to the slightly lower, actual matrix potential of the soil.

Only slow-type tensiometer reactions are shown at a depth of 65 mm. One cup (T13) even showed a first reaction long after simulated rainfall had stopped. For the 125-mm depth, again, both reaction types were present, which indicates that some continuous macropores were not intercepted at the 65 mm level.



**Figure 3** *Reconstruction of methylene blue staining patterns for sample 179. Patterns were drawn at depths of 15, 25, 45, 65, 90, 110, 125, and 160 mm in the sample. The tensiometer locations and the serial numbers at the three depths are also shown.*

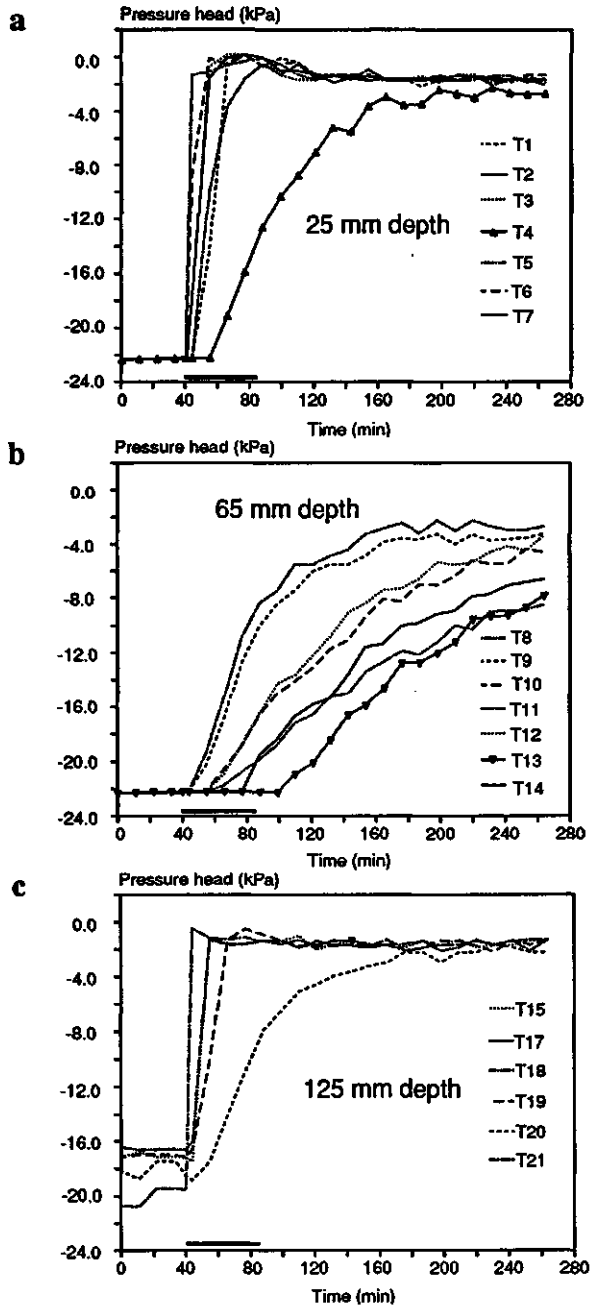
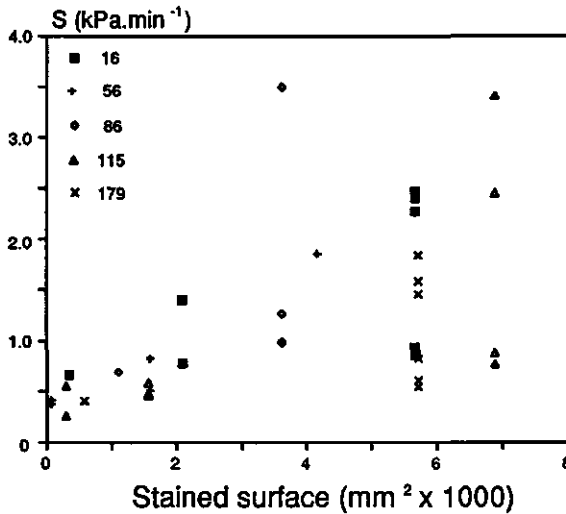


Figure 4 Tensiometric measurements of soil-water pressure heads for sample 179 at depths (a) 25, (b) 65 and (c) 125 mm below soil surface. T1, T2, etc., denote tensiometer numbers.

The different tensiometer reactions were characterized by three parameters: (i) the time after the start of simulated rainfall at which a first reaction was observed ( $t_1$ , min); (ii) the intensity of this first reaction, i.e., the gradient of the tensiometer reaction curve ( $S$ ), calculated from the baseline and the first two points after the first reaction; and (iii) the behavior after simulated rainfall has stopped; either wetting (increase of pressure head,  $+\Delta h$ ) or drying (decrease of pressure head,  $-\Delta h$ ). Wetting is an indication of the effects of internal catchment. The tensiometers were installed at random in the 3 layers, which means that some of them were in or near a macropore, and others were in the middle of a ped. Different locations should result in different reaction types, as defined by  $t_1$ ,  $S$  and  $\Delta h$ .

**Relating Morphological to Physical Data**

First, the relation was explored between  $t_1$  and  $S$  and the measured distance of the tensiometer cups to blue-colored stains, the latter being derived from the drawings of stains.



**Figure 5** Relationship between blue stained planar surface area and tensiometer reaction-intensity  $S$  for tensiometer reactions of category 2, which become dryer after termination of the simulated rainfall. The data are for the core numbers indicated.



Twenty-five cups that were located inside or within < 5 mm of a blue-colored macropore were associated with  $S$  values ranging from 0.26 to 3.5, with an average of  $1.15 \text{ kPa}\cdot\text{min}^{-1}$ . For the other 77 cups, there was no clear relation between the distance to a blue stained macropore and reaction time, or intensity. In order to more specifically express relations between tensiometer reactions and staining patterns, a stratification was carried out in terms of three categories of reactions after the end of the simulated rainfall:

1. wetting,
2. drying,
3. no clear reaction

Stratified according to these criteria, the intensity of the reaction ( $S$ ) was expressed as a function of the planar blue-stained surface area at that particular depth (Fig. 5). As the blue-stained area increased,  $S$  values increased for tensiometers of Category 2. The correlation coefficient of 0.52 was significant at 0.01 probability. Reactions of Category 1 show no correlation with reaction intensity ( $S$ ), because dynamics of water flow are particularly governed by the conductivity of the soil matrix and not by water movement in the macropores. Reaction intensity ( $S$ ) was also plotted against tensiometer depth in the sample.

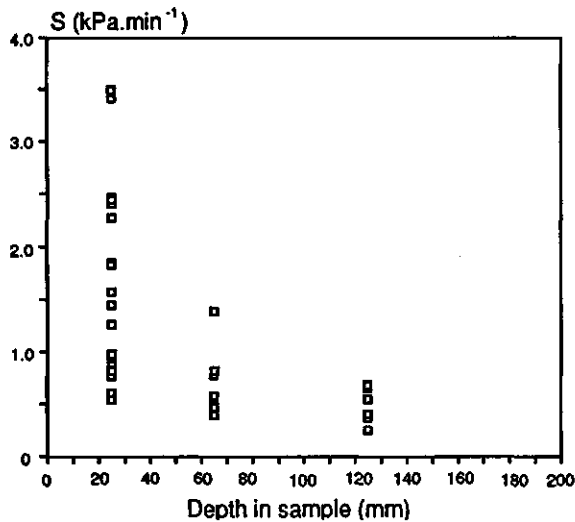


Figure 6 Changes with depth of the tensiometer reaction intensity  $S$  for tensiometer reactions of category 2 which become dryer after termination of the simulated rainfall.

Figure 6 shows the results for reactions of Category 2. Highest S values are found in the top of the sample. The S values in the lower part of the sample appear to be low, but are still more than twice as high as S values calculated for reaction types of Category 1. The calculated correlation coefficient of -0.52 is significant at 0.01 probability level.

Due to the limited depth resolution of the horizontal cross sections, a more pronounced relation between cup reaction type and distance to methylene blue stains cannot be derived. To determine such a pronounced relation, measurements with a much higher depth resolution, such as computerized axial tomography (CAT), are necessary.

Table 1 presents all 102 tensiometer reactions, as measured in the five samples, grouped in the categories as explained above (three of the originally 105 installed tensiometers were damaged during installation and omitted from the analysis).

**Table 1** *Tensiometric response categories for the five column experiments; Category 1: number of tensiometer with reactions becoming wetter after termination of the simulated rainfall; category 2: number of reactions becoming dryer; category 3: no clear reaction.*

Depth in sample (mm)	Category 1	Category 2	Category 3
25	8	22	5
65	20	8	7
125	15	4	13
Total	43	34	25

As mentioned above, tensiometer reactions of Category 2 indicate closeness to vertically continuous water-conducting macropores. Tensiometers with reactions of Category 1 indicate internal catchment nearby. Considering tensiometer reactions as a soil physical point count, we conclude that, in the top 25-mm of the sample 63% of the soil volume was in direct contact with continuous water-conducting macropores and 23% was influenced by internal catchment. For the 65-mm depth, a shift towards internal catchment is obvious, as the percentages were 23% and 57% respectively. At 125-mm depth, this trend continues, in

agreement with the morphological trends, illustrated in Fig. 3, showing a strong decrease of stained (continuous) pores with depth.

**Table 2**      *Estimated mass balances of the five experimental columns.*

Sample	simulated outflow		infiltration		internal catchment
	rainfall		surface	lateral	
	(mm)				
16	10	4.2	1.2	0.3	4.3
56	10	5.2	1.2	0.3	3.3
86	10	5.8	1.2	0.3	2.7
115	10	4.4	1.2	0.3	4.1
179	10	6.5	1.2	0.3	2.0
Average	10	5.2 ± 0.96	1.2	0.3	3.3 ± 0.96

Considering the entire soil volume of the five cores, we conclude that: 33% of the volume was in direct contact with continuous water-conducting macropores, 42% was being influenced by internal catchment, and 25% of the volume cannot clearly be classified in either category.

This characterization indicates that internal catchment plays a prominent part in processes of water flow in structured clay soils. To further illustrate this point, mass balances of the five experiments are presented in Table 2. In every experiment, 10 mm of water was applied with the same intensity. Measured outflow ranged between 4.2 and 6.5 mm, with an average of 5.2 mm. Matrix infiltration at the soil surface has been calculated by using an unsaturated hydraulic conductivity value at a slightly negative pressure head of -1.0 kPa (exclusion of the macropores). This surface infiltration was calculated to be 1.2 mm, considering the time from the start of the simulated rainfall, until ponded water ceased (Hillel, 1980, p. 20-24). Hoogmoed and Bouma (1980) calculated lateral absorption from macropores by using a diffusivity equation. They concluded that lateral infiltration of water from macropores into the soil matrix during bypass flow is in the order of only a few percent; we calculated 0.3 mm. The estimated value for internal catchment is 3.3 mm ± 0.96 mm, which is one third of the applied amount of water.

## CONCLUSIONS

This study shows that flow of water in structured soils is more complex than is suggested by the concept of mobile/immobile water, which is widely being used in the literature. A third phase, water that is intercepted in discontinuous macropores (internal catchment), should be added to this concept. Soil structure, measured under field conditions, should be taken into account when characterizing bypass flow. Macropore continuity, in particular, governs bypass phenomena, including internal catchment. Point measurements with small tensiometer cups are useful to express these processes in quantitative terms.

## ACKNOWLEDGEMENT

This study was funded by the European Community project: "Nitrate in soils" (EV4V.0098-NL).

## REFERENCES

- Andreini, M.S., and T.S. Steenhuis. 1990. Preferential paths of flow under conventional and conservation tillage. *Geoderma* 46:85-102.
- Beven, K., and P. Germann. 1982. Macropores and water flow in soils. *Water Resour. Res.* 18:1311-1325.
- Bouma, J., C.F.M. Belmans, and L.W. Dekker. 1982. Water infiltration and redistribution in a silt loam subsoil with vertical worm channels. *Soil Sci. Soc. Am. J.* 46:917-921.
- Bouma, J., and L.W. Dekker. 1978. A case study on infiltration into dry clay soil. I. Morphological observations. *Geoderma* 20:27-40
- Bouma, J., L.W. Dekker, and C.J. Muilwijk. 1981. A field method for measuring short-circuiting in clay soils. *J. Hydrol.* 52:347-354.
- Buishands, T.A., and C.A. Velds. 1980. Neerslag en verdamping. *Climate in the Netherlands. R. Dutch Meteorol. Inst. De Bilt, the Netherlands*
- Edwards, W.M., R.R. van der Ploeg, and W. Ehlers. 1979. A numerical study of the effects of noncapillary-sized pores upon infiltration. *Soil Sci. Soc. Am. J.* 43:851-856.
- Hillel, D. 1980. *Applications of soil physics.* Academic Press, NY.
- Hoogmoed, W.B., and J. Bouma. 1980. A simulation model for predicting infiltration into cracked clay soil. *Soil Sci. Soc. Am. J.* 44:458-461.
- Klute, A. 1973. Soil water flow theory and its application in field situations. p. 9-31. In R. R. Bruce et al. (ed.), *Field soil water regime, SSSA Spec. Publ. 5.* SSSA, Madison, WI.
- Kung, K-J.S., 1990. Preferential flow in a sandy vadose zone: 2. Mechanism and implications. *Geoderma* 46:51-58.
- Lauren, J.G., R.J. Wagenet, J. Bouma, and J.H.M. Wösten. 1988. Variability of saturated hydraulic conductivity in a Glossaquic Hapludalf with macropores. *Soil Sci.* 145:20-28.
- Lawes, J.B., J.H. Gilbert, and R. Warington. 1882. *On the amount and composition of the rain and drainage waters collected at Rothamsted.* Williams Clowes and Sons, London.
- Soil Survey Staff. 1975. *Soil taxonomy: A basic system of classification for making and interpreting soil surveys.* USDA-SCS Agric. Handb. 436, . U.S. Gov. Print. Office, Washington DC.
- Valocchi, A.J. 1990. Use of temporal moment analysis to study reactive solute transport in aggregated porous media. *Geoderma* 46:233-247.
- Van Ommen, H.C., L.W. Dekker, R. Dijkma, J. Hulshof, and W.H. van der Molen. 1988. A new technique for evaluating the presence of preferential flow paths in nonstructured soils. *Soil Sci. Soc. Am. J.* 52:1192-1194.

*Van Stiphout, T.P.J., H.A.J. Van Lanen, O.H. Boersma, and J. Bouma. 1987. The effect of bypass flow and internal catchment of rain on the water regime in a clay loam grassland. J. Hydrol. 95:1-11*

*White, R.E. 1985. The influence of macropores on the transport of dissolved and suspended matter through soil. Adv. Soil Sci. 3:95-121.*

## CHAPTER 4

# SENSITIVITY ANALYSIS ON PROCESSES AFFECTING BYPASS FLOW

Published in: *Hydrological Processes volume 7*  
*page 33-43 (1993)*

# **SENSITIVITY ANALYSIS ON PROCESSES AFFECTING BYPASS FLOW**

**H.W.G. Booltink and J. Bouma**

*Departement of Soil Science and Geology, Agricultural University, P.O. Box 37, 6700 AA Wageningen, The Netherlands.*

## **ABSTRACT**

Bypass flow in structured soils is dominated by soil hydrological processes, such as rain intensity, initial pressure head of the soil, surface storage of rain, horizontal contact area and absorption rate and hydraulic conductivity of the soil matrix. This study was conducted to determine the relative impact of these processes in different soil types. A quasi 3-dimensional simulation model was used to calculate the effects of these soil hydrological input parameters on surface infiltration, macropore flow (with related horizontal absorption) and drainage. For light textured soils, surface infiltration was the most important term in the water balance. Heavy textured soils, on the contrary, had drainage as the main term. In the latter soils bypass flow, when occurring, was almost equal to the amount of rain applied, indicating that absorption processes were strongly reduced. Lateral absorption on macropore walls was a minor fraction in the total mass balances, due to limited contact area and relatively weak diffusivity forces. Surface infiltration is a crucial parameter in bypass flow and is mainly dependent on rain intensity, initial pressure head and conductivity of the soil matrix. This requires measurement methods for hydraulic conductivity that specifically consider the effect of macropores.



## INTRODUCTION

Bypass flow, defined as flow of free water along macropores in unsaturated soils, is a common phenomenon in structured soils (Beven and Germann, 1982 White, 1985). Different factors that govern bypass flow in these soils were summarized by Bouma (1990). Flow of water into macropores occurs when, during a rain event, rain intensity is higher than the absorption capacity of the soil surface. Depending on the soil microrelief, a certain amount of water will be stored on the soil surface. When this storage capacity is exceeded, water will start flowing into macropores.

Macropores can be either continuous or non-continuous. In the latter, water will accumulate at some depth and start infiltrating from there. This process of "Internal Catchment" has first been described by Van Stiphout et al. (1987). Water flowing along the walls of air-filled macropores will be laterally absorbed. In case of continuous macropores the final excess of water will be added to the ground water or will flow to greater depths. Magnitude and intensity of these processes is controlled by external conditions, such as rain intensity, but also by internal conditions e.g. soil texture and soil structure with characteristically different hydraulic properties (Jarvis and Leeds, 1987).

Identical macropores function therefore differently in different soil materials due to different flow processes in the soil groundmass (Bouma et al., 1983).

A statistical frame work, consisting of uniform distributions of channel radii and depths, was used by Beven and Clark, (1986). In this model infiltration radially moved away from a water filled channel into the soil matrix.

In this study a sensitivity analyses was carried out on soil physical processes, related to bypass flow, such as surface infiltration, horizontal infiltration from macropores and outflow. Four different soil types, varying from loamy sand to heavy clay were used to compare magnitude and intensity of the processes among the selected soils. The object of this sensitivity analysis is to derive generalized relationships for bypass flow phenomena allowing easier characterizations in modelling.

The sensitivity analyses was carried out with a quasi 3-dimensional simulation model developed by Hoogmoed and Bouma (1980). This model combines two existing physical simulation models for vertical and horizontal infiltration.

## MATERIAL AND METHODS

### Simulation model

The simulation model used was developed by Hoogmoed and Bouma (1980), it describes the following processes:

(A) Vertical infiltration of water into the upper surface of a homogenous soil with a specified initial water content. (B) Flow of water into cracks, (C) horizontal absorption of water into the crack walls. (D) Drainage.

(A) A one-dimensional simulation model considering, from the top to the bottom, 9 compartments of 2.0 cm, 1 of 1.5 cm and a top compartment of 0.5 cm, was used to calculate vertical infiltration in the surface of the soil matrix. Water flow between underlying layers was simulated with the Darcy equation [1] using  $K(\theta)$  and  $\theta-\psi$  relations in a table. Physical boundary conditions are as follows:

$$z=0 \quad -K \delta H/\delta z = R \quad 0 < T < T(p) \quad [1a]$$

$$0 < H < w \quad T(p) \leq T \leq T(c) \quad [1b]$$

$$H = w \quad T > T(c) \quad [1c]$$

$$z=20 \quad -K \delta H/\delta z = \text{constant} \quad [1d]$$

where  $z$  = depth (cm) below the top of the soil,  $T(p)$  = time (days) when ponding starts,  $T(c)$  = time when ponding reaches the maximum surface storage  $w$  (cm),  $R$  = rain intensity ( $\text{cm}\cdot\text{day}^{-1}$ ), and  $H$  = hydraulic head (cm water).

(B) If the infiltration capacity of the soil is less then the applied rain intensity, ponding will occur at time  $T(p)$ . When a preset threshold value for surface storage ( $w$ ) is reached the excess of water, between rainfall and vertical infiltration, will flow into the cracks.

- (C) Water flowing into cracks is absorbed laterally. For this a one-dimensional simulation model [2], based on the diffusivity equation (Van der Ploeg and Benecke, 1974) was used.

$$\delta/\delta x [D \delta \theta / \delta x] = \delta \theta / \delta t \quad [2a]$$

With the following boundary conditions:

$$x=0 \quad \delta \theta / \delta x = 0 \quad T > T(c) \quad [2b]$$

$$x > x_t \quad \delta \theta / \delta x = 0 \quad T > T(c) \quad [2c]$$

Where  $x$  = horizontal distance (cm) from infiltration surface,  $\theta$  = moisture content,  $x$  = penetration depth of the wetting front at time  $t$ , and  $D$  is the diffusivity -  $\theta$  relation.

This model calculates lateral absorption, in a horizontal homogeneous soil column (divided into 0.2 cm compartments), as a function of time. Bouma and Dekker, 1978, found that water flowing into cracks formed small bands on horizontal ped faces. The total surface area of bands at a given depth is referred to as: "Contact Area". This surface area is only a very small percentage of the total surface area available on vertical ped faces. Contact area increases with time since new bands develop during the bypass flow process. For each time step, new bands develop and they are associated with initial, high, absorption rates in relatively dry soil. In this way series of contact areas with different absorption rates are simultaneously considered in the model.

- (D) Water which is not laterally absorbed at the bottom of the 20 cm soil column is considered as drainage.

Output of the model is cumulative surface infiltration (CUMINF), cumulative lateral absorption (CUMABS) and cumulative drainage (CUMDRN). The sum of these three factor plus the threshold value for surface ponding should equal the amount of rain applied.

The model was written in CSMP III language, by using a first order Euler integration method with a fixed time step of  $10^{-5}$  day. The model has been run

on the VAX 8600 computer of the Agricultural University Wageningen. Mass balance errors were always smaller than 0.5 %.

Further details on the model are given by Hoogmoed and Bouma (1980), Van der Ploeg and Benecke (1974), Van Keulen and Van Beek (1971), and Hillel (1977).

### Sensitivity analyses

In order to stress the effects of similar hydrological processes in different soils, the sensitivity analyses was carried out for four different soil types (Wösten, 1987). Texture data and Van Genuchten parameters, describing soil physical and hydrological characteristics (Van Genuchten, 1980), are presented in table 1. Soil physical parameters on which the sensitivity analysis was carried out are presented in table 2. A set with standard parameters was selected as our basic data set (underlined values in table 2.).

**Table 1** *Texture data and Van Genuchten parameters for four surface soils. Texture in percentage of mineral soil.(Wösten et al., 1987).*

soil type	<2 $\mu\text{m}$ (%)	water cont. saturated ( $\text{cm}^3 \cdot \text{cm}^{-3}$ )	water cont. residual ( $\text{cm}^3 \cdot \text{cm}^{-3}$ )	saturated conductivity ( $\text{cm} \cdot \text{day}^{-1}$ )	alpha ( $\text{cm}^{-1}$ )	n (-)	l (-)
loamy sand	< 12	0.45	0.0	18	0.0152	1.412	-0.213
sandy loam	12- 18	0.40	0.0	23	0.0313	1.200	-3.578
clay loam	25- 35	0.44	0.0	31	0.0519	1.126	-6.552
clay	50-100	0.57	0.0	98	0.1689	1.068	-10.286

A standard pressure head of 25 kPa is considered to be a realistic initial value under many field conditions. A rain intensity of  $25 \text{ cm} \cdot \text{day}^{-1}$  during 2 hours has, for Dutch climatological circumstances, a probability of occurrence of once a year,  $15 \text{ cm} \cdot \text{day}^{-1}$  during 2 hours, a probability of twice a year and  $40 \text{ cm} \cdot \text{day}^{-1}$  during 2 hours a probability of once per ten years (Buishand and Velds, 1980). Contact area represents the vertical surface area on which horizontal absorption takes place. Bouma and Dekker, (1978), observed such infiltration patterns in  $0.5 \text{ m}^2$  plots as a function of rain intensity and amount. They found that water flowed along macropores in small vertical bands occupying 2 percent or less, of

the potential available contact area. Which were the vertical faces of 10 cm large soil prisms. Since little information about this parameter is known we selected a broad range of values with 5 percent contact area (which corresponds with 250 cm<sup>2</sup> for a 0.5 m<sup>2</sup> area with large soil prisms) as a standard.

Surface storage is a parameter which is hard to measure. Surface roughness will provide some information about potential storage, but the actual value depends mainly on number, size and surface appearance of macropores conducting water to greater depths. A value of 0.1 cm has been selected as the standard.

**Table 2** *Parameter settings as used in sensitivity analyses (standard parameter settings underlined)*

initial pres. head (kPa)	rain intensity (cm.day <sup>-1</sup> )	contact area (cm <sup>2</sup> )	surface storage (cm)	conductivity at pres. head (kPa)
2.5	5	25	0.005	0.1
5.0	10	50	0.010	0.2
10.0	15	100	0.020	0.3
<u>25.0</u>	20	175	0.040	0.4
<u>50.0</u>	<u>25</u>	<u>250</u>	0.070	<u>0.5</u>
100.0	30	325	<u>0.100</u>	0.6
500.0	35	400	0.150	0.7
999.9	40	500	0.200	0.9
	45	600	0.250	1.0
	50	700	0.300	

Saturated hydraulic conductivity is often measured by shallowly ponding water on a saturated soil sample and by measuring outflow from the bottom under steady state flow conditions (e.g., Klute 1986). The value for the saturated hydraulic conductivity is therefore dominated by flow through macropores. In order to use a K-value representing the saturated hydraulic conductivity of the soil matrix, excluding the effects of macropores, we used a K-value at a slightly negative pressure head of 0.5 kPa.

Conductivities for the four soils are presented in table 3. The sharp drop of the conductivity upon desaturation in soils with macropores is illustrated by comparing the saturated hydraulic conductivity (h=0 kPa) with the values for 0.1

kPa (table 3). This drop is most pronounced for the clay soil, where most macropores occur.

The sensitivity analysis was carried out, as is usual, by changing only one parameter at a time and keeping all the others constant.

**Table 3** *Conductivities for the loamy sand, sandy loam, clay loam, and clay at different pressure heads.*

pressure head (kPa)	Hydraulic conductivity (cm.day <sup>-1</sup> )			
	loamy sand	sandy loam	clay loam	clay
0.0	17.810	22.900	31.100	98.200
0.1	12.034	5.805	3.144	1.594
0.2	10.384	4.301	2.130	0.891
0.3	9.261	3.472	1.626	0.603
0.4	8.398	2.920	1.314	0.446
0.5	7.694	2.518	1.099	0.349
0.6	7.101	2.210	0.941	0.284
0.7	6.590	1.965	0.820	0.237
0.9	5.743	1.597	0.647	0.175
1.0	5.387	1.456	0.583	0.153

## RESULTS

Mass balances for the sandy loam, clay loam, and clay, using standard parameter settings, are shown in Figs. 1a-c. For the loamy sand no mass balance is given since the simulation with standard parameter settings produced no bypass flow, the rain shower was completely absorbed by surface infiltration.

Figures 1a-c show cumulative amounts of rain, infiltration (CUMINF), horizontal absorption (CUMABS), and drainage (CUMDRN). Values for T(p) and T(c) represent start times of ponding and bypass flow. Differences in T(p) and T(c) among the soils are pronounced. For the clay soil ponding starts within 2 minutes after starting irrigation and bypass flow after 12 minutes. For the clay loam and sandy loam ponding starts after 9 and 23 minutes respectively. Bypass flow for the latter two starts after 24 and 44 minutes from the start of irrigation.

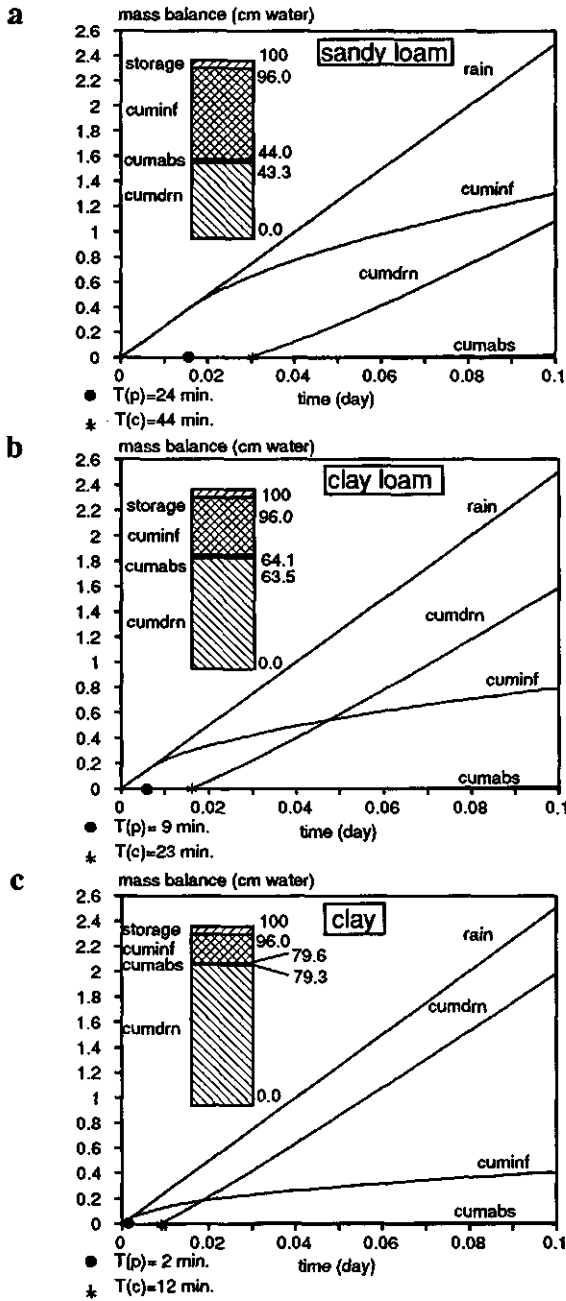


**Figure 1** Mass balances for the sandy loam (1a), clay loam (1b) and, clay (1c), using standard parameter settings. Values in window represent relative amounts.

A substantial reduction of the contribution of cumulative infiltration on the mass balances (sandy loam, 52 percent, clay loam, 31.9 percent, and clay, 16.4 percent) can be seen as the clay content increases. This decrease of infiltration is proportionally related to an increase of the cumulative drainage. Cumulative horizontal absorption is only a small fraction of the total balances, which decreases from 0.7 percent for sandy loam to 0.3 percent for clay. Standardized surface storage of 0.1 cm corresponds with 4 percent of the mass balances. The importance of drainage in the mass balance, especially for the clay loam and clay is also illustrated by the almost immediate constant intensity of the drainage curve, 19 cm.day<sup>-1</sup> for the clay loam and 22 cm.day<sup>-1</sup> for the clay soil, which nearly equals rain intensity (25 cm.day<sup>-1</sup>). This implies that most of the water, applied after time T(c), will flow into cracks and lead to drainage.

For the loamy sand bypass flow was only observed when (i) initial pressure head was lower than 10 kPa, (ii) rain intensities were higher than 30 cm.day<sup>-1</sup>, and (iii) for surface storage having a value lower than 0.02 cm.

The relative impact for the different input parameters on calculated surface infiltration, horizontal absorption, and drainage are presented in Fig. 2a, 3a and 4a for the sandy loam, Fig. 2b, 3b and 4b for the clay loam, and Fig. 2c, 3c and 4c for the clay soil. In these graphs the relative input and output is calculated by dividing the used input and output values by the standard values of input and output. The coordinates (1,1) represent standard input/output.

### Surface infiltration

Surface infiltration is mainly influenced by initial pressure head, rain intensity and, to a lesser extent, by the saturated hydraulic conductivity of the soil matrix. For pressure head values lower than 10 kPa the sensitivity is high. After 25 kPa the sensitivity becomes reduced. This sensitivity performs identical for all three soils; clay loam and clay are a little more sensitive for dryer initial conditions. Surface infiltration is also sensitive for low rain intensities. The three soils behave quite differently. The sandy loam is very sensitive for intensities lower than 15 cm.day<sup>-1</sup>. The clay loam only for intensities less than 10 cm.day<sup>-1</sup>, and the clay shows no sensitivity at all. A soil is only sensitive for rain intensity as long as rain intensity restricts the potential infiltration capacity of that soil. When rain intensity is higher than the potential infiltration capacity, it is no longer a limiting factor and becomes therefore insensitive.



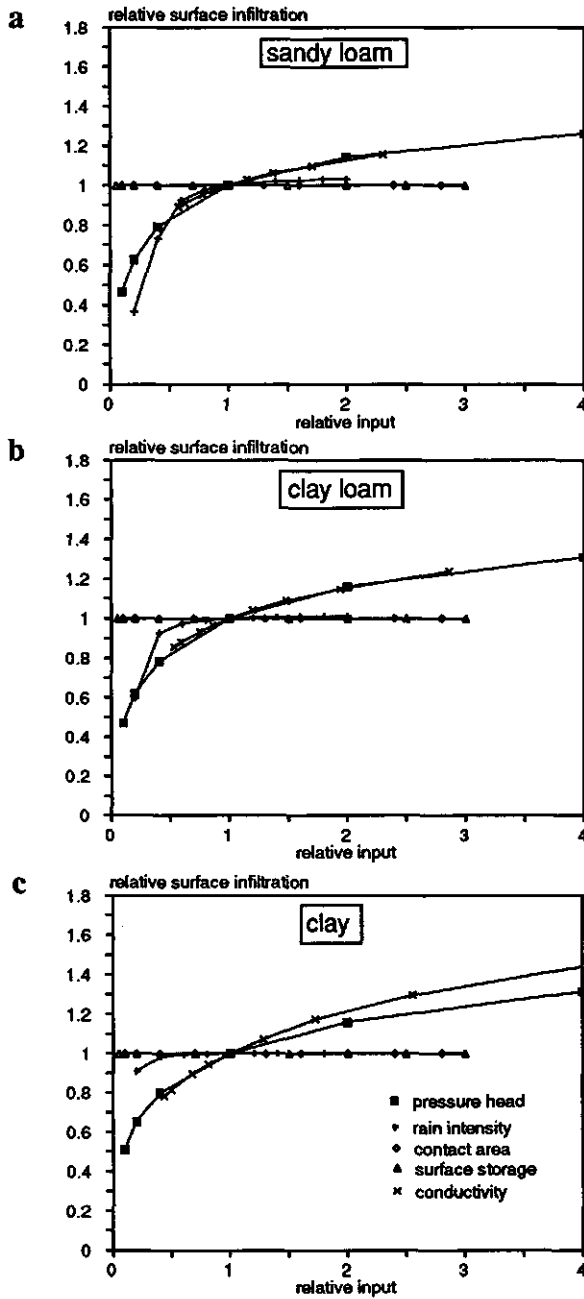
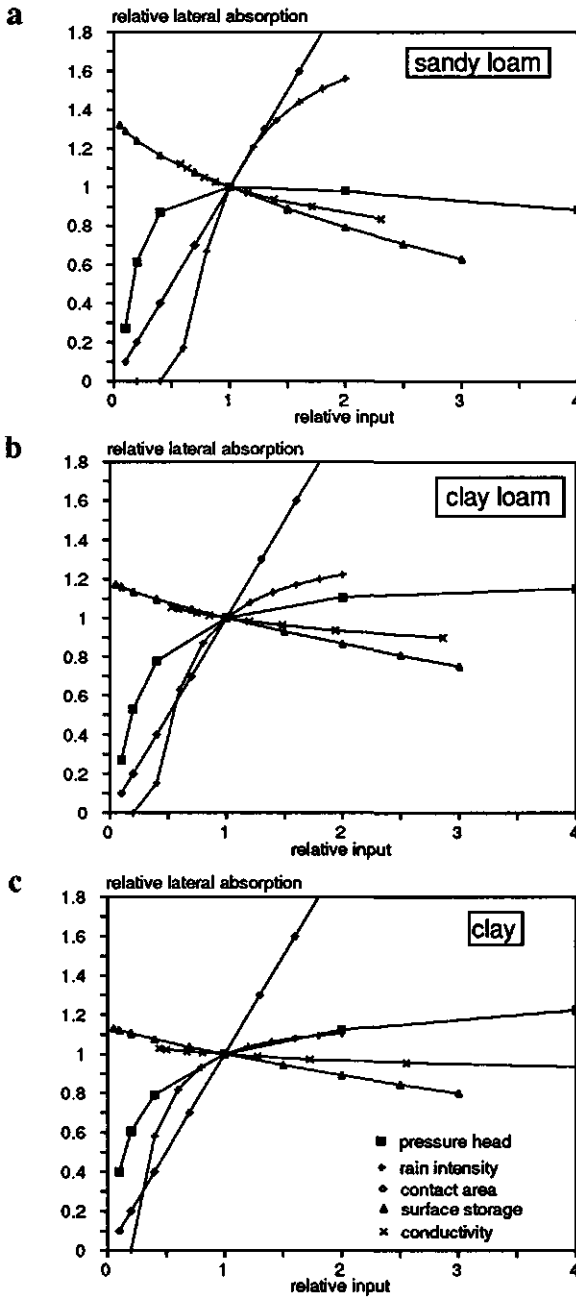
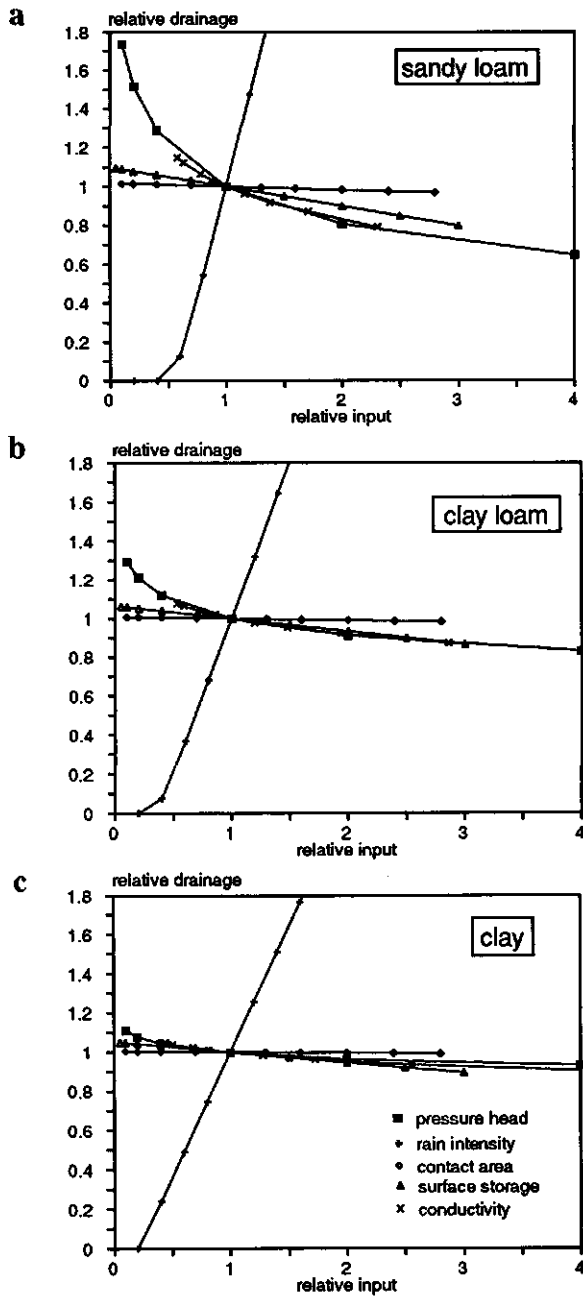


Figure 2 Relative sensitivity of surface infiltration for the sandy loam (2a), clay loam (2b) and clay (2c). Standard input/output is indicated by (1,1).



**Figure 3** Relative sensitivity of lateral absorption for the sandy loam (3a), clay loam (3b) and clay (3c). Standard input/output is indicated by (1,1).



**Figure 4** *Relative sensitivity of drainage for the sandy loam (4a), clay loam (4b) and clay (4c). Standard input/output is indicated by (1,1).*

The saturated hydraulic conductivity for the soil matrix is also a sensitive parameter for all soils, with a tendency of increasing sensitivity for clay soils. This is also a result of the infiltration capacity of a soil, which in the model is calculated as a function of moisture content and conductivity of the top layer. Sensitivities for initial pressure heads and conductivity are therefore much alike. The effect of an increased surface infiltration, due to the head  $w$ , was always small. The clay loam showed an increase of less than 1 percent with a surface storage capacity of 0.3 cm. The sensitivity for this parameter is determined by a combination of two factors: the height of the water head  $w$  and the saturated hydraulic conductivity of the soil matrix. Some additional simulations with the clay loam, using a rain intensity of  $50 \text{ cm}\cdot\text{day}^{-1}$ , an extreme surface storage of 2.0 cm and, a  $K$  at  $h=5$  cm, showed an increased surface infiltration of 4 percent. However, a combination of, a rain intensity of  $50 \text{ cm}\cdot\text{day}^{-1}$ , a 2.0 cm surface storage and, a high conductivity ( $K$  at  $h=1$  cm), increased surface infiltration with 12 percent.

### Lateral absorption

Contact area gives a 1:1 sensitivity for input versus output. Doubling the surface for lateral absorption leads to the same increase of lateral absorption.

The typical shape of the sensitivity line for initial pressure head is partly a reflection of the diffusivity - water content function. For most soils diffusivity shows a sharp decrease in the wet part of the curve, which is reflected as the sensitive part for low pressure heads.

Sensitivity for the other parameters is a result of the effects of these parameters on surface infiltration and ponding capacity. Lateral absorption starts if crack flow occurs according to calculated absorption function, which means, that, for identical initial pressure heads, the amount of lateral absorption is directly related to  $T(c)$ .

Although lateral absorption seemed to be affected by a number of parameters the effects on the absolute values is practically negligible. An increase of lateral absorption with a factor 10 represents (on an absolute scale) for the clay soil only an increase from 0.3 to 3 percent on the total mass balance.

### Drainage

Parameters dominating the cumulative amount of drainage from the bottom of the column are rain intensity and initial pressure head (sandy loam). Because drainage is calculated in the model as an excess term, sensitivity for initial pressure head is a reversed function of the sensitivity of that parameter for surface infiltration. This is illustrated by the decreased sensitivity for the clay loam and clay soil.

Rain intensity shows an extreme sensitivity. For the sandy loam an increase of 20 percent of rain intensity gives a increase of 34 percent on drainage, for the clay loam and clay these values are 26 and 22 percent respectively. Part of this sensitivity is caused by the effects of rain intensity on surface infiltration. Without this effect sensitivity would show a 1:1 line as is nearly the case for clay, where rain intensity is the only parameter influencing drainage (see also Fig. 1).

## DISCUSSION

The sensitivity analyses reported, show that identical rain intensities and quantities have different effects on different soil types. Bypass flow, from the bottom of 20 cm long soil columns, containing 4 soil types, ranging from loamy sand to heavy clay, varied from 0 to 79 percent. Calculated lateral absorption, during bypass flow, was always less than 1 percent and seems not to be an important parameter. However, the model used was only able to consider strictly vertical and continuous macropores. Absorption in macropores which have a more complex geometry may become more important. In skew or partially horizontal macropores infiltration will be dominated by gravitation forces and not, as in our model, by diffusivity flow only. This will lead to increased absorption. Such effects, and the effect of non-continuous macropores can only be simulated correctly if soil structure is taken into account in terms of vertical macropore continuity.

Surface infiltration is mainly governing the overall process of bypass flow. An increased surface infiltration will lead to delayed ponding and, finally, reduced bypass flow. Especially for heavy clay soils, where surface infiltration and lateral absorption decrease rapidly after the start of irrigation, this delay is

determining the final amount of bypass flow. Hatano and Booltink (1992) reported excellent regression between measured amount of outflow from the column and  $T(c)$  ( $r^2=0.99$ ). This implies that, when modelling bypass flow, special attention should be paid to a correct simulation of surface infiltration and that an accurate prediction of  $T(c)$  is an important criterion in model simulations. Parameters dominating this process are mainly: rain intensity and saturated conductivity of the soil matrix. Calculating surface infiltration by using the saturated hydraulic conductivity, including the effects of macropores, will lead to an overestimation of infiltration. Bouma (1982) distinguished between the saturated hydraulic conductivity of a soil including ( $K_{sat}$ ), and excluding ( $K_{(sat)}$ ), the effects of macropores.  $K_{(sat)}$ , which is equivalent to the saturated hydraulic conductivity of the soil matrix, was defined as the minimum conductivity value were the soil matrix potential is still zero. Determination of this value requires special methods such as the disk permeameter (Perroux and White, 1988) or suction crust infiltrometer (Booltink et al., 1991). For the soils reported on, surface storage is only important when it exceeds high values of more than 1 cm with a high saturated hydraulic conductivity.

## ACKNOWLEDGEMENT

This study was funded by the European Community project STEP-0032-C

## REFERENCES

- Beven, K., and P. Germann. 1982. *Macropores and water flow in soils*. *Water Resour. Res.* 18:1311-1325.
- Beven, K., and R.T. Clarke. 1986. *On the variation of infiltration into a homogeneous soil matrix containing a population of macropores*. *Water Resour. Res.* 22:383-388.
- Booltink, H.W.G., J. Bouma, and D. Giménez. 1991. *Suction crust infiltrometer for measuring hydraulic conductivity of unsaturated soil near saturation*. *Soil Sci. Soc. Am. J.* 55:566-568.
- Bouma, J. 1982. *Measuring the hydraulic conductivity of soil horizons with continuous macropores*. *Soil Sci. Soc. Am. J.* 46:438-441.
- Bouma J. 1990. *Using Morphometric expressions for macropores to improve soil physical analyses of field soils*. *Geoderma* 46:3-11.
- Bouma, J., and L.W. Dekker. 1978. *A case study on infiltration into dry clay soil. I. Morphological observations*. *Geoderma* 20:27-40.
- Bouma, J., C. Belmans, L.W. Dekker, and W.J.M. Jeurissen. 1983. *Assessing the suitability of soils with macropores for subsurface liquid waste disposal*. *J. Environ. Qual.* 12:305-311.
- Buishand, T.A., and C.A. Velds. 1980. *Neerslag en verdamping. Climate in the Netherlands. Royal Dutch Meteorological Institute (in Dutch)*.
- Hatano, R. and H.W.G. Bootink. 1992. *Using fractal dimensions of stained flow patterns in a clay soil to predict bypass flow*. *J. Hydr.* 135:121-131.
- Hillel, D. 1977. *Computer simulation of soil water dynamics IDRC, Ottawa*.
- Hoogmoed, W.B., and J. Bouma. 1980. *A simulation model for predicting infiltration into cracked clay soil*. *Soil Sci. Soc. Am. J.* 44:458-461.
- Jarvis, N.J., P.B. Leeds-Harrison. 1987. *Modelling water movement in drained clay soil. I. Description of the model, sample output and sensitivity analyses*. *J. of Soil Sci.* 338:487-498.
- Klute, A. (ed.) 1986. *Methods of soil analysis. Part 1. 2nd ed. Agron. Monogr. 9. ASA and SSSA, Madison, WI*.
- Perroux, K.M., and I. White. 1988. *Designs for disc permeameters*. *Soil Sci. Soc. Am. J.* 52:1205-1215.
- Stiphout, T.P.J., H.A.J. Van Lanen, O.H. Boerma, and J. Bouma. 1987. *The effect of bypass flow and internal catchment of rain on the water regime in a clay loam grassland soil*. *J. Hydr.*, 95(1/2):1-11.
- Van Genuchten, M. Th. 1980. *A closed-form equation for predicting the hydraulic conductivity of unsaturated soils*. *Soil Sci. Soc. Am. J.* 44:892-898.

- Van Keulen, H., and C.G. M. van Beek. 1971. *Water movement in layered soil; A simulation model*. *Neth. J. Agric. Sci.* 19:138-153.
- Van der Ploeg, R.R., and P. Benecke. 1974. *Unsteady, unsaturated n-dimensional moisture flow in soil: A computer simulation program*. *Soil Sci. Soc. Am. Proc.* 38:881-885.
- White, R.E. 1985. *The influence of macropores on transport of dissolved and suspended matter through soil*. In: B.A. Stewart (ed.), *Advances in soil science*. Volume 3. Springer, New York, N.Y. Vol. 3:95-120.
- Wösten, J.H.M. 1987. *Description of the water retention and conductivity characteristics from the Staring series with analytical functions*. Report nr. 2019. Staring Centre, Wageningen, Netherlands. (in Dutch).



## CHAPTER 5

# USING FRACTAL DIMENSIONS OF STAINED FLOW PATTERNS IN A CLAY SOIL TO PREDICT BYPASS FLOW

Published in: *Journal of Hydrology* volume 135  
page 121-131 (1992)

# USING FRACTAL DIMENSIONS OF STAINED FLOW PATTERNS IN A CLAY SOIL TO PREDICT BYPASS

R. Hatano<sup>1</sup> and H.W.G. Booltink<sup>2</sup>

<sup>1</sup> Faculty of Agriculture, Hokkaido University, Sapporo, Japan

<sup>2</sup> Departement of Soil Science and Geology, Agricultural University, P.O. Box 37, 6700 AA Wageningen, The Netherlands.

## ABSTRACT

Methylene blue staining patterns of five undisturbed unsaturated soil cores, 200 mm long and 200 mm in diameter, taken from a well-structured clay soil classified as a Hydric Fluvaquent, were characterized by using the fractal dimension of structure in order to predict measured bypass flow. Cumulative outflow curves in all cores were well described by a spherical model. Outflow in each core started after a significant time-lag from the start of irrigation. Outflow rates during irrigation in all cores were almost equal to irrigation rates, which means that nearly all the water applied, after outflow had started, contributes to bypass flow. Total amount of outflow ( $O_m$ , mm) was regressed on the time-lag ( $T_l$ , min) as:

$$O_m = -0.181 T_l + 9.85$$

This time-lag was caused by the effect of internal catchment of discontinuous macropores and surface storage. The three-dimensional fractal dimension of structure ( $D_{s3}$ ) was calculated for the upper and lower half of the core, by using values of  $D_{s2}$  and stained area in cross sections. A statistically significant empirical equation, relating the total amount of outflow ( $O_m$ ) to both upper and lower values of  $D_{s3}$  and to the volume fraction of stained parts ( $V_s$ ) is:

$$O_m = -230.6(V_s D_s^3 - 1)_{upper} + 234.4(V_s D_s^3 - 1)_{lower} + 12.6$$

Thus, a greater  $D_s^3$  value in the upper half of the core and a lower  $D_s^3$  in the lower half of the core induce larger amounts of outflow: hence vertically continuous macropores, such as fragments of cracks or tubes, play a significant role in the process of bypass flow.

## INTRODUCTION

Water and solute movement in well structured clay soils is affected by macropores (White, 1985). Movement of free water along macropores through an unsaturated soil matrix has been defined as bypass flow, while subsurface infiltration of bypass water at the bottom of dead-end macropores has been referred to as internal catchment (e.g. Bouma, 1984; Van Stiphout et al. 1987). Booltink and Bouma (1991) studied bypass flow and internal catchment in five large (6 l) undisturbed cores, sampled from a heavy clay soil. They applied 10 mm of water at an intensity of 13 mm.hr<sup>-1</sup> and added methylene blue to stain the walls of macropores along which water movement took place; 102 small tensiometers measured water flow patterns in the soil at different depths. After the experiment, each column was cut into six to eight slabs, about 2 cm high, and staining patterns on the horizontal surfaces were observed and digitized to allow manipulation of these morphological data. Attempts to predict bypass independently using the staining patterns were not successful.

Hatano et al. (1992) used similar morphological techniques to calculate the fractal dimensions of staining patterns of methylene blue, in this study macroporosity and fractal dimensions of staining patterns were successfully related to Brenner numbers for Cl<sup>-</sup> breakthrough.

This paper investigates the feasibility of using fractal dimensions of morphological staining patterns, established during bypass flow, to predict bypass flow phenomena in terms of the first moment of outflow and total outflow.

## MATERIAL AND METHODS

### Soil used

Soil samples were taken at a depth of 15 - 35 cm in steel cylinders (200 mm in diameter and 200 mm long) at five randomly chosen locations within a field at the experimental farm "The Kandelaar" in the former southern sea polder Eastern Flevoland in the Netherlands. Aggregate size in the sample was approximately 30 to 50 cm<sup>3</sup>, which implies that 120 to 200 peds were present in a sample, which should be ensure that the sample is representative (Lauren et al., 1988).

The soil is classified as a mixed mesic Hydric Fluvaquent (Soil Survey Staff, 1975). Soil sampling procedure, treatment of the samples and a profile description are presented elsewhere (Booltink and Bouma, 1991).

### Experimental set up

In the laboratory, the five cylinders were brought to similar initial soil physical conditions (Booltink and Bouma, 1991). Initial moisture content of the five samples varied between 0.42 to 0.48 cm<sup>3</sup>.cm<sup>-3</sup>. Twenty one small tensiometer cups (5 mm in diameter and 10 mm long) were installed at three depths in each sample. After that the samples were placed on a funnel, which was connected to a transducer- equipped outflow collector and a thin film of methylene blue powder was spread over the sample surface.

Each of the five samples was subjected to a rain shower of 10 mm, at an intensity of 13 mm.hr<sup>-1</sup>. In the Netherlands, such a rain event has a probability of occurrence of once per two years (Buishands and Velds, 1980). The shower caused nearly immediate ponding on top of the samples, which had a saturated hydraulic conductivity of approximately 50 mm.day<sup>-1</sup>.

Outflow, always an intense blue colour, was measured every 30 s by a computer connected to the outflow collector.

After termination of the experiment the sample was sectioned in layers at depths: 15, 25, 45, 60, 90, 110, 125 and 160 mm from the top of the sample; for every layer a cross section of the methylene blue staining patterns was drawn on transparent sheets. The sheets were digitized and converted in a raster database (1 x 1 mm grid cell mesh) using software a geographical information system.

**Parameterization of outflow curves**

To parameterize cumulative outflow curves a spherical model (Davis, 1986) was fitted through the individual outflow curves. The model is defined as:

$$O_f = 0 \qquad T - T_l < 0 \qquad [1a]$$

$$O_f = O_m [1.5(T - T_l)T_m^{-1} - 0.5(T - T_l)^3 T_m^{-3}] \qquad T - T_l < T_m \qquad [1b]$$

$$O_f = O_m \qquad T - T_l > T_m \qquad [1c]$$

where  $O_f$  is the outflow (mm),  $O_m$  is the fitted total amount of outflow for the sample (mm),  $T$  is the time (min),  $T_l$  is the time-lag for outflow to begin after irrigation has started (min), and  $T_m$  is the period during which outflow occurred (min).

**Fractal dimensions of structure**

The two-dimensional fractal dimension of staining patterns,  $D_2$ , can be derived by fractionalizing a horizontal, stained, cross section into squares (pixels) of side  $r$ , and then counting the number of stained pixels  $N_2(r)$ . By repeating this process with increasing  $r$  values a range of  $N_2(r)$  values is obtained. Double logarithmic plots of  $N_2(r)$  against  $r$  show a straight line (Hatano et al., 1992) from the slope of which the fractal dimension  $D_2$  is estimated. This model is written as:

$$\log N_2(r) = -D_2 \log r + c \qquad [2]$$

where  $c$  is constant.

The three-dimensional fractal dimension can be obtained in a similar way. In this case cubes of side  $r$  are considered, instead of squares (pixels).

The model for the 3-d fractal dimension is:

$$\log N_3(r) = -D_{s3} \log r + c \quad [3]$$

where  $c$  is a constant.

Measurement of  $D_{s3}$  necessitates three-dimensional image data, which requires vertical sampling, on horizontal cross sections, at an interval with adequate resolution. Pixel size was 1 mm in the case of the measurement using a digitizer. It is impossible to create such thin horizontal cross-sections. Therefore,  $D_{s3}$  was calculated by interpolating two dimensional image data measured on cross sections.

The value of  $D_{s3}$  can be obtained from the slope of the regression line for the double logarithmic relationship between the relative width of a cube with side ( $r$ ) and the number of cubes containing stains [ $N_3(r)$ ]. If  $N_3(r)$  is multiplied by the volume of a cube of side  $r$ , an approximation to the total volume of stained parts is obtained. When  $r = 1$ , the size of the smallest pixel, this approximates to the total volume.

The total volume is calculated by vertically integration of the products of depth and area of each cross-section, created after vertical interpolation. The area can be approximated as a product of  $N_2(r)$  and the area of a pixel of side  $r$ . The value of  $N_3(r)$  can be calculated from the integral of the interpolated values of  $N_2(r)$  at an interval of  $r$ .

The fractal dimension  $D_{s3}$  is determined from eqn [3].  $N_3(r)$  was estimated by linear interpolation in a vertical direction.

Hatano (1991) took  $D_{s2}$  values for dots, lines and planes as 0, 1 and 2, respectively.  $D_{s3}$  values for vertical straight lines, vertically extended planes and solid space are 1, 2 and 3, respectively. Furthermore, a horizontal section of an object, with  $D_{s3}$  in space, has a  $D_{s2}$  equal to  $D_{s3}-1$ .

## RESULTS AND DISCUSSION

### Bypass flow

Figure 1 shows measured outflow from cores. All outflow curves were well described by the spherical model, as goodness of fit was always higher than 0.98 (Table 1). Outflow from all cores started after a significant time lag from the start of irrigation.

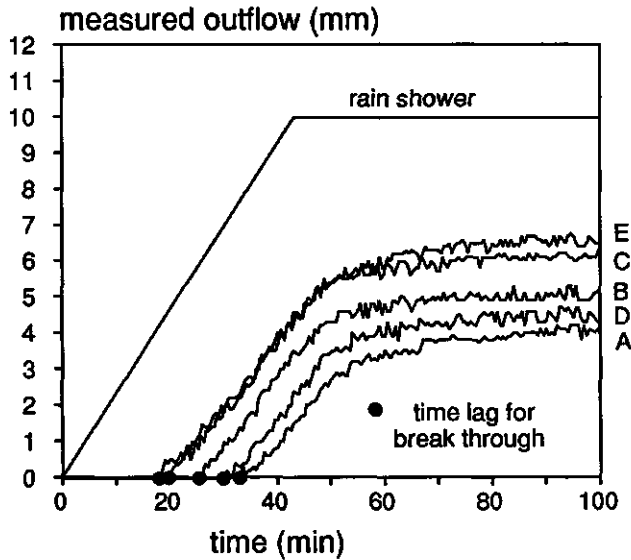


**Figure 1** Measured outflow curves for sample A,B,C,D, and E.

Outflow rates for each core, during irrigation of 40 minutes, were almost equal to the applied irrigation rate of  $13\text{mm}\cdot\text{hr}^{-1}$ . This implies bypass flow through vertically continuous macropores; absorption processes, surface infiltration and lateral absorption in these macropores have been minimal. As soon as irrigation ceased, outflow reduced remarkably and stopped after a few minutes.

Furthermore, the total amount of outflow ( $O_m$ ) which ranged from 4.0 to 6.5 mm can be represented as a function of time-lag ( $T_l$ ).

$$O_m = -0.181 T_l + 9.85 \quad [4]$$

with a correlation coefficient of 0.996. This indicates that the time-lag for outflow was induced by internal catchment (storage of water in vertically non-continuous macropores) and surface storage.

**Table 1** Values of the spherical model parameters (eqn. [1]) to describe outflow.

Sample	$O_m$ (mm)	$T_m$ (min)	$T_l$ (min)	Goodness of fit
A	4.02	44	32	0.99
B	5.01	37	26	0.98
C	6.07	44	21	0.99
D	4.34	36	31	0.98
E	6.54	54	19	0.99

### Fractal dimension of staining patterns

Figure 2 shows the vertical distribution of fractal dimensions in horizontal cross-sections ( $D_s$ ) through each soil core.  $D_s$  values for all cores and all depths ranged from 0.85 to 1.67. Analysis of variance showed that differences for individual curves were significant at the 5% level. To stress the significance for individual points, the least significant difference at a 5% level (LSD-5) has been added to Fig. 2.

As an example, relating  $D_s$  values to staining patterns, images of staining patterns of methylene blue in horizontal cross sections at depths of 45 mm and 110 mm in the cores of A, B and D are presented in Fig.3. Although three images at a depth of 45 mm in the cores of A, B and D have almost the same stained area, the staining pattern in core A is longer and more slender, the staining pattern in core B is more extensive and the staining pattern in core D is more crowded than the others.  $D_s$  values of 1.18 for A, 1.35 for B and 1.30 for D reflect the staining characteristics very well. Three images at a depth of 110 mm have smaller stained areas but show similar staining patterns; a long and slender pattern for core A, a fragmentary pattern for core B and an extensive pattern for core D. Their  $D_s$  values are 1.09, 1.02 and 1.67, respectively.



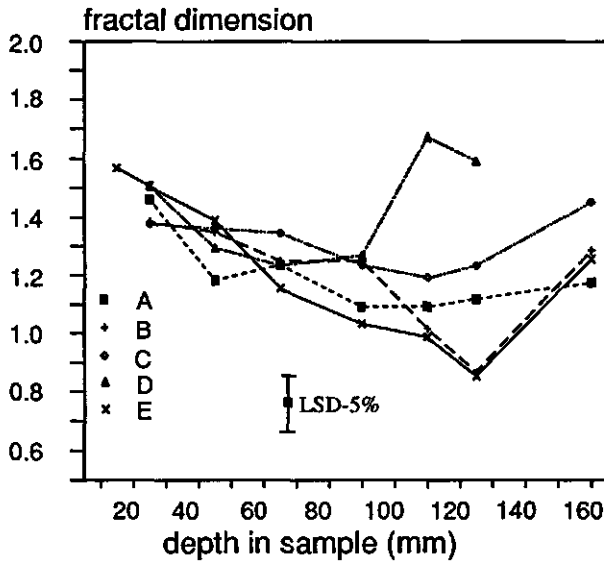


Figure 2 Vertical distribution of fractal dimensions for the two-dimensional structure of stains, observed in horizontal cross-sections in soil cores.

The average values of  $D_{s2}$  for the upper half (25 - 90 mm) and lower half (110 - 160 mm) of the core as well as for the whole core are shown in Table 2. Staining patterns in the upper half are relatively similar but those in the lower half vary considerably.

Considering this difference, the three-dimensional fractal dimension of structure ( $D_{s3}$ ) was calculated for the upper and lower halves of the core as well as for the whole core. Values of  $D_{s3}$  are given in Table 3. These values seem more or less equal to the averages of  $D_{s2}$  plus 1. However, there is significant disagreement in the values for the whole of core B and lower half of core B and the whole of core E and the upper half of core E.

If an object has an isotropic structure,  $D_{s3}$  equals  $D_{s2}+1$ .  $D_{s2}$  values and stained area, measured for the samples, however, varied with depth.  $D_{s3}$  values would, therefore, not strictly equal the sum of the depth average of  $D_{s2}$  plus 1. Samples B and E, which showed significant discrepancy between  $D_{s2}+1$  and  $D_{s3}$ , had relatively large variation in the vertical distribution of  $D_{s2}$  and the stained area. A better approximation of the depth average of  $D_{s2}$  is, therefore, given by  $D_{s3}-1$ ,

which incorporates the effect of an anisotropic structure.  $D_{3-1}$  was, therefore, used to characterize outflow from the cores.

**Table 2** *Two-dimensional fractal dimensions of staining patterns ( $D_2$ ) in horizontal cross-sections.*

Sample	Whole column	Upper column	Lower column	Number of data points	Goodness of fit
A	1.19	1.24	1.13	6	0.99
B	1.20	1.31	1.06	6	0.99
C	1.31	1.33	1.29	6	0.99
D	1.43	1.33	1.63	6	0.99
E	1.17	1.27	1.03	6	0.99

**Table 3** *Three-dimensional fractal dimensions of staining patterns ( $D_3$ ).*

Sample	Whole column	Upper column	Lower column
A	2.27	2.29	2.08
B	2.32	2.36	2.20
C	2.33	2.39	2.28
D	2.39	2.38	2.58
E	2.42	2.43	2.04

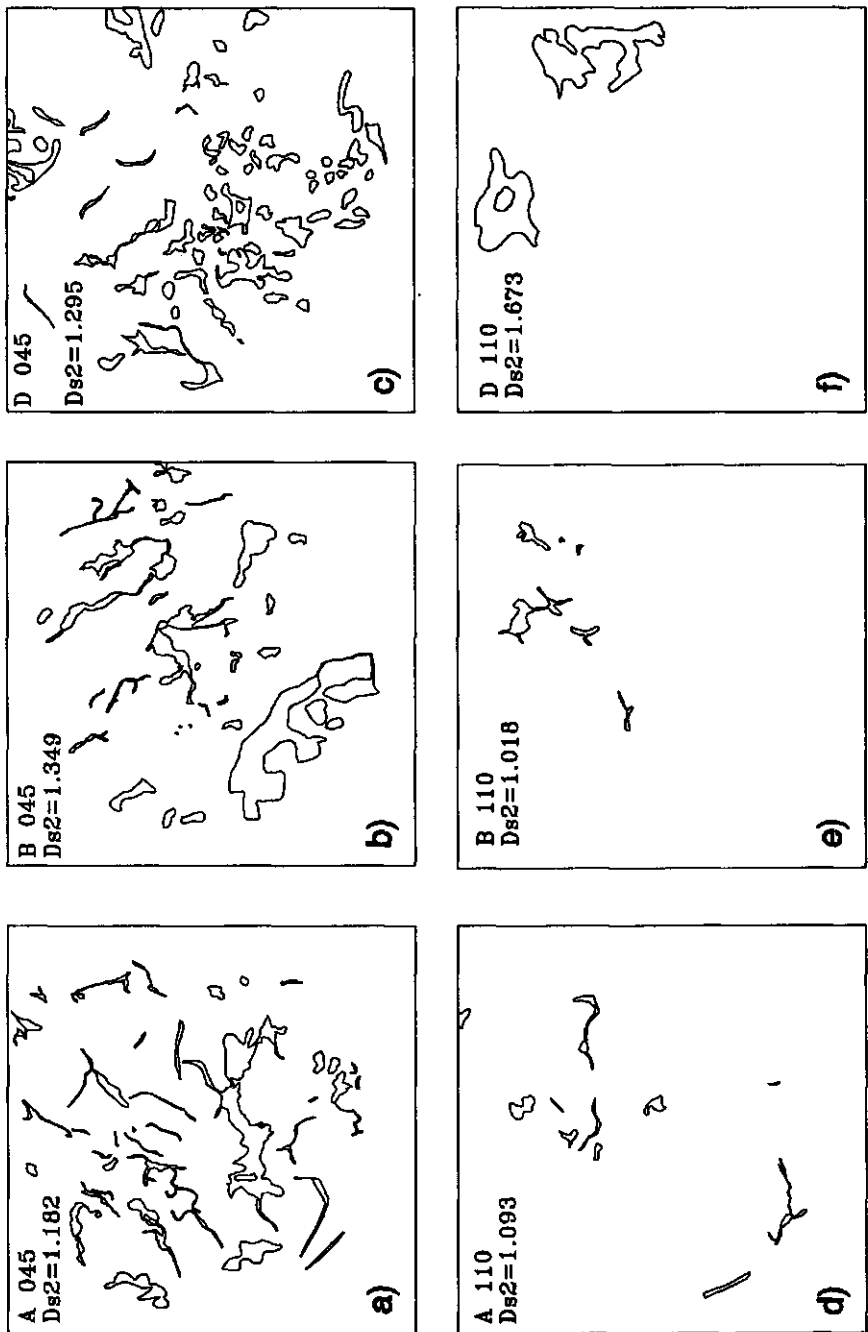


Figure 3 Some typical examples of staining patterns in horizontal cross-sections in soil cores at depths of 45 mm (a-c) and 110 mm (d-f), respectively.

**Fractal dimension and bypass flow**

The total amount of outflow ( $O_m$ , Table 1) controlled by bypass flow, can be represented as a function of time lag ( $T_l$ , Table 1), caused by the effect of the internal catchment and surface storage. On the other hand, morphological data on staining patterns can be regarded as a result of both bypass flow and internal catchment. The volume fraction of staining ( $V_s$ ) is, therefore, important in explaining bypass flow and internal catchment.  $V_s$  was obtained from the number of the smallest unit cubes [N3(1)]. Values of  $V_s$  for the upper and lower half of the core as well as for the whole core are summarized in Table 4.

**Table 4** *The volumetric fraction of stained parts in soil core ( $V_s$ )*

Sample	Whole column	Upper column	Lower column
A	0.037	0.087	0.007
B	0.035	0.083	0.003
C	0.048	0.090	0.021
D	0.046	0.098	0.037
E	0.032	0.085	0.004

Table 5 shows the results of some trials to explain the total amount of outflow. Although there is no direct physical relationships between  $O_m$  and  $V_s$ ,  $V_s$  and  $D_s^{3-1}$ , for the upper half of core, can explain the amount of outflow. The equation is:

$$O_m = 187.1 V_s D_s^{3-1} + 12.0 \quad [5]$$

with a correlation coefficient of 0.894, which is significant at a 5% confidence level. The shape of this equation indicates that smaller values  $V_s$  and greater value of  $D_s^{3-1}$  increased the total amount of outflow.  $D_s^{3-1}$  is the depth-weighted average of  $D_s^2$ , indicating that a two-dimensional structure is able to describe outflow.

The amount of outflow cannot be explained by using only morphological data for the lower half of the core. However, data for both data the upper and lower

halves of the core used in a multiple regression analysis gave with a correlation coefficient of 0.995 which is significant at a 1% confidence level. This equation is:

$$O_m = -230.6(V_s D_s^{3-1})_u + 232.4(V_s D_s^{3-1})_l + 12.6 \quad [6]$$

where subscripts u and l represent the upper and lower halves of the core, respectively. Both regression coefficients were statistically significant at the 1% level.

The shape of this equation indicates that the contribution, of staining patterns in the lower half of the cores, to bypass flow differs to that in the upper half of core; that is, greater values of  $V_s$  and smaller values  $D_s$  in the lower half of the column increase the total amount of outflow. A physical morphological explanation for this phenomenon is that stains in the upper half of the cores develop around relatively small pedes and are mostly not continuous. In the lower half, where the number of stains has been sharply decreased, only vertical continuous macropores, which dominate bypass flow, remain. This tendency was also found by Hatano et al. (1992).

**Table 5.** *Examples to explain the amount of outflow ( $O_m$ , Table 1) by using the fractal dimension ( $D_s$ , Table 2) and the volumetric fraction of stained parts ( $V_s$ , Table 3). Subscripts of u and l represent the upper and lower half of core.*

Equation	Correlation coefficient
$O_m = -62.1 V_{su} + 10.7$	0.340
$O_m = -19.8 V_{sl} + 5.5$	0.262
$O_m = -187.1 (V_s^{D_s^{3-1}})_u + 12.0$	0.894*
$O_m = 16.2 (V_s^{D_s^{3-1}})_l + 5.1$	0.033
$O_m = -4.6 V_{su} + 1.7 V_{sl} + 43.7$	0.516
$O_m = -230.6 (V_s^{D_s^{3-1}})_u + 232.4 (V_s^{D_s^{3-1}})_l + 12.6$	0.995**

Subscripts of \* and \*\* represent that the equation is significant at 5% and 1% levels, respectively.

## CONCLUSIONS

This study shows that morphology of flowpaths is an important factor in prediction of bypass flow. Methylene blue is useful as a tracer to define flow paths. The fractal analysis shown in this paper can simplify the complex interpretation of staining patterns in terms of fractal dimensions of structure, such as dots, lines, planes and their intermediate structures. A regression analysis of, the relationship between bypass flow and fractal dimension, showed that the depth weighted average of the fractal dimension of a two-dimensional structure is a useful tool to describe outflow. In the upper half of the soil cores, flow paths with greater fractal dimensions were derived from interpedal macropores developed around relatively small peds; in the lower half, flow paths with smaller fractal dimension, derived from fragments of cracks, contributed to greater bypass flow. Macropores whose vertical continuity is dominant induce significant bypass flow.

## ACKNOWLEDGEMENT

The authors are indebted to Professor Dr. J. Bouma (Wageningen Agricultural University) for many helpful suggestions. R. Hatano acknowledges a travel grant from the Ministry of Education, Science and Culture of Japan. This study was funded partly by the EC project STEP-0032-C.

## REFERENCES

- Booltink, H.W.G. and Bouma, J., 1991. *Physical and morphological characterization of bypass flow in a well-structured clay soil. Soil Sci. Soc. Am. J.* 55:1249-1254.
- Bouma, J., 1984. *Using soil morphology to develop measurement methods and simulation techniques for water movement in heavy clay soils. In: J. Bouma and P.A.C. Raats (eds.), Water and Solute Movement in Heavy Clay Soils. Int. Soc. Soil Science (ISSS) Symp. Inst. Land Reclamation and Irrigation (ILRI), Wageningen, the Netherlands. Publ. No. 37, pp. 298-316.*
- Buishands, T.A. and Velds, C.A., 1980. *Neerslag en verdamping. Climate in the Netherlands. Royal Dutch Meteorological Institute De Bilt, the Netherlands, pp 115-118 (in Dutch).*
- Davis, J.C., 1986. *Statistics and data analysis in geology. 2nd edn. Wiley, Singapore. pp 246-248.*
- Hatano, R., Kawamura, N., Ikeda, J. and Sakuma, T. 1992. *Evaluation of the effect of the morphological features of flow paths on solute transport by using fractal dimensions of methylene blue staining pattern. Geoderma, 53:31-44.*
- Lauren, J.G., Wagenet, R.J., Bouma, J. and Wösten, J.H.M., 1988. *Variability of saturated hydraulic conductivity in a Glossaquic Hapludalf with macropores. Soil Sci. 145: 20-28.*
- Soil Survey Staff. 1975. *Soil Taxonomy; a basic system of classification for making and interpreting soil surveys. SCS-USDA, Government printing office, Washington DC, Agricultural Handbook, No. 436, 754pp.*
- Van Stiphout, T.P.J., Van Lanen, H.A.J., Boersma, O.H. and Bouma, J., 1987. *The effect of bypass flow and internal catchment of rain on the water regime in clay loam grassland. J. Hydrology, 95:1-11.*
- White, R.E., 1985. *The influence of macropores on the transport of dissolved and suspended matter through soil. Adv. Soil Sci. 3:95-120.*

## CHAPTER 6

# MEASUREMENT AND SIMULATION OF BYPASS FLOW IN A STRUCTURED CLAY SOIL: A PHYSICO-MORPHOLOGICAL APPROACH

Published in: *Journal of Hydrology* volume 148  
page 149-168



# MEASUREMENT AND SIMULATION OF BYPASS FLOW IN A STRUCTURED CLAY SOIL: A PHYSICO-MORPHOLOGICAL APPROACH

H.W.G. Booltink<sup>1</sup>, R. Hatano<sup>2</sup> and J. Bouma<sup>1</sup>

1) *Department of Soil Science & Geology, Agricultural University, Wageningen, The Netherlands.*

2) *Faculty of Agriculture, Hokkaido University, Sapporo, Japan*

## ABSTRACT

Water flow in structured clay soils is strongly influenced by the presence and geometry of macropores. This study was conducted to develop a method which could measure bypass flow, provide a morphological analysis of the water-conducting macropore system, and combine physical and morphological data in a simulation model for prediction purposes. The effects of different physical boundary conditions on bypass flow, such as rain intensity, the conductivity of the soil, soil micro relief and initial pressure head in the soil, were tested with a computer controlled measuring device. Measurements were carried out on large undisturbed soil cylinders in the laboratory. Macropore geometry was subsequently characterized by using fractal dimensions of staining patterns on horizontal cross sections and was a very important parameter to explain the measured outflow. A pedotransfer function, based on this geometry, was used to calculate the time of initial breakthrough at the bottom of the soil cylinders. This pedotransfer function was then used in a computer model which simulated bypass flow successfully in fifteen large soil columns. Total amount of outflow was not directly influenced by rain intensity but more by the amount of rain applied.

## INTRODUCTION

Bypass flow has been defined as the flow of free water along macropores into and through an unsaturated soil matrix (Bouma, 1984). Occurrence of free water and unsaturated soil at the same depth in a soil, cannot be described by classical one-dimensional flow theory which defines a particular water content for any given depth at any given time. Bypass flow occurs widely in the field when water infiltrates into open macropores in dry or moist soil (e.g. Beven and Germann, 1982; White, 1985). Increased concern for water use efficiency during irrigation and deep penetration of pollutants leads to the necessity to characterize bypass flow in quantitative terms. Bouma et al. (1981) presented a simple field method to measure bypass flow. The method, however, did not utilize rigid instrumentation.

Different approaches for simulating bypass flow have been developed but a generally acceptable model is not yet available. Germann and Beven (1985) and Germann (1990) applied kinematic wave theory in combination with a sink term to describe macropore flow and sorption of water in the surrounding soil. A system of uniformly distributed channels with different widths and depths was used by Beven and Clark (1986). Chen and Wagenet (1992) simulated water and chemical transport by combining the Richard's equation for transport in the soil domain in combination with the Hagen-Poiseuille and Chezy-Manning equations for macropore transport. Hatano and Sakuma (1991) designed a plate model to simulate transport of water and solutes in an aggregated soil. They distinguished a mobile, immobile and a mixing phase for water and chemical interactions.

In all these models real soil structure, defined as the physical constitution of a soil material, as expressed by the size, shape, and arrangement of the elementary particles and voids, is not considered as a starting point. Bronswijk (1988) and Jarvis and Leeds (1987,1990) define sizes and continuities of macropores as determined by the swelling and shrinkage characteristics of the soil matrix rather than by observations of the macropores themselves. Hoogmoed and Bouma (1980) developed a model based on soil morphology, describing surface storage and lateral absorption of water and drainage. Although this model is based on soil morphological observations it does, however, not include the effects of tortuous water transport through macropores.

Bouma et al. (1977) and Ringrose-Voase and Bullock (1984) developed a technique for measuring macropores in undisturbed soil, by using methylene blue staining patterns. They stratified macropores into categories of channels, vughs and planar voids and discussed functional physical properties of different types of macropores in descriptive, qualitative terms.

Fractal theory is a useful tool for the quantitative characterization of macropore systems. Bartoli et al. (1991) used fractal dimensions to characterize soil structure. Crawford et al. (1993) used fractal and fracton dimensions to explain diffusion processes in heterogenous soils. Hatano and Booltink (1992) used fractal dimensions of stained flow patterns to predict cumulative amounts of bypass flow.

This manuscript describes a general method for measuring and simulating bypass flow in soils with macropores. The use of large, undisturbed field samples in which functional macropores are stained is emphasized.

## MATERIALS AND METHODS

### Soil

Fifteen soil samples were taken, close to each other in a regular grid of 0.5 m, in steel cylinders (0.20 m diameter by 0.20 m length), at the Kandelaar Experimental farm in Eastern Flevoland in the Netherlands. Sampling was carried out by pressing the cylinders slowly into the soil using a hydraulic sampling device (Eijkelpamp Agrisearch Equipment, The Netherlands). The cylinders had sharpened lower edges and the inside cylinder wall was covered with grease to avoid boundary flow along the cylinder wall.

Ten soil samples with a volume of  $3.0 \times 10^{-4} \text{ m}^3$  were taken at the same location for the determination of the soil hydraulic conductivity and retentivity curves using the one-step outflow method (Doering, 1965; Kool and Parker, 1987; Booltink et al., 1991b) and 2 additional steel cylinders (0.20 m length and diameter for the suction crust infiltrometer (Booltink et al., 1991a).

The soil was classified as a mixed mesic Hydric Fluvaquent (Soil Survey Staff, 1975), with the following horizons:  $A_p$  (0.0-0.30 m), clay (42% clay) with a moderate, medium angular blocky structure and an abrupt wavy boundary; 2C (0.30-0.70 m), clay loam (40% clay), strong, very coarse prismatic structure; 3C

(0.70-1.03 m), silty clay loam (30% clay), strong, very coarse prismatic structure; and 4BCb (1.03-1.20 m), sand, single grain. The macropores present were mainly interpedal planar voids.

Soil samples were taken at a depth of 0.15 m, since this appeared to be the most restrictive layer (Booltink and Bouma, 1991). The volume of the natural soil peds was estimated to be approximately  $2.0 \times 10^{-5} \text{ m}^3$ . About 300 peds were, therefore, present in the samples of  $6.0 \times 10^{-3} \text{ m}^3$ . Samples can therefore be considered to be representative for the soil being studied (Lauren et al., 1988).

### Experimental set up

The experimental laboratory set up is shown in Fig. 1. Soil samples were placed on a funnel connected to an outflow collector equipped with a pressure transducer. To prevent erosion of the sample, a disk, perforated with approximately 75,  $2.0 \times 10^{-3} \text{ m}$  holes, was placed at the bottom. Rain showers of  $1.5 \times 10^{-2} \text{ m}$  were applied on top of the soil samples by using a small rain simulator, consisting of an adjustable tube pump and a needle irrigator. Rain intensities applied on the soil samples were:  $2.778 \times 10^{-6}$  (2 samples),  $5.556 \times 10^{-6}$ ,  $8.333 \times 10^{-6}$  (each 5 samples) and  $11.11 \times 10^{-6} \text{ m.s}^{-1}$  (3 samples). All intensities induced bypass flow in this type of soil.

Two tensiometers were installed, one at the top and one at the bottom of the sample. These tensiometers provide information on: (i) the initial pressure head in the soil; (ii) the time when water starts to infiltrate in macropores (top tensiometer) and (iii) the hydraulic conditions at the bottom of the soil column. Installation of the tensiometer cups should be carried out at a slightly upward angle to prevent water flow from macropores into the cavity in which the cups are placed. Tensiometers should be sufficiently large to represent hydraulic soil conditions adequately and were  $5.0 \times 10^{-2} \text{ m}$  long with a diameter of  $0.5 \times 10^{-2} \text{ m}$ . All measurements were controlled by a computer, equipped with a 14 bit 16 channel analog-digital convertor. The measurement interval is flexible with a minimum of 5 s. Output was shown graphically on the screen and stored in a file.

To measure breakthrough curves and/or adsorption of chemical species the basic set up can be extended easily with, for example, a specific ion electrode or a spectrophotometer.

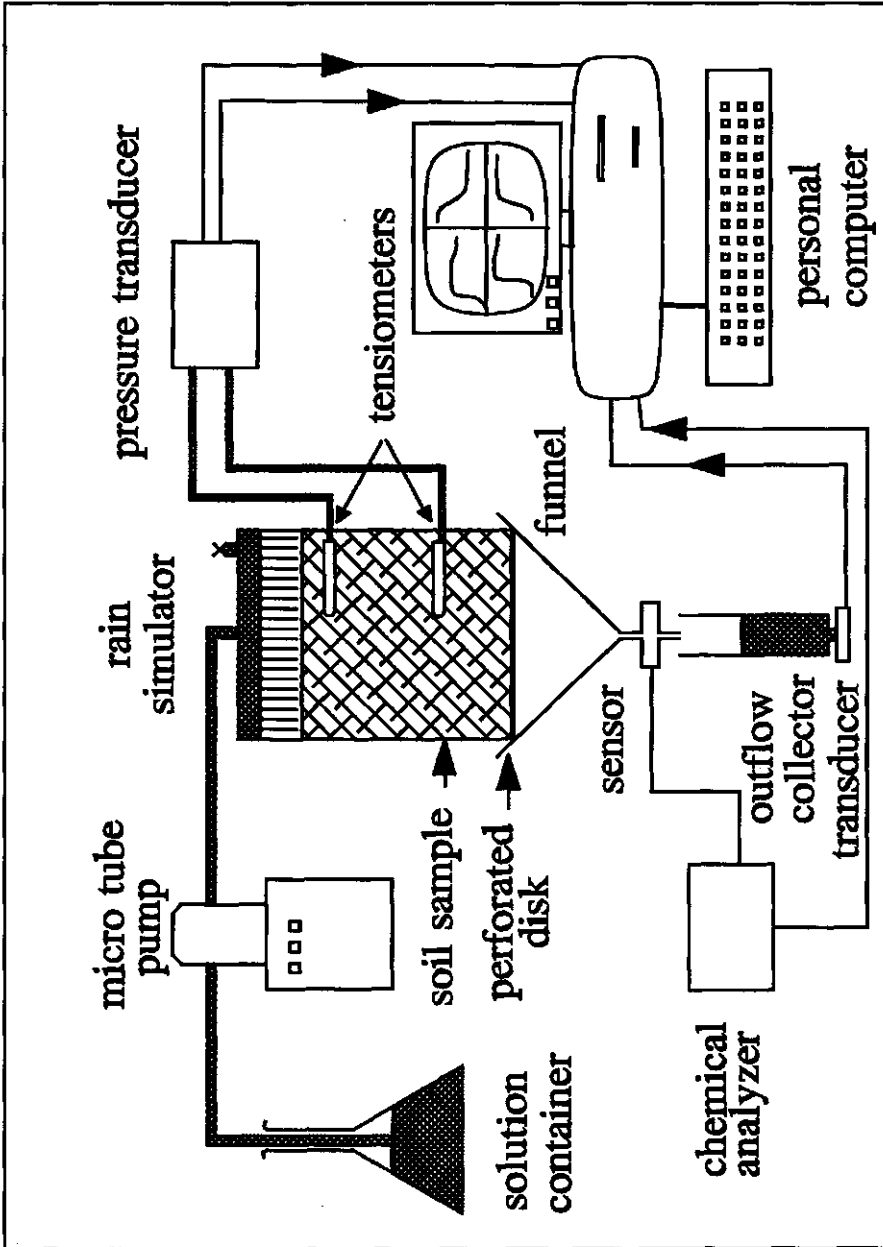


**Figure 1** Schematical set up of the computer controlled device for measuring bypass flow.

**Morphological methods**

Before starting the experiment the soil surface was exposed carefully by chipping away soil aggregates, in order to create an undisturbed, natural infiltration surface.

Water applied on top of the sample contained 0.01 molar methylene blue.

After the experiment, the sample was peeled off in layers of  $2.0 \times 10^{-2}$  m thickness. The methylene blue patterns were photographed and later analyzed by an image analyzer (Nexus 6400). The areas and perimeters of all individual stains were calculated directly by the Nexus. The bitmaps produced by the image analyzer were used for further analyses. The 2-D fractal dimensions of the staining patterns were determined by the so called box counting procedure (Hatano et al., 1992). Three dimensional fractal dimensions (Ds3) and the total volume of stained patterns (Vs) were calculated by vertical integration of the 2-D data, measured on cross sections (Hatano and Booltink 1992).

The criteria for the ratio between area and perimeter ( $A/Pe^2 < 0.015$ ), as described by Bouma et al. (1977), were used to stratify staining patterns in terms of vertical cracks and horizontal pedfaces of structure elements.

Area of the cracks was calculated following equation [1]:

$$A = \sum_{j=1}^{10} \sum_{i=1}^n \Delta Z * Pe \tag{1}$$

In which A is the total sample area of the vertical cracks, j and i are respectively the layer number and stain number,  $\Delta Z$  segment thickness and Pe the perimeter of the stain.

The incorporation of measured soil geometrical characteristics, such as fractal dimensions, in existing deterministic simulation models can be facilitated by the use of pedotransfer functions which relate easily obtainable soil characteristics to more complex ones (Bouma and Van Lanen, 1986). Analysis of the data obtained in this experiment augmented by data from previous experiments (Booltink and Bouma, 1991), and suggested that the time lag for initial breakthrough at the bottom of the soil column,  $T_{(d)}$ , could be estimated with a linear regression equation containing the parameters  $V_{s1}$  (the volume stained at the lower part of soil column) and  $Ds_{3-1}$  (the depth weighted fractal dimension of the lower part of the soil samples).

Thus:

$$\frac{1}{T_{(d)}} = a * \left[ \frac{Vs_l}{100} \right]^{(Ds3 - 1)} + b \quad [2]$$

Parameters a and b in equation [2] are empirical constants.

High values of  $Vs_l$ , are an indication of either a large number of small macropores, or a few big water conducting macropores, will lead to a reduction of  $T_{(d)}$ . The fractal dimension on the other hand gives information on the geometry of water conducting macropores. A macropore system with a  $Ds3$  value of 2 consists of mainly vertically oriented cracks; a value of 3 on the other hand indicates that horizontal cracks dominate the system (Hatano and Booltink (1992)).

The value of  $T_{(d)}$ , computed with eq. [2], was used to calculate the propagation of the waterfront in macropores.

### Simulation model

A quasi- three dimensional simulation model, used by Hoogmoed and Bouma (1980), was applied to quantify flow processes during bypass flow. Processes considered are:

A. Vertical infiltration of water in the upper soil surface and water flow between underlying layers, simulated with the Darcy equation [3].

$$z=0 \quad -K \delta H / \delta z = R \quad 0 < T < T(p) \quad [3a]$$

$$0 < H < w \quad T(p) \leq T \leq T(c) \quad [3b]$$

$$H = w \quad T > T(c) \quad [3c]$$

$$z=20 \quad -K \delta H / \delta z = \text{constant} \quad [3d]$$

where  $z$  = depth (m) below the top of the soil,  $T_{(p)}$  = time (s) when ponding starts,  $T_{(c)}$  = time when water enters the macropores,  $w$  = surface storage (m),  $R$  = rain intensity ( $m.s^{-1}$ ), and  $H$  = hydraulic head (m water).

- B. Flow of water in macropores when a threshold value for surface storage is reached.
- C. Lateral absorption of water into vertical crack walls (Van der Ploeg and Benecke, 1974) [4].

$$T > T_{(c+lag)} \quad 0 < x \leq x_t \quad \frac{\delta}{\delta x} \left[ D \frac{\delta \theta}{\delta x} \right] = \frac{\delta \theta}{\delta t} \quad [4a]$$

With the following boundary conditions:

$$T > T_{(c+lag)} \quad x = 0 \quad \frac{\delta \theta}{\delta x} = 0 \quad [4b]$$

$$T > T_{(c+lag)} \quad x > x_t \quad \frac{\delta \theta}{\delta x} = 0 \quad [4c]$$

Where  $x$  = horizontal distance (m) from the infiltration surface,  $\theta$  = moisture content,  $x_t$  = penetration depth of the wetting front at time  $t$ ,  $lag$  is the time lag between  $T_{(c)}$  and the arrival of the wetting front at depth  $z$ , and  $D$  is the diffusivity -  $\theta$  relation.

- D. Water not absorbed at the bottom of the soil column was calculated as drainage.

An extended model description was provided by Hoogmoed and Bouma (1980), Van der Ploeg and Benecke (1974), and Bootink and Bouma (1992).

To improve the description of the bypass flow processes, some model modifications were made:

1. At the start of a bypass flow event not all the vertical macropores are instantly available for conducting water due to surface roughness. The accessibility of macropores at the soil surface was proportionally divided between a minimum and a maximum threshold value for surface storage, as derived from visual observations.



2. Lateral water absorption in vertical continuous macropores is based on absorption described by a diffusivity equation (eq. [4]). Vertical water absorption on the horizontal pedfaces of structure elements inside the soil is, however, largely dominated by gravity forces, described by the Darcy equation (eq. [3]). To simulate this latter process a module which calculates a Darcy subsurface infiltration similar to the infiltration of water into the upper soil surface was added.
3. The model of Hoogmoed and Bouma did not consider the effects of tortuous water transport in terms of absorption and breakthrough. They assumed cracks to be vertically continuous and straight. Water running into such cracks, exits very rapidly. In reality pathways are tortuous. The pedotransfer function (eq. [2]) for estimating the time lag for initial breakthrough was incorporated in the model and used to calculate the rate of propagation of the waterfront in macropores.

In summary, inputs of the model are: retentivity, conductivity and diffusivity curves; initial moisture content; the applied rain amount and intensity; surface storage of ponded water; and the surface area and fractal dimensions of methylene blue staining patterns in the sample, indicating areas where infiltration into the soil matrix can occur.

To test model performance in relation to the pedotransfer function, three series of simulations were carried out: (i) the time lag for initial breakthrough calculated according the developed pedotransfer function, was used as model input and simulation results were compared with measurements. (ii) To check the quality and sensitivity of the pedotransfer function independently an independent data set of 4 randomly selected samples, 1 sample for each rain intensity, was created from the original data base of 20 samples (15 from this experiment and 5 from previous experiments, (Booltink and Bouma, 1991), and the pedotransfer function was calculated for the remaining 16 samples. Subsequently the time lag for initial breakthrough was estimated by this new equation and used to simulate data for the 4 randomly selected soil columns, and (iii) simulated amounts of outflow, using time lags calculated with the pedotransfer function, were compared with simulations performed with measured time lags.

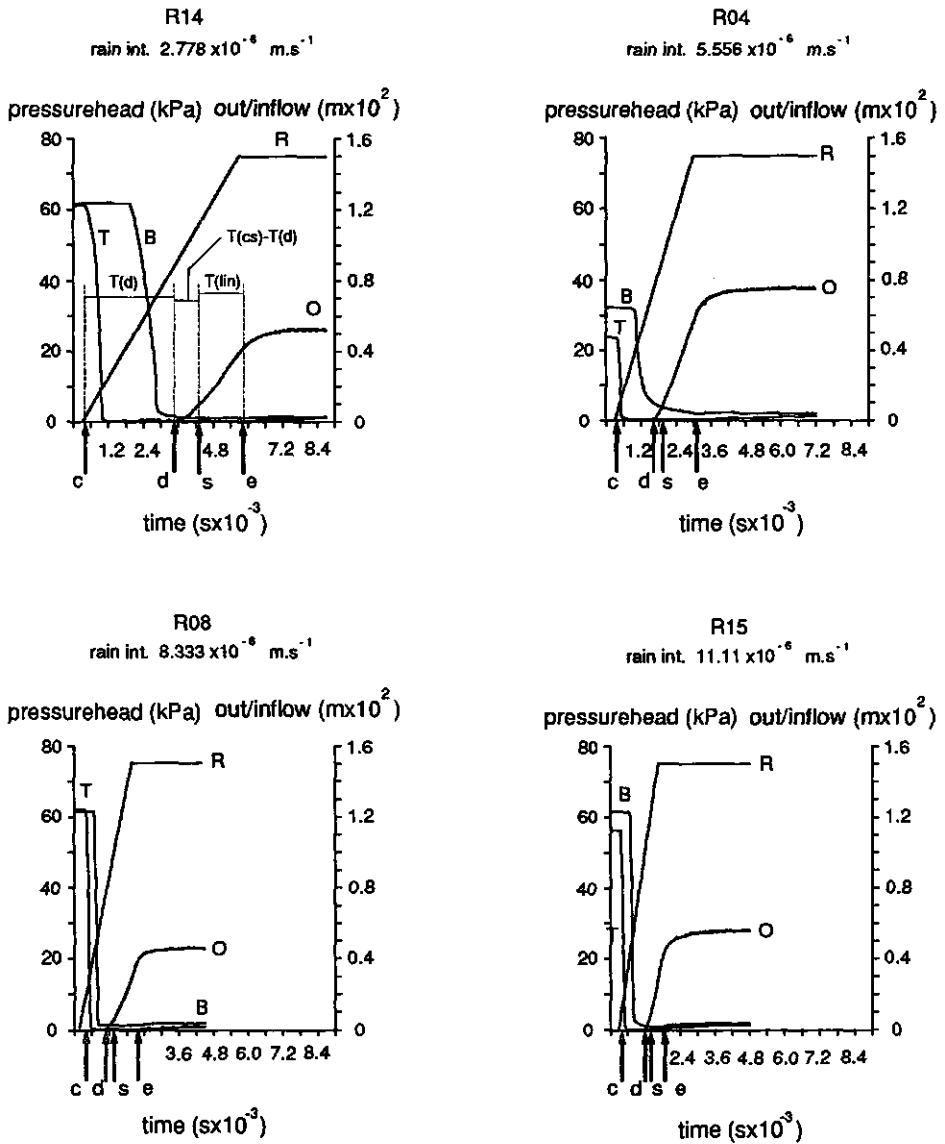


**Figure 2** Results of measurements for 4 different rain intensities. Arrows indicate characteristic points in time: c refers to start of water entering the macropores ( $T_{(c)}$ ), d to the point of initial breakthrough ( $T_{(d)}$ ), s to the starting point of the linear outflow ( $T_{(cs)}$ ), and e to the end point of linear outflow ( $T_{(ce)}$ ). B and T are referring to the bottom and top tensiometer respectively. R refers to the cumulative rain applied and O the cumulative outflow.

## RESULTS AND INTERPRETATIONS

### Morphological

The area and number of pores decreased with depth for the first 0.1 m in the soil sample. For the lower 0.1 m, area and number of pores were more or less constant. The boundary, which equals 0.25 m depth in the field soil profile, coincides more or less with the depth of the plough layer in the field. The upper and lower part of the columns have, therefore, been considered separately in further analyses.

Table 1 shows stained volumes and fractal dimensions for all 15 samples.

The total volume stained averaged 5.10% of the sample volume ( $\sigma=1.74\%$ ) which equals  $3.00 \times 10^{-4} \text{ m}^3$ . Except for sample R17, the stained volume at the lower part of the cores is only a small fraction of the total volume. Average fractal dimensions of stains in the upper part of the columns were 2.28 compared with 2.01 for the lower part. This indicates that, in the upper part, relatively more horizontal pedfaces are present, whereas in the lower part, the system is dominated by vertically continuous cracks.

The total area of horizontal pedfaces and vertical cracks are presented in table 1. Values were based on average structure element sizes of  $2.0 \times 10^{-5} \text{ m}^3$ . Except for sample R06, where horizontal cracks are the main macropores, the macropore system is dominated by vertical cracks.

### Physical

Figure 2 shows the experimental results of 4 representative samples with rain intensities of  $2.778 \times 10^{-6}$ ,  $5.556 \times 10^{-6}$ ,  $8.333 \times 10^{-6}$  and  $11.11 \times 10^{-6} \text{ m.s}^{-1}$  respectively. For all experiments, irrigation was started after monitoring initial conditions for 300 s and was continued until  $1.5 \times 10^{-2} \text{ m}$  of water was applied. The top tensiometers all react within a few minutes of irrigation starting, indicating that water has entered the macropores. After the experiment, this was confirmed by the presence of methylene blue stains on the cups. These top tensiometers provide, therefore, reliable information on the time  $T_{(c)}$ , expressed in seconds after starting the rain shower, when water enters the macropores. The time intervals (T) were determined by scanning the computer measured output file (measuring interval 5 s.)

## Morphometric methods for simulation of water flow

**Table 1** *Morphological results. Ds<sub>3</sub> refers to the 3-D fractal dimension; the subscripts u, l refer to the upper and lower parts of the soil cores, respectively, while the subscript w indicates the whole core; V<sub>s</sub> (%) is the stained volume, Ver. C. (m<sup>2</sup>x10<sup>4</sup>) the total area of vertical cracks (eq. [1]), and Hor. pedf. (m<sup>2</sup>x10<sup>4</sup>) the total area of horizontal pedfaces (Bouma et al., 1977).*

Sample	V <sub>s<sub>u</sub></sub> (%)	V <sub>s<sub>l</sub></sub> (%)	V <sub>s<sub>w</sub></sub> (%)	Ds <sub>3<sub>u</sub></sub> (-)	Ds <sub>3<sub>l</sub></sub> (-)	Ds <sub>3<sub>w</sub></sub> (-)	Ver.C. (m <sup>2</sup> x10 <sup>4</sup> )	Hor. Pedf. (m <sup>2</sup> x10 <sup>4</sup> )
<hr/> $2.778 \times 10^{-6} \text{ m.s}^{-1}$ <hr/>								
R13	6.522	0.188	3.884	2.261	1.74	2.239	1099	47
R14	3.569	0.161	2.161	2.069	1.90	2.067	401	37
<hr/> $5.556 \times 10^{-6} \text{ m.s}^{-1}$ <hr/>								
R03	7.481	0.261	4.491	2.246	1.947	2.231	756	59
R04	8.866	0.326	5.260	2.345	2.048	2.334	1079	48
R05	11.990	0.986	7.374	2.425	2.016	2.380	1420	52
R06	3.044	0.584	2.075	2.201	2.001	2.160	380	452
R07	11.240	0.132	6.605	2.356	2.226	2.351	1250	48
<hr/> $8.333 \times 10^{-6} \text{ m.s}^{-1}$ <hr/>								
R08	9.752	2.121	6.532	2.355	1.992	2.284	1216	66
R09	8.055	0.958	5.066	2.291	1.901	2.236	900	52
R10	6.050	1.515	4.053	2.180	2.062	2.145	774	53
R11	10.640	0.756	6.491	2.287	1.910	2.250	1581	63
R12	7.113	0.925	4.502	2.224	1.845	2.163	823	47
<hr/> $11.11 \times 10^{-6} \text{ m.s}^{-1}$ <hr/>								
R15	8.363	2.069	5.980	2.377	2.162	2.333	1079	50
R16	6.077	1.320	4.031	2.300	2.010	2.247	807	54
R17	7.301	7.906	7.951	2.208	2.274	2.233	1715	105

The bottom tensiometers show a behaviour which is related to rain intensity. The verification of methylene blue stains on the bottom cups was positive in only a few cases, which makes the use of these cups very limited.

The cumulative outflow curves as measured, all show identical behaviour. After the point when outflow starts,  $T_{(d)}$ ; an exponential progression between the times  $T_{(d)}$  and  $T_{(cs)}$  (start of linear outflow) can be seen. Between  $T_{(cs)}$  and  $T_{(ce)}$  (end of linear outflow) there is a nearly linear outflow pattern, and after  $T_{(ce)}$  an

exponential fade out pattern is shown. T values are expressed in seconds after starting the rain shower. The five elements constituting bypass flow will now be discussed separately:

#### *A. Surface storage*

When rain intensity exceeds the infiltration capacity of the soil matrix, a water layer starts to build up on the soil surface. The thickness of this water layer, surface storage, is highly variable due to the roughness of the soil surface and can, therefore, not be measured directly.

A minimum and a maximum surface storage is distinguished. The minimum value indicates when the very first macropore starts to conduct water and can be derived from the tensiometer reaction in the top of the sample. Infiltration until the start of macropore flow was calculated by using the two-parameter infiltration equation as developed by Stroosnijder (1976). Minimum surface storage can now be calculated by subtracting the infiltrated amount of water from the applied amount (table 2). By following this procedure for all cores, the amounts of surface storage calculated, for all samples averaged  $0.74 \times 10^{-3}$  m with a standard deviation of  $0.30 \times 10^{-3}$  m water.

The minimum surface storage is an important boundary condition in the entire bypass flow process, as it determines the time of incipient bypass flow and the amount of water which infiltrates at the soil surface after cessation of bypass flow.

Since not all the macropores present start to conduct water after  $T_{(c)}$ , we also defined a maximum surface storage, i.e. the level of ponding at which all macropores, accessible for bypass flow, conduct water. No direct measurements for this parameter were carried out during the experiment. An estimate can be made by determining the amount of water leaving the soil column after the rain shower has stopped. This water represents the amount of water still present on the soil surface and in the macropores. For these experiments maximum surface storage average  $2.67 \times 10^{-3}$  m, standard deviation  $0.62 \times 10^{-3}$  m. This value agreed fairly well with visual observations during the experiments.

#### *B. Initial breakthrough*

The time of initial breakthrough [ $T_{(d)}$ ], at the bottom of the soil cylinder, is related strongly to the applied rain intensity. However, the rather large variation

**Morphometric methods for simulation of water flow**

between  $T_{(d)}$  values within one rain intensity, e.g. sample R08 and sample R11 (table 2) indicates that geometry of the water conducting macropores is an important variable in the flow process.

**Table 2** *Physical results.  $T_{(d)}$  refers to the time of initial breakthrough,  $T_{(cs)}-T_{(d)}$  represents the duration of the exponential start of outflow (ESO), and  $O/I_i$  is the outflow rate expressed as a fraction of the inflow rate.  $T$  values are expressed in seconds after starting the rain shower.*

Sample	minimum surf. stor ( $m \times 10^2$ )	maximum surf. stor ( $m \times 10^2$ )	$T_{(d)}$ ( $s \times 10^2$ )	$T_{(cs)}-T_{(d)}$ ( $s \times 10^2$ )	ESO ( $m \times 10^2$ )	$O/I_i$ (-)	Total outflow ( $m \times 10^2$ )
$2.778 \times 10^{-6} \text{ m.s}^{-1}$							
R13	0.117	0.237	22.98	22.62	0.217	0.67	0.51
R14	0.039	0.169	31.98	8.82	0.124	0.74	0.52
$5.556 \times 10^{-6} \text{ m.s}^{-1}$							
R03	0.089	0.279	15.12	5.88	0.082	0.69	0.50
R04	0.039	0.209	12.30	3.90	0.067	0.78	0.75
R05	0.078	0.308	15.78	3.12	0.036	0.77	0.62
R06	0.056	0.146	15.72	8.88	0.051	0.39	0.22
R07	0.100	0.340	19.80	1.56	0.046	0.70	0.52
$8.333 \times 10^{-6} \text{ m.s}^{-1}$							
R08	0.084	0.314	5.88	6.12	0.100	0.56	0.47
R09	0.034	0.234	7.98	2.82	0.055	0.71	0.66
R10	0.067	0.317	4.08	10.02	0.133	0.84	0.69
R11	0.117	0.237	10.50	3.30	0.080	0.56	0.44
R12	0.125	0.235	7.62	7.98	0.086	0.38	0.31
$11.11 \times 10^{-6} \text{ m.s}^{-1}$							
R15	0.055	0.305	8.40	2.16	0.046	0.71	0.57
R16	0.045	0.345	7.08	0.72	0.069	0.77	0.85
R17	0.067	0.327	3.96	4.32	0.063	0.66	0.71

By applying a regression analysis, parameters a and b in the pedotransfer function (eq. [2]) were calculated to be 3.46506 and 0.02849 respectively. The correlation coefficient r was 0.812 which is significant at 1% (n=20). Although this pedotransfer function is strictly empirical it has a clear physical meaning.

An increase of the volume of stained macropores ( $V_s$ ) shortens the time lag. A high fractal dimension ( $D_{s3-1}$ ), significant for a soil system dominated by horizontal pedfaces, on the contrary, extends the time lag.

The regression analysis was also performed for the upper part of the soil column. No significant relation could be found there. This makes clear that the lower parts of the samples restrict bypass flow.

### C. Exponential start of outflow

At low rain intensities the exponential start of outflow (ESO), between  $T_{(d)}$  and  $T_{(cs)}$  is clearly present e.g. sample R14 in Fig. 2. At high rain intensities, e.g. sample R15, ESO is hardly visible. Bouma and Dekker (1978) found that water flowing into macropores, during bypass flow, formed small bands on the vertical walls of structure elements. The number and length of the bands were strongly related to the amount and intensity of rain applied. The development of new bands, and the creation of new initial infiltration areas, are important at low intensities. At high intensities, due to the fast propagation of the macropore wetting front, the potential available capacity for developing new bands is used relatively fast. This latter capacity is defined as the, rain intensity dependent, maximum area of the structure elements in contact with bypass flow water (Ver. C. and Hor. Pedf. in table 2).

ESO is also influenced by the initial pressure head in the sample. A low initial pressure head reduces absorption along the macropore walls which leads to a short ESO period, e.g. sample R04 in Fig.2.

Internal catchment, defined as the accumulation of water in vertically discontinuous macropores (Van Stiphout et al., 1987), leads to high ESO values, especially in the early stage of the flow process, when dead-end macropores are first filled.

The times of ESO, indicated by  $T_{(cs)}-T_{(d)}$  and the amount of outflow in that period are presented in table 2.

### D. Linear outflow

In the time span  $T_{(cs)}$  and  $T_{(ce)}$ , outflow is linear ( $T_{(lin)}$  in Fig. 2) for all samples (i.e. the time derivative for outflow is constant) as has been observed consistently in earlier measurements (e.g. Bouma et al., 1981; Van Stiphout et al., 1987). A quasi steady-state condition is thus suggested between absorption processes and applied rain intensity. In table 2 outflow rate during steady state flow is expressed as a fraction of the inflow rate ( $O_f/I_r$ ).

Relevant parameters which determine the absorption rate (rain intensity minus the outflow rate) have been examined using multiple regression techniques

(Statistical Package for Social Studies, SPSS (1991)). The total explained variance when correlating the absorption rate with the parameters, mentioned in table 3, was 0.688 (n=15). Table 3 shows that geometry of the macropore system ( $V_{s_l}^{Ds_3}$ ), defined as the volume stained ( $V_s$ ) raised to the power of the fractal dimension ( $Ds_3$ ), is even more important in explaining the absorption rate than the initial pressure head of the soil ( $\Psi_{(init)}$ ). The low correlations of stained volume and geometry in the upper parts of the soil cylinders indicate once more that bypass flow is governed by the most restrictive layer.

**Table 3** *Correlation coefficients for soil physical and morphological characteristics with the absorption gradient of water.  $V_{s_u}$  and  $V_{s_l}$  refer to the stained volume fractions of upper and lower part of the soil core respectively.  $V_{s_u}^{Ds_3}$  and  $V_{s_l}^{Ds_3}$ , represents the stained volume fraction raised to the power of the fractal dimension.  $\Psi_{(init)}$  is the initial pressure head in the sample.*

Parameter	Correlation coefficient
$V_{s_u}$	0.029
$V_{s_u}^{Ds_3}$	0.062
$V_{s_l}$	0.414
$\Psi_{(init)}$	0.484
$V_{s_l}^{Ds_3}$	0.636*

\* indicates 0.01 1-tailed significance

### E. Total outflow

Cumulative total outflow at the end of the experiment is presented in table 1. Average measured outflow over the 15 samples was  $5.6 \times 10^{-3}$  m (standard deviation  $1.6 \times 10^{-3}$  m) which is 37% of the applied amount.

Although rain intensity has an important effect on several individual processes, there was no significant relationship between the applied rain intensity and the total amount of outflow. At low rain intensities the time of initial breakthrough is much larger compared to high intensities but this effect is compensated by the duration of the rain shower.



The initial pressure head seems to have some impact. This effect, however, was not significant statistically, as can be explained by the dominating effect of the geometry on absorption, as already shown in table 3.

**Model simulations**

Figure 3 presents results for the simulations by using the model in combination with the pedotransfer function for predicting time lag for initial breakthrough (eq. [2]). Simulated and measured outflow have been plotted as a scatter diagram.

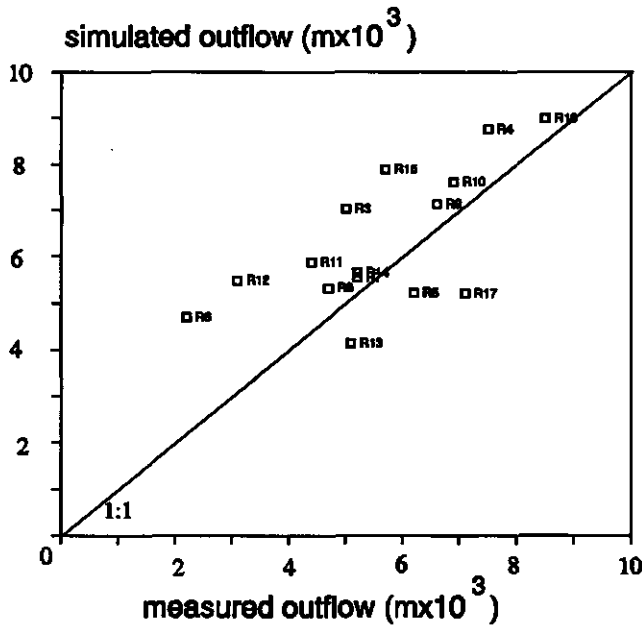


Figure 3. Scatter diagram for measured versus simulated outflow by using the pedotransfer function (eq. [2]).

The model overestimates the outflow slightly since data points are not quite evenly distributed around the 1:1 line. To test the quality of the model: (i) the average measured outflow was compared with average simulated outflow by means of a t-test. Simulation results did not differ significantly from the

measured data with a probability of 95%. (ii) The regression coefficient ( $r=0.6639$ ) of measured versus simulated outflow deviates from the 1:1 line ( $r=1.0$ ). This indicates that the model results show a rather less dynamic behaviour than the measured data. However,  $r$  was significant at a 1% probability level, indicating that the relation is well described.

Average values for simulation results are presented in table 4.

**Table 4** Average mass balances for the model simulations on all 15 samples.

	Average ( $\text{m} \times 10^2$ )	Standard dev. ( $\text{m} \times 10^2$ )
Rain	1.50	-
Surface infiltration	0.54	0.115
Absorption		
vertical cracks	0.26	0.120
horizontal pedfaces	0.07	0.064
Outflow	0.63	0.149

Outflow is the most important term in the mass balance. Due to the relatively dry initial condition and the water remaining on top of the sample, surface infiltration is high compared with previous experiments (Booltink and Bouma, 1991). Absorption into horizontal pedfaces seems hardly relevant. For sample R06 where the area of horizontal pedfaces dominates the system (table 1), this becomes, however, an important sink term.

Measured time lags in table 5, for the samples R03, R08, R14, and R16, were compared with time lags obtained from the pedotransfer function (eq. [2]). To check the pedotransfer function independently, the parameters  $a$  and  $b$  of eq. [2] were calculated excluding data of the samples R03, R08, R14 and R16; time lags calculated agreed fairly well with measured time lags. The apparently large deviation for sample R14 is, however, related to the duration of the rain shower, of the same order of magnitude as the time lag of sample R16.

Table 5 further shows the results of the comparison between simulations with measured data for the time lag and values obtained with the independent values for a and b in eq. [2].

Since time lag has no influence on surface infiltration this term was disregarded. Although differences in time lag can be considerable (e.g. R14) the effect on the simulated sink terms is rather small, indicating that the model is not very sensitive for small variations of this, especially in combination with relative low rain intensities.

**Table 5** *Sensitivity of simulated parameters for measured and calculated values, using the transfer function eq. 2 (Trans fun), for time lag.*

Sample		Time lag (sx10 <sup>2</sup> )	Drainage (mx10 <sup>2</sup> )	— Absorption — vert. cracks (mx10 <sup>2</sup> )	horpedf (mx10 <sup>2</sup> )
R03	measured	15.12	0.71	0.18	0.05
	trans fun	14.88	0.70	0.18	0.05
R08	measured	5.88	0.53	0.37	0.07
	trans fun	5.94	0.53	0.37	0.07
R14	measured	31.98	0.58	0.15	0.04
	trans fun	25.50	0.56	0.17	0.04
R16	measured	7.08	0.88	0.19	0.05
	trans fun	8.58	0.90	0.17	0.04

## CONCLUSIONS

1. The experimental set up provides a simple and flexible measuring system and can measure bypass flow rapidly. Data obtained can be used to characterize physically and morphologically the flow system it can also serve as input in simulation models to predict, or analyze further, bypass flow phenomena.
2. Stratification of macropores in terms of vertical continuous cracks and horizontal pedfaces of structure elements, together with the use of fractal

- dimensions to describe soil geometry derived from measured methylene blue staining patterns, are a promising operational method for the morphological characterization of soil structure. Other structures should be characterized as well to explore the application of this method further.
3. Saturated hydraulic conductivity at the soil surface and surface storage of water are crucial in determining the starting time of bypass flow. (Hoogmoed and Bouma, 1980; Booltink and Bouma, 1992). However, the absorption of water in the soil and, related to that, the point of initial breakthrough at the bottom of the soil cylinder is affected more by the geometry of the macropores than by the soil physical properties of the soil. In this study a pedotransfer function was developed to predict independently the time of initial breakthrough based on morphological features such as volume and fractal dimensions of stains.  
Since contact time of water and soil is important in calculating absorption processes, this pedotransfer function can be used to describe the propagation of tortuous water transport through a macropore system.
  4. Rain intensities applied, have a significant impact on the time scale of processes such as the start of bypass flow and initial breakthrough. Total bypass flow, however, is not influenced by rain intensity and seems more dependent on the amount of applied rain. For irrigation practices, a proper combination of application intensity and amount, dependent on soil texture and structure, can reduce bypass flow and increase irrigation efficiency.
  5. The extended version of the simulation model of Hoogmoed and Bouma (1980) could simulate the column experiments on bypass flow with significant accuracy. The relatively low explained variance probably reflects the depth averaging of the fractal dimensions, and contact areas. In future techniques such as CT-scanning or NMR may facilitate tracing the pathways of bypass flow continuously and the calculation of fractal dimensions from 3-D data directly.  
Internal catchment was not explicitly simulated by the model but could be well replaced by the stratification of infiltration in terms of vertically continuous cracks and horizontal pedfaces of structure elements. Internal catchment in this type of soil originates probably more from micro storage of water along macropore walls than from accumulation of water in dead-

end macropores. Especially on horizontal pedfaces this type of infiltration is likely to be an important sink term. These assumptions on internal catchment are of course valid only for this particular type of soil and cannot be transferred freely to other types. However, the methodology developed can be used to characterize other soils as well.

6. Further collection of data and validating, on different soil types, the pedotransfer function developed is recommended for the future. Coupling of this data to soil profile and structure descriptions in existing soil data bases may then enhance the usefulness of existing soil data.

## ACKNOWLEDGEMENT

This study was partly funded by the EC-research project STEP-0032-C.

R. Hatano is thankful for a travel grant from the Ministry of Education, Science and Culture of Japan.

The authors would like to thank Mr. T. Ito (Hokkaido University) for analyzing the staining patterns.

## REFERENCES

- Bartoli, F., R. Philippy, M. Doirisse, S. Niquet, and M. Dubuit. 1991. Structure and self-similarity in silty and sandy soils: the fractal approach. *J. of Soil Sci.*, 42:167-185.
- Beven, K., and P., Germann. 1982. Macropores and water flow in soils. *Water Resour. Res.*, 18:1311-1325.
- Beven, K., and R.T. Clarke. 1986. On the variation of infiltration into a homogeneous soil matrix containing a population of macropores. *Water Resour. Res.*, 22:383-388.
- Booltink, H.W.G. and Bouma, J., 1991. Physical and morphological characterization of bypass flow in a well-structured clay soil. *Soil Sci. Soc. Am. J.*, 55:1249-1254.
- Booltink, H.W.G., and J. Bouma. 1992. Sensitivity analyses on processes affecting bypass flow. *Hydrological Processes*, 7:33-43.
- Booltink, H.W.G., J. Bouma, and D. Giménez. 1991. Suction crust infiltrometer for measuring hydraulic conductivity of unsaturated soil near saturation. *Soil Sci. Soc. Am. J.*, 55:566-568.
- Booltink, H.W.G., C. Kosmas, E. Spaans, P.D. Peters. 1991. Application of the one-step outflow method for determining hydraulic properties of soils. *Soil and groundwater research report II: Nitrate in soils. Commission of the European communities. Luxembourg.*, pp:116-127.
- Bouma, J. 1984. Using soil morphology to develop measurement methods and simulation techniques for water movement in heavy clay soils. pp. 298-316. In J. Bouma and P.A.C. Raats (ed.) *Proc. ISSS Symp. Water and solute movement in heavy clay soils, Wageningen, The Netherlands. 27-31 Aug. 1984. Publ. 37. Inst. for Land Reclamation and Improvement, Wageningen, The Netherlands.*
- Bouma, J., and L.W. Dekker. 1978. A case study on infiltration into dry clay soil. I. Morphological observations. *Geoderma*, 20:27-40.
- Bouma, J., and H.A.J., Van Lanen. 1986. Transferfunction and threshold values: from soil characteristics to land qualities. in: K.J. Beek, P.A. Burrough and D.E. McCormack (Eds): *Quantified Land Evaluation Procedures. ITC, International Institute for Aerospace Survey and Earth Sciences, Publication no. 6. Enschede*, pp.106-110.
- Bouma, J., L.W. Dekker, and C.J. Muilwijk. 1981. A field method for measuring short-circuiting in clay soils. *J. Hydr.*, 52:347-354.

- Bouma, J., A. Jongerius, O. Boersma, A. de Jager, and D. Schoonderbeek. 1977. The function of different types of macropores during saturated flow through four swelling soil horizons. *Soil Sci. Soc. Am. J.*, 41:945-950.
- Bronswijk, J.J.B. 1988. Modeling of water balance, cracking and subsidence of clay soils. *J. Hydr.*, 97:199-212.
- Chen, C., and R.J., Wagenet. 1992. Simulation of water and chemicals in macropore soils. Part I. representation of the equivalent macropore influence and its effect on soilwater flow. *J. Hydr.*, 130:105-126.
- Crawford., J.W., K.R., Ritz, and I. Young. 1993. Quantification of fungal morphology, gaseous transport and microbial dynamics in soil. An integrated frame work utilising fractal geometry. *Geoderma*, 56:157-172.
- Doering, E.J. 1965. Soil-water diffusivity by the one-step method. *soil Sci.*, 99, 332-326.
- Germann, P.F. 1990. Preferential flow and the generation of runoff 1. Boundary layer flow theory. *Water Resour. Res.*, 26:3055-3063.
- Germann, P.F., and K. Beven. 1985. Kinematic wave approximation to infiltration into soils with sorbing macropores. *Water Resour. Res.*, 21:990-996.
- Hatano, R., and T., Sakuma. 1991. A plate model for solute transport through aggregated soil columns. I. Theoretical description. *Geoderma*, 50:13-23.
- Hatano, R., and H.W.G. Booltink. 1992. Using fractal dimensions of stained flow patterns in a clay soil to predict bypass flow. *J. Hydr.*, 135:121-131.
- Hatano, R., N. Kawamura, J. Ikeda, and T. Sakuma. 1992. Evaluation of the effect of morphological features of flow paths on solute transport by using fractal dimensions of methylene blue staining pattern. *Geoderma*, 53:31-44.
- Hoogmoed, W.B., and J. Bouma. 1980. A simulation model for predicting infiltration into cracked clay soil. *Soil Sci. Soc. Am. J.*, 44:458-461.
- Jarvis, N.J., and P.B., Leeds-Harrison. 1987. Modelling water movement in drained clay soil. I. Description of the model, sample output and sensitivity analysis. *J. Soil Sci.*, 38:487-498.
- Jarvis, N.J., and P.B., Leeds-Harrison. 1990. Field test of a water balance model of cracking clay soils. *J. Hydr.*, 112:203-218.
- Kool, J.B., and J.C. Parker. 1987. Estimating soil hydraulic properties from transient flow experiments: SFIT user's guide. Electric Power Research Institute, Palo Alto, California, USA.
- Lauren, J.G., J. Wagenet, J. Bouma, and J.H.M. Wösten. 1988. Variability of saturated hydraulic conductivity in a Glossoaquic Hapludalf with macropores. *Soil. Sci.*, 145:20-28.
- Ploeg, R.R. van der, and P. Benecke. 1974. Unsteady, unsaturated n-dimensional moisture flow in soil: A computer simulation program. *Soil Sci. Soc. Am. Proc.*, 38:881-885.
- Ringrose-Voase, A.J., and P. Bullock. 1984. The automatic recognition and measurement of soil pore types by image analysis and computer programs. *J. of Soil Sci.*, 35:673-684.
- Soil Survey Staff. 1975. *Soil Taxonomy; a basic system of classification for making and interpreting soil surveys.* Agr. Handb. no. 436, SCS-USDA. Government Printing office, Washington DC.
- Statistical Package for Social Sciences, SPSS. 1991. *Base manual.* SPSS Inc. 444 N. Michigan Avenue, Chicago IL 60611. USA.

- Stroosnijder, L. 1976. Cumulative infiltration and infiltration rate in homogeneous soil. Agric. Res. Rep. 847., pp. 69-99.*
- Van Stiphout, T.P.J., H.A.J. Van Lanen, O.H. Boerma, and J. Bouma. 1987. The effect of bypass flow and internal catchment of rain on the water regime in a clay loam grassland soil. J. Hydr., 95(1/2):1-11.*
- White, R.E. 1985. The influence of macropores on transport of dissolved and suspended matter through soil. In: B.A. Stewart (ed.), Advances in soil science. Volume 3. Springer, New York, N.Y. Vol. 3:95-120.*



## **CHAPTER 7**

# **FIELD MONITORING OF NITRATE LEACHING AND WATER FLOW IN A STRUCTURED CLAY SOIL**

Submitted to: *Agriculture, Ecosystems & Environment*

# FIELD MONITORING OF NITRATE LEACHING AND WATER FLOW IN A STRUCTURED CLAY SOIL

**H.W.G. Booltink**

*Departement of Soil Science and Geology, Agricultural University, P.O. Box 37, 6700 AA Wageningen, The Netherlands.*

## ABSTRACT

Bypass flow and nitrate leaching from an experimental field at the Kandelaar farm in Eastern Flevoland in the Netherlands was measured in drain outflow for a period of 4 year. Automated monitoring equipment registered precipitation, ground water level and drain discharge continuously and was complemented with manually collected data on soil water potentials and soil mineral nitrogen. Occurrence of bypass flow was established because air-filled porosity in the soil was more than adequate to accept the rain in a soil without macropores. During bypass flow events in summer, 30% of the precipitation was directly discharged via the drains. In winter periods this amount corresponded to 84% of the precipitation. Bypass flow induced nitrate leaching from the fine aggregated top soil towards the ground water. In periods with an active growing crop nitrate leaching was negligible. A catchcrop grown directly after slurry application in late summer had a strong reducing effect on nitrate leaching during the entire winter season. In the subsoil, large amounts of inaccessible nitrogen are present in the soil, within large soil peds. Soil structure strongly influences bypass flow and can be used as a management tool for farmers to decrease nitrate leaching.

## INTRODUCTION

Nitrate leaching from agricultural soils has been widely studied (e.g. Addiscot and Cox, 1976; White et al., 1983; Verdegem and Baert 1984; Wild 1972). In the Netherlands attention has mainly been focused on sandy soils: clay soils are usually not regarded as being soils with high nitrate leaching potential. However, bypass flow, defined as: "the flow of water through a system of large pores that allow fast velocities and bypasses the unsaturated soil matrix" (Beven and Germann, 1982), can lead to rapid transport of water and dissolved matter to the ground water (e.g. White, 1985). Bypass flow phenomena can not be adequately described by flow theory, based on Richard's equation (e.g. Klute, 1973), or convective dispersive transport equations (Nielsen and Biggar, 1962). Dekker and Bouma (1984) studied nitrogen leaching in pastures on cracking clay soils in the Netherlands. They found that the amount of leached nitrate strongly depended on applied rain intensities. Nitrogen losses, due to bypass flow, averaged 30% at high rain intensities. Prewetting the soil before fertilizer application could reduce nitrate losses to 8% of the applied amount. Smaling and Bouma (1992) measured nitrogen losses of 20 kg N per ha from a single addition of 50 kg N per ha, during one bypass flow event in Kenya. These experiments were carried out by the procedure as described by Bouma et al. (1981), using large undisturbed soil samples and artificial rain events. In both experiments the amount of rain applied, would not have led to outflow from the soil cores in a homogenous soil. Such column experiments, however, can hardly be used to predict nitrate leaching rates on a field scale. For this, long term field monitoring studies on nitrate leaching are required. White et al. (1983) measured water flow rates and nitrate concentrations on catchment scale by monitoring drain outflow. In this study, however, no data on soil mineral nitrogen were presented, which made interpretation of data in terms of leaching processes difficult. On the contrary, Garwood and Ryden (1986) mainly concentrated on the analysis of soil mineral nitrogen and paid little attention to nitrogen concentrations in drainage water. To obtain insight in the process of nitrate leaching in structured clay soils both water outflow and soil mineral nitrogen profiles have to be determined to allow interpretations of nitrate contents in drainage water.

Agricultural management also has a large impact on nitrate leaching as indicated by, for example, Steenvoorden (1989). Time and amount of application of organic and inorganic fertilizers strongly influence the nitrate concentration in ground water. The application of catchcrops to reduce nitrate leaching was studied by Finke (1993).

In this study long term monitoring of bypass flow and soil mineral nitrogen contents was used to: (i), investigate bypass flow and related nitrate leaching in conjunction with different fertilizing and land management treatments and (ii), define procedures for farmers for reducing nitrate leaching and fertilizer use efficiency.

## MATERIAL AND METHODS

### Soil

The study area was located at the experimental farm The Kandelaar in Eastern Flevoland, the Netherlands. The soil, reclaimed in 1958 and first used for agricultural purposes in 1967, was characterized as a mixed, mesic Hydric Fluvaquent (Soil Survey Staff, 1975). A soil profile description is presented in Table 1. Macropores present were both vertical and horizontal interpedal planar voids (Fig. 1).

**Table 1** *Soil profile description of the study site at the Kandelaar experimental farm.*

A <sub>p</sub>	0.00 - 0.30 m:	clay (42% clay) with a moderate, medium angular blocky structure and an abrupt wavy boundary
2C	0.30 - 0.70 m:	clay loam (40% clay), strong, very coarse prismatic structure
3C	0.70 - 1.03 m:	silty clay loam (30% clay), strong, very coarse prismatic structure
4BC <sub>o</sub>	1.03 - 1.20 m:	sand, single grain

Field experiments with iodide tracers (Van Ommen et al., 1988), in combination with methylene blue laboratory experiments (Booltink and Bouma, 1991; Bootink et al., 1993) showed that, as a result of annual tillage practices, the number of continuous macropores rapidly decreased at the bottom of the A<sub>p</sub> horizon. Macropores present below that depth (see Fig. 1), originated from

irreversible shrinkage during reclamation, and were continuous over the profile until the 4BC<sub>o</sub> horizon.

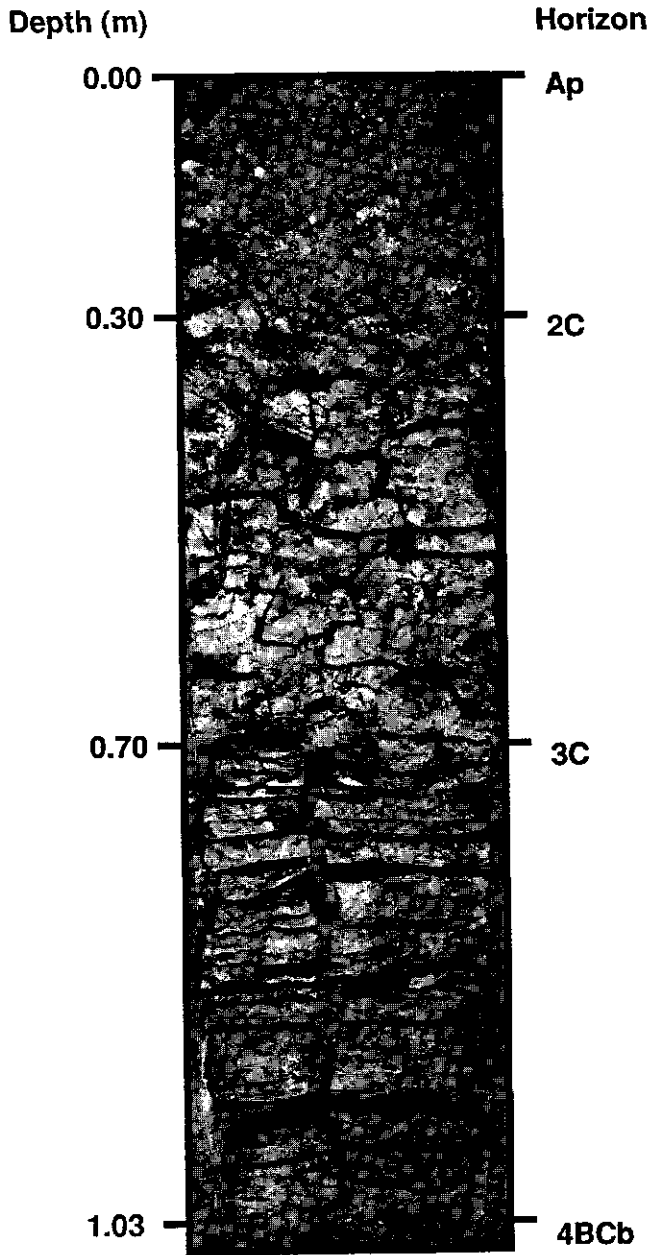


**Figure 1** Soil profile and layer codes. Codes refer to table 1.

**Experimental set up**

The study site was used by the Research Station for Arable Farming and Field Production of vegetables (PAGV, Lelystad, The Netherlands) for research on the applicability of organic manure in arable land systems, especially with respect to crop yields. Different combinations of organic, inorganic, green manure and management practices were compared. A complete overview of the fertilizer and management treatments is presented in table 2.

**Table 2** *Experimental set up for the fertilizer and management experiments.*

Inorg. fert (kg N.ha <sup>-1</sup> )	Org. fert. (kg P <sub>2</sub> O <sub>5</sub> .ha <sup>-1</sup> )	Land management
N0 0	X 0	A stubble + straw residues
N1 75	Y 125	B stubble + straw + catchcrop
N2 150	Z 250	C stubble + catchcrop
N3 225		D stubble + stubble-ploughing + catchcrop
		E stubble + straw + stubble- ploughing + catchcrop

The fertilizer experiments were carried out on 60, randomly distributed, small 12 x 7.5 m plots (Fig. 2) and were continuous over a period of 6 years starting in 1986. Three replicates (I, II, and III) of the experiment were performed.

An inorganic fertilizer application of 150 kg N per ha (N2) corresponds with the standard fertilizer advice, based on N mineral samples taken in march. The levels of N1 (75 kg. ha<sup>-1</sup>) and N3 (225 kg. ha<sup>-1</sup>) correspond with the advice ± 50%. This amount was given in one application in spring. Calculation of the fertilizer advice was carried out by the Laboratory for Soil and Crop Testing (Oosterbeek, The Netherlands).

Besides the inorganic fertilizer application, organic fertilizer was applied once every two year in autumn. A poultry slurry application of 250 kg P<sub>2</sub>O<sub>5</sub> per ha (level Z in table 2) included a nitrogen application of approximately 285 kg.ha<sup>-1</sup> (about 150 kg.ha<sup>-1</sup>NH<sub>4</sub><sup>+</sup>-N and 135 kg.ha<sup>-1</sup> organic N). Slurry was applied with a slurry injector to minimize volatilization losses of ammonia.

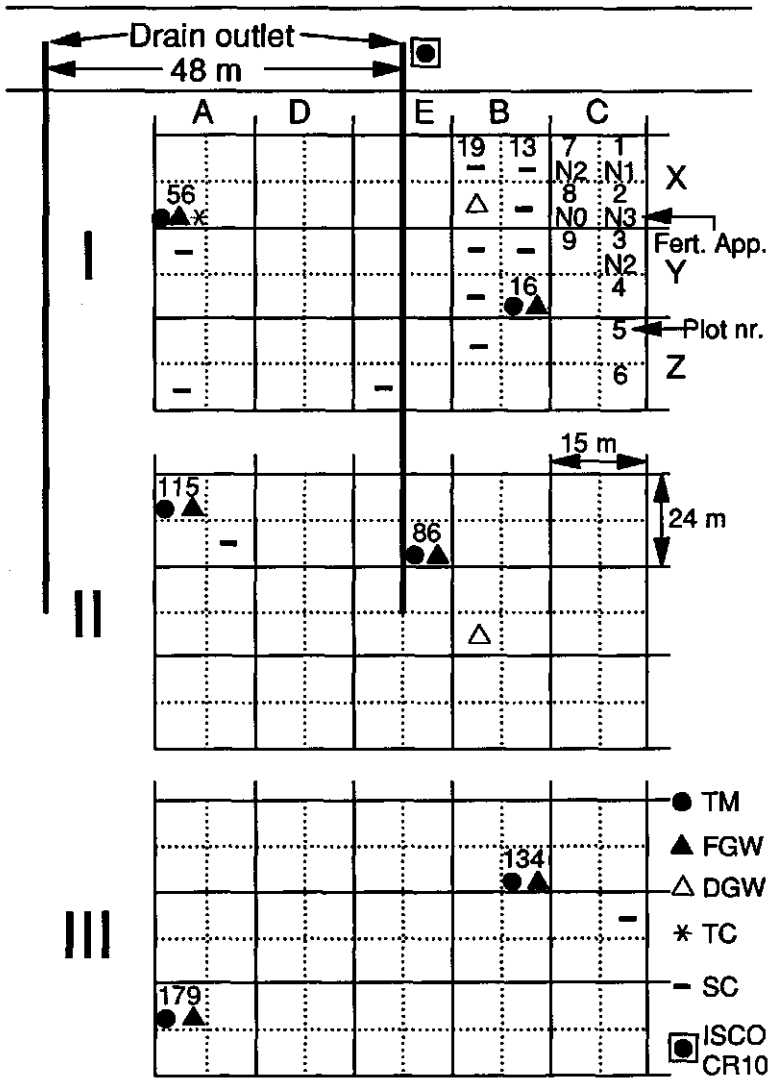


**Figure 2** *Lay out of the experimental set up at the study area, at the Kandelaar. Codes for fertilizer and management treatments, A-E, X,Y,Z and N1-3, refer to table 2. TM represents the plots where tensiometer profiles were installed, FGW stands for freatic groundwater level, DGW for deep groundwater level, TC for thermocouple profile and SC for ceramic suction cups. The location of the datalogger and sequential sampler are indicated by respectively CR10 and ISCO.*

**Data collection**

The monitoring set up at the study area is illustrated in figure 3. On 6 plots in the research site tensiometers were installed at 0.05, 0.25, 0.35, 0.50, 0.80 and 1.00 m depth (TM in Fig. 2.) Phreatic ground water piezometers were installed on every one of the 6 plots (FGW in Fig. 2) and on a line perpendicular to the tile drains in replication I. Deep ground water (4.5-5.0 m) was monitored on two plots (DGW). Thermocouples (TC) were installed on one plot at 0.05, 0.10, 0.20, 0.50, and 1.00 m depth. Except in periods of agricultural activities, such as harvesting and ploughing, a fortnightly monitoring scheme was maintained as much as possible during the year.

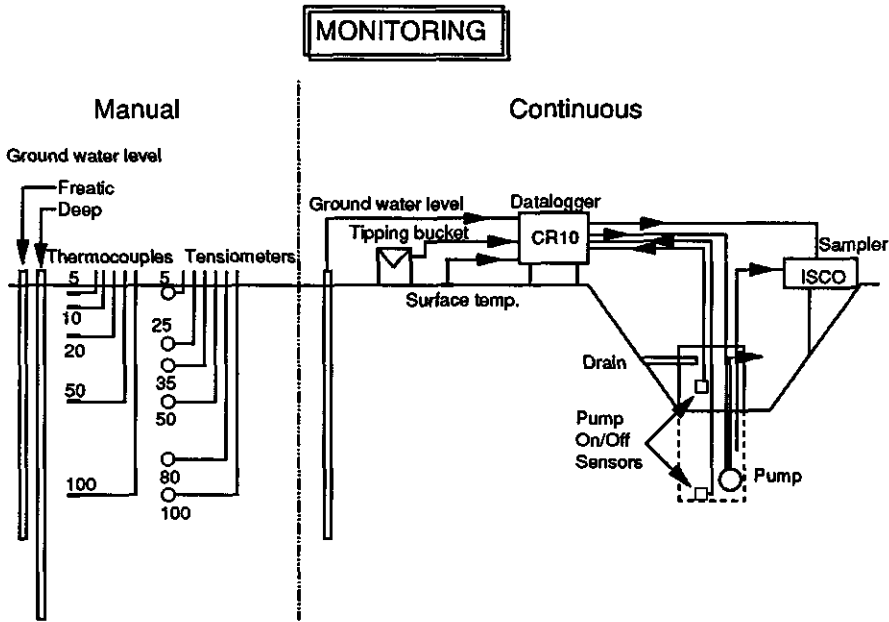


**Figure 3** Schematic overview of the monitoring set up.

A CR10-datalogger (Campbell) was used for continuous monitoring drain discharge on one tile drain in the centre of the study area. Drain depth varied from approximately 0.90 m at the beginning to 1.10 m at the end.



Drain discharge was stored in a  $0.220 \text{ m}^3$  vessel with an electronic switch in the top and bottom (Fig. 3). The datalogger checked the sensors every 3 s and switched the pump on and off if the water level in the vessel reached the respective switches. Time and date for switching the pump on and off were stored in the datalogger and were used to calculate drain discharge intensity. Catchment area of the drain was approximately  $7200 \text{ m}^2$ , discharge resolution of the drain outflow apparatus was, therefore,  $0.03 \times 10^{-3} \text{ m}$  water head. Water samples were taken every  $0.06 \times 10^{-3} \text{ m}$  of discharge, using a sequential water sampler (ISCO). Eight samples were mixed in a sample bottle by the sampler. In this way, flow was proportionally sampled representing  $0.48 \times 10^{-3} \text{ m}$  of discharge per sample bottle. Drain water samples were analyzed for  $\text{NO}_3^-$ ,  $\text{NH}_4^+$  and  $\text{Cl}^-$  in the laboratory. Concentrations measured in drain outflow are a mixture of all plots in replica I and part of replica II, and can not be transformed into values for individual plots.

Rain amount, the soil/air-interface temperature and ground water level was continuously measured during 180 s interval by the CR10-datalogger and, except for the rain amount, was averaged over 900 s periods.

Soil samples for mineral nitrogen ( $\text{N}_{\text{min}}$ ) analysis were taken at irregular time intervals in the fertilizer plots, up to 4 or 5 times per year. Four different sub-samples, taken on a cross section within a plot, were mixed to a representative plot sample. Boundaries of the sample depth intervals for standard sampling were: 0.00, 0.30, 0.60 and 0.90 m minus soil surface, or 0.00, 0.20, 0.35, 0.50, 0.70, 0.80, 0.95 and 1.10 m for additional sampling. Monitoring was started in October 1989 and continued until April 1992.

Nitrate concentration in soil solution at 0.9 m depth was monitored approximately once per month on 13 representative plots (SC in Fig. 2). In every of the 13 plots, 4 ceramic suction cups (0.05 m long and 0.015 m diameter) were installed and connected with plastic tubing to 1 stock bottle.

## RESULTS AND DISCUSSION

### Bypass flow

Measured precipitation intensity and ground water level for the winter season 1989/1990 are presented in Fig. 4. Bypass flow is illustrated by the nearly

immediate reaction of ground water to high precipitation intensities. Instant drain discharge occurs when ground water is at a depth less than 0.80 m minus soil surface. During the measuring period of 2.5 year a total of 38 bypass events were registered.

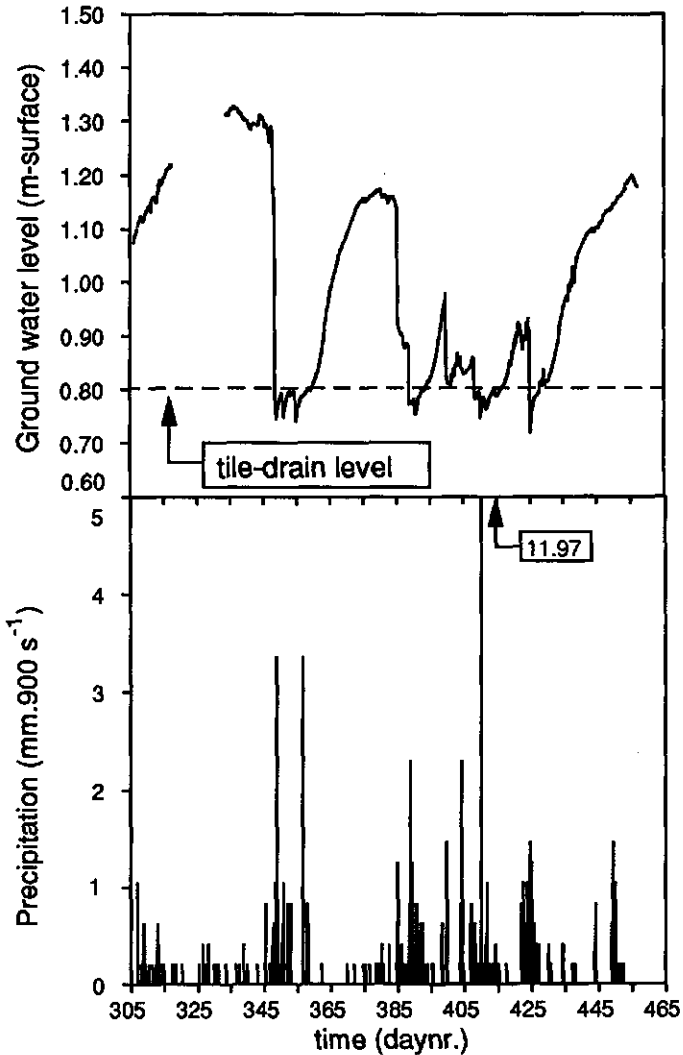


**Figure 4** *Precipitation intensity and ground water fluctuations in the winter season 1989/1990 (1 january 1989 is daynr. 1).*

**Morphometric methods for simulation of water flow**

Time lags for initial breakthrough of bypass flow to the groundwater, for 17 individual bypass flow events, are presented in table 3. Initial breakthrough is fast, within 1800 s, if rain intensity is high or, since the non structured 4BC<sub>6</sub> sand horizon reduces the breakthrough peak, the groundwater level is within 1.00 m depth.

**Table 3** *Timelags for initial breakthrough of bypass flow water ( $T_{lag}$ ) to the groundwater in relation with initial groundwater level ( $GW_{init}$ ) and rain intensity ( $Rain_{int}$ ) (1 january 1989 is daynr. 1).*

Daynumber	Month	$GW_{init}$ (m-surf.)	$Rain_{int}$ ( $mx10^3.900 s^{-1}$ )	$T_{lag}$ (s)
350	dec	0.80	0.63	11700
385	jan	1.13	2.31	4500
388	jan	0.85	3.15	2700
410	feb	0.78	11.97	1800
497	may	0.98	5.46	1800
625	sep	1.34	3.57	4500
628	sep	1.29	4.20	2700
632	sep	1.11	2.94	2700
902	jun	1.10	4.20	2700
902	jun	1.08	5.88	1800
904	jun	0.98	6.30	1800
906	jun	0.94	1.68	6300
908	jun	0.90	13.86	900
1038	nov	1.40	5.25	3600
1041	nov	1.25	3.78	2700
1082	dec	1.22	3.78	2700
1083	dec	0.97	2.10	1800

Table 4 presents data on drain discharge during clearly distinguished periods with bypass flow events. Notice that one period consists of one or more individual bypass flow events. The discharge/rain ratio varies between 0.30 to 0.84. This difference is mainly caused by the storage of bypass flow water in the 4BC<sub>6</sub> horizon, as indicated by the initial groundwater levels just before the bypass flow event.

**Table 4** *Total drain outflow related to the total precipitation during periods of bypass flow. Initial groundwater level before the bypass flow event is indicates as  $GW_{init}$ , drain/rain represents the ratio between drain discharge and the amount of precipitation during the period considered (1 january 1989 is daynr. 1).*

Daynumber	$GW_{init}$ (m-surf.)	Precipitaion ( $mx10^3$ )	Drain outflow ( $mx10^3$ )	Drain/Rain (-)
348- 362	1.16	50.6	32.2	0.636
380- 396	1.13	29.8	19.8	0.664
411- 418	0.78	17.2	14.5	0.843
497- 498	1.18	4.6	1.4	0.312
670- 672	1.23	22.1	6.5	0.296
784- 792	1.03	14.5	12.2	0.842
905- 912	1.12	92.4	41.7	0.452
1041-1052	1.25	85.5	33.6	0.393
1082-1092	1.22	31.3	22.3	0.713
1100-1106	1.02	42.0	32.5	0.773

Bypass flow is also demonstrated by measured tensiometer profiles. In Fig. 5 fortnightly tensiometer data at 0.50 m depth are combined with measured rain intensities. A nearly immediate response on rain events can be seen for e.g. plot 56 and 115. Plot 16 and 179, on the contrary, show a strongly delayed reaction on rain events. For plot 179 it even takes 2 months before equilibrium is reached. Cups with a fast reaction can, therefore be regarded as being close to water conducting macropores (Booltink and Bouma 1991). Slowly reacting cups, on the contrary, are located inside structure elements where only little water displacement occurs due to diffusion processes. These techniques are, therefore, unsuitable for predictive purposes, such as nitrate leaching, or for validation of solute transport models. Recently installed automated TDR (Time Domain Reflectometry) equipment (Topp et al., 1990; Heimovaara, 1991) integrates water contents over an area of 0.025 m<sup>2</sup> and, therefore, seems to be a good alternative for laborious and manifold tensiometer measurements.

#### Drain discharge: effects of structure

In Fig. 6 a drainage discharge peaks, over a period of 5 days in february 1990 (day numbers 411 to 416) is taken as an example to illustrate solute fluxes

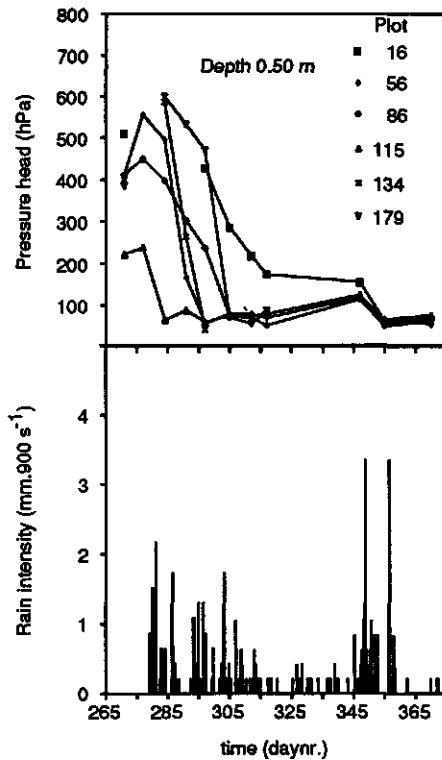


**Figure 5** Measured rain intensities with corresponding tensiometer reactions at 0.50 m depth. Period 5 october to 31 december 1991 (1 january 1989 is daynr. 1).

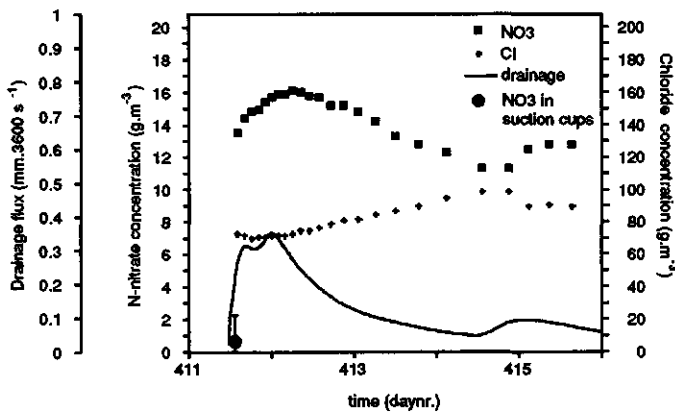


**Figure 6** Drain discharge and concentrations of nitrate and chloride in the drainage water in february 1990 (1 january 1989 is daynr. 1).

during that period. The tile drains discharged  $14.5 \times 10^3$  m (84%) of the  $17.2 \times 10^3$  m precipitation in the particular period of 5 days. Even though the profile was relatively wet before this bypass flow period, water storage capacity, measured by tensiometers, was approximately 0.10 m. In a non-macroporous soil this rain event would, therefore, not have lead to drain discharge. In Fig. 6 drain discharge rate is presented in combination with chloride and nitrate concentration. Due to dilution of ground water with high chloride concentration with bypass flow water with low chloride concentration, the chloride concentration in drain discharge decreases proportionally with the discharge rate. Nitrate, on the contrary, shows the opposite effect. Nitrate concentration is increasing proportionally with drain discharge rate. This effect is caused by the dissolution of easily accessible nitrate in the top layer of the soil. Due to the relatively small structure elements in the plough layer, there is a good contact between bypass water and soil material, which allows dissolution of nitrate as was previously suggested by Addiscot and Cox (1976). Increasing nitrate concentration with discharge rates was also reported by MacDuff and White (1976), Martin and White (1982), and White et al. (1983). However, the origin of this nitrate was not determined.

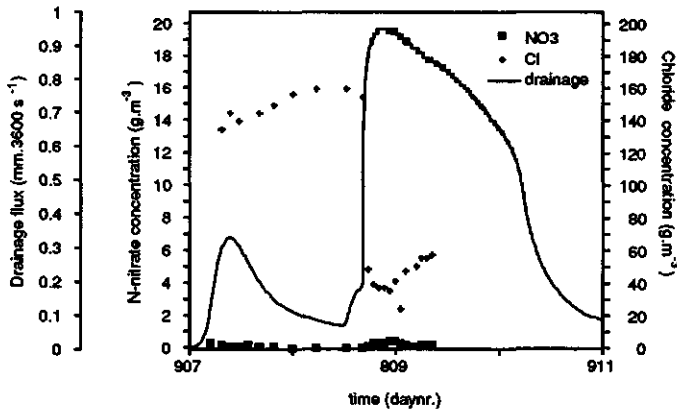


**Figure 7** Drain discharge and concentrations of nitrate and chloride in the drainage water in June 1991 (1 January 1989 is daynr. 1).

Although there is a considerable amount of mineral nitrogen in the subsoil this nitrogen has no effect on the leaching process, as is illustrated by a bypass event

in June 1991 (Fig. 7). During this event, nitrate concentrations in drain water remained low. Nitrate in the topsoil, either applied by spring fertilizing or mineralised from the soil, had all been consumed by an active growing winter wheat crop. Since rooting depth at that time had not yet reached the subsoil (plants were 0.20 m high), conditions for nitrate leaching in the subsoil can be compared to those in the winter period.

### Effects of cropping

In 1989 yellow mustard (*Brassica nigra*) was sown directly after the slurry application. Italian rye-grass (*Lolium multiflorum*) was sown in the spring of 1991. The slurry application was equivalent to an average of 143 kg total N per ha<sup>-1</sup> (75 kg ha<sup>-1</sup> NH<sub>4</sub><sup>+</sup>-N and 63 kg ha<sup>-1</sup> organic N).

By studying time series of nitrate concentrations, an increase of the nitrate concentration in bypass flow water can be seen during the winter season. Table 5 shows that for the period 1989-1990 the increase over time is rather small, in the winter period of 1991-1992 this increase, however, is very pronounced. These differences are mainly caused by the effect of the catchcrop. During the 1989-1990 period the yellow mustard was well developed. This catchcrop, which covered 80% of the study site, consumed all the easily available nitrogen. After mixing the catchcrop with soil by ploughing, nitrogen is slowly released again. The Italian rye-grass in 1991 was poorly developed and covered only 40% of the study area. This resulted in small nitrate crop-uptake and high nitrate concentrations in bypass flow water, already early in winter (Dec 1991 in table 5). Mineral soil N data collected during the periods 1989-1990 and 1991-1992 confirmed the processes as described above. In Fig. 8a-f average soil mineral N profiles are presented. Fig. 8a and d represent the N<sub>min</sub> status directly after harvest but before manure application in August in both periods. N<sub>min</sub> profiles in Fig. 8b and e were taken just before winter cultivation. Differences in N<sub>min</sub> profiles are distinct. Due to the poorly developed catchcrop in 1991 the N<sub>min</sub> content (80 kg ha<sup>-1</sup>) is high compared to 1989 (39 kg ha<sup>-1</sup>) in which year the catchcrop was well developed. Most pronounced differences were found in the layers below 0.30 m depth. Mineralization over the winter period was considerable in 1989/1990. Total N<sub>min</sub> content in February 1990 was 117 kg ha<sup>-1</sup> (Fig. 8c), an increase of 78 kg ha<sup>-1</sup>. In the winter period of 1991/1992 this

increase was only 8 kg.ha<sup>-1</sup> (Fig. 8f), indicating that the conservation effect of the catchcrop was negligible for this latter period.

**Table 5** *Effects of cropping and agricultural management on nitrate concentration during two comparable winter periods.*

Season	1989-1990		1991-1992	
Average nitrate and peak concentrations (g.m <sup>-3</sup> )	avg	peak	avg	peak
nov.	-	-	11.9	22.5
dec.	7.0	8.6	36.5	43.1
jan.	10.0	12.1	-	-
feb.	14.3	16.1	-	-
Catchcrop name	yellow mustard		italian rye-grass	
cover	80%		40%	
development	good		poor	
Application of slurry	august 24		september 2	
Winter cultivation	november 24		october 22	
Summer crop	spring barley		winter wheat	

- indicates that no data were available for this period.



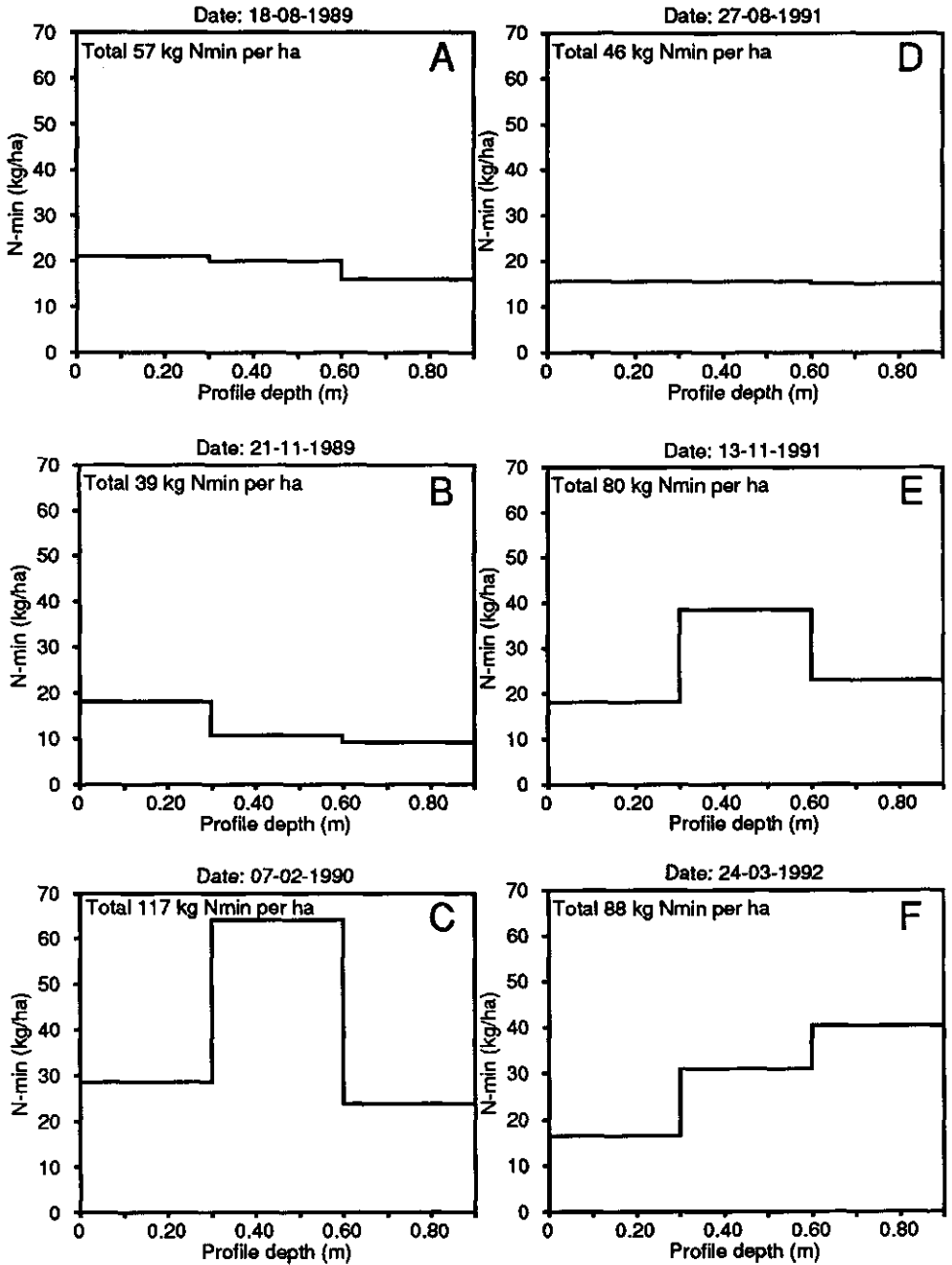


Figure 8 Average mineral N profiles of 6 fields during the winter seasons of 1989-1990 and 1991-1992.

### Unsuitability of suction cups for measuring solute components

The location of suction cups in the soil peds strongly influences its ability for extracting soil moisture. Cups in close contact with water conducting macropores will be able to extract bypass water. Cups inside soil peds, on the contrary, can only extract water from the soil matrix, which has a different chemical composition. Since the precise location of these cups is never known, suction cups have to be regarded as unsuitable for extracting soil solution in this type of soil because of the high heterogeneity of results obtained. As an example, nitrate concentrations in soil water, collected with suction cups, during a bypass flow event are presented in Fig 6. Nitrate concentrations collected with suction cups (De Boer, 1992), in all 13 plots (total 53 cups) were an order of magnitude lower than values determined in the drain outflow at the same time. Error bars represent 95% confidence intervals.

## CONCLUSIONS

1. In structured clay soils bypass flow is an important term of the water balance. Field monitoring data on bypass flow indicate that up to 80 percent of precipitation is nearly directly transported to the ground water. Since nitrate concentrations, measured in drain discharge, increased during bypass flow, bypass flow increases the nitrate load to ground water.
2. Occurrence of small soil aggregates reduces bypass flow but has a negative effect on nitrate leaching. Small structure elements with large contact areas along their walls, increased nitrate leaching.
3. In this study the Dutch standard level for surface water quality of 10 g N-NO<sub>3</sub><sup>-</sup> per m<sup>3</sup>, as measured in drain outflow, was exceeded only during the winter season. The order of magnitude and the time in winter when high concentrations occurred, were strongly influenced by management practices.
4. A catchcrop, grown directly after slurry application could strongly reduce nitrate concentrations in drain water. For two comparable winter seasons, this reduction was estimated to be 75 percent.
5. Soil solution sampling by suction cups, with or without mixing into an average sample, seems to be an unsuitable procedure in the type of soil

being considered. Nitrate values vary greatly and concentrations are significantly lower than those in drain discharge. Monitoring nitrate concentrations by means of drain discharge is a good method for measuring nitrate leaching of larger areas. If data are needed for smaller sub-areas small scale lysimeters can be an alternative.

## ACKNOWLEDGEMENTS

The author wishes to thank Ing W. de Boer from the Winand Staring Centre and Ing J. Alblas from the Research Station for Arable Farming and Field Production of Vegetables (PAGV) for additional experimental data, Ing F. Nieuwland and Ing A. Rops of the Kandelaar experimental farm for their cooperation during the experiments and Prof. Dr. J. Bouma for critically reading the manuscript. This study was financed by the EC-research projects "Nitrate in soils" (EV4V.0098-NL) and STEP-0032-C.

## REFERENCES

- Addiscot, T.M., and D. Cox. 1976. Winter leaching of nitrate from autumn-applied calcium nitrate, ammonium sulphate, urea and sulphur-coated urea in bare soil. *J. Agric. Sci. Camb.* 87:381-389.
- Beven, K., and P. Germann. 1982. Macropores and water flow in soils. *Water Resour. Res.* 18:1311-1325.
- Boer, W. de. 1992. Personal communication.
- Booltink, H.W.G. and Bouma, J., 1991. Physical and morphological characterization of bypass flow in a well-structured clay soil. *Soil Sci. Soc. Am. J.*, 55:1249-1254.
- Booltink, R. Hatano, and J. Bouma. 1993. Measurement and simulation of bypass flow in a structured clay soil: a physico-morphological approach. *J. Hydr.* (in press).
- Bouma, J., L.W. Dekker, and C.J. Muilwijk. 1981. A field method for measuring short-circuiting in clay soils. *J. Hydr.* 52:347-354.
- Dekker, L.W., and J. Bouma. 1984. Nitrogen leaching during sprinkler irrigation of a Dutch clay soil. *Agricultural Water Management* 9, 37-45.
- Finke, P.A. 1993. Field scale variability of soil structure and its impact on crop growth and nitrate leaching in the analysis of fertilizer scenario's. Accepted for publication in *Geoderma*.
- Garwood, E.A., and J.C. Ryden. 1986. Nitrate loss through leaching and surface runoff from grassland: effects of water supply, soil type and management. In: Meer, H.G. van der, J.C. Ryden, and G.C. Ennik (eds.). *Nitrogen fluxes in intensive grassland systems*. Martinus Nijhoff publishers, Dordrecht, The Netherlands.
- Heimovaara, T.J. 1991. A computer controlled TDR system for measuring soil water contents. Report 41. Lab. of Phys. Geography and Soil Sci. Univ. of Amsterdam.
- Klute, A. 1973. Soil water flow theory and its application in field situations. p.9-31. In R. R. Bruce et al. (ed.), *Field soil water regime*, SSSA Spec. Publ. 5. SSSA, Madison, WI.
- MacDuff, J.H., and R.E. White, 1984. Components of the nitrogen cycle measured for cropped and grassland soil-plant systems. *Plant and Soil.* 76:35-47

- Martin, R.P., R.E. White. 1982. Automatic sampling of stream water during storm events in small remote catchments. *Earth. Surf. Proc. and Landforms*. 7:53-61.
- Nielsen, D.R., and J.W. Biggar. 1962. Miscible displacement III. Theoretical considerations. *Soil Sci. Soc. of Am. Proc.* 26:216-221.
- Smaling, E.M.A., and J. Bouma. 1992. Bypass flow and leaching of nitrogen in a Kenyan vertisol at the onset of the growing season. *Soil use and management*. Vol. 8.1:44-48.
- Steenvoorden, J.H.A.M. 1989. Agricultural practices to reduce nitrogen losses via leaching and surface runoff. In: *Management systems to reduce impact of nitrates*. p.72-80. Elsevier applied Science, Amsterdam, The Netherlands.
- Soil Survey Staff. 1975. *Soil Taxonomy; a basic system of classification for making and interpreting soil surveys*. Agr. Handb. no. 436, SCS-USDA. Government Printing office, Washington DC.
- Topp, G.C., T.L. Davis, and A.P. Annan. 1980. Electromagnetic determination of soil water content in coaxial transmission lines. *Water Resour. Res.* 16:574-582.
- Van Ommen, H. C., L. W. Dekker, R. Dijkma, J. Hulshof and W. H. van der Molen. 1988. A new technique for evaluating the presence of preferential flow paths in non-structured soils. *Soil Sci. Soc. Am. J.*, 52: 1192-1194.
- Verdegem, L., and L. Baert. 1984. Losses of nitrate nitrogen in sandy and clayey soils. *Pedologie*, XXXIV-3:235-255.
- White, R.E. 1985. The influence of macropores on the transport of dissolved and suspended matter through soil. *Advances in Soil Science* 3:95-121.
- White, R.E., S.R. Wellings, and J.P. Bell. 1983. Seasonal variations in nitrate leaching in structured clay soils under mixed land use. *Agric. Cult. Water Manag.* 7:391-410.
- Wild, A., 1972. Nitrate leaching under bare fallow at a site in northern Nigeria. *J. Soil Sci.* 23:315-324.

## **CHAPTER 8**

# **DISTRIBUTED MODELLING OF BYPASS FLOW ON FIELD SCALE IN A HEAVY TEXTURED CLAY SOIL**

Submitted to: *Water Resources Research*

# DISTRIBUTED MODELLING OF BYPASS FLOW ON FIELD SCALE IN A HEAVY TEXTURED CLAY SOIL

**H.W.G. Booltink**

*Departement of Soil Science and Geology, Agricultural University, P.O. Box 37, 6700 AA Wageningen, The Netherlands.*

## ABSTRACT

Water transport in structured soils is strongly influenced by macropores. This study was conducted to develop a water transport model able to simulate bypass flow processes on a field scale. The LEACHW-model was extended with subroutines describing bypass flow, tortuous water transport through macropores and absorption of water along macropore walls. The model was tested on measured data from an experimental site in the Netherlands. A Monte-Carlo analysis in combination with a Rotated-Random-Scan procedure was carried out to take into account variability of model parameters and to subsequently calibrate the model. A sensitivity analysis showed that the conductivities of the top soil layers were the most sensitive parameters in the model. Validation of the model on independent data showed that the model was capable of simulating bypass flow realistically. The Rotated-Random-Scan procedure was a valuable tool for the quantification of ill-defined model parameters.

## INTRODUCTION

The occurrence of macropores in soils has an important impact on water and solute movement. Beven and Germann (1982) and White (1985) reviewed the

experimental evidence that water flow in soils containing macropores cannot be described accurately by models based on Darcian flow theory only.

Macropore or bypass flow was defined as: "the flow of free water along macropores into and through an unsaturated soil matrix" by Bouma (1984), or by Beven and Germann (1982) as: "the flow of water through a system of large pores that allows fast velocities and bypasses the soil matrix".

Increased awareness of a need to improve water-use efficiency and the risks of rapid transport of pesticides and fertilizers to deeper soil layers leads to the necessity to describe bypass flow in quantitative terms.

Several modelling approaches have been followed in the past. Edwards et al. (1979) used a two-dimensional model which simulates infiltration and redistribution of water into a soil surface containing a cylindrical macropore. Beven and Clark (1986) defined a uniform distribution of macropores with different widths and depths, from which water moved away radially and vertically. Darcian flow in the soil matrix was combined with Hagen-Poiseuille transport in macropores by Chen and Wagenet (1992). Germann and Beven (1985) and Germann (1990) used kinematic wave theory to simulate bypass flow. In their approach the soil matrix and macropores are considered as one domain in which the water propagates as a kinematic pulse. Hatano and Sakuma (1991) used a combined capacity-bypass flow model to simulate transport of water and reactive solutes in an aggregated soil. They distinguished mobile, immobile and mixing phases for water and chemical interactions. However, in all these modelling approaches "real" soil structure, defined as the physical constitution of a soil material, as expressed by the size, shape and arrangements of the elementary particles and voids, is not considered.

Booltink et al. (1993) incorporated measured soil structure characteristics, such as fractal dimensions of macropore-stains formed by bypass flow, into a simple simulation model which could simulate bypass flow on laboratory scale. This model, based on previous work of Hoogmoed and Bouma (1980), can, however, not be used to simulate bypass flow on a field scale.

Studies on simulation of bypass flow on a field scale are rare. Bronswijk (1988) modelled water flow in a heavy clay soil with strong swelling and shrinkage. Shrinkage characteristics were used to calculate volume changes which were converted into cracking and subsidence of the soil. This model was field tested by comparison to measured data on cracking volume, ground water levels and



water contents. Jarvis and Leeds-Harrison (1987a) described a two-domain water balance model which explicitly accounts for the effect of soil structure. This model, which operates on a one day basis, was tested on a large undisturbed lysimeter (Jarvis and Leeds-Harrison, 1987b). The model was further developed by Jarvis (1991) to include transpiration and root water uptake, exchange processes between the two domains and water flow in the soil matrix. In these studies no attention was paid to variability of model parameters.

In the underlying field study an existing water transport model, LEACHW, (Wagenet and Hutson, 1992) was extended with subroutines describing bypass flow and interaction of bypass flow and surrounding soil, based on concepts as described by Booltink et al. (1993). Special attention is given on the effects of variability of model parameters and soil physical properties as characterized by using a Monte-Carlo procedure. This Monte-Carlo procedure was also used to calibrate the model. Finally, the calibrated model was validated on an independent data set.

## SIMULATION MODEL

The numerical simulation model LEACHM (Leaching Estimation and Chemistry Model) was used as the base model (Wagenet and Hutson 1992). LEACHM considers different processes in a variable soil profile, with or without plant growth. Processes included are: transient fluxes of water, fluxes and transformation of nitrogen, pesticides and salts; evapotranspiration and rainfall. In this study we used the water flow sub model LEACHW. A brief description of the model is given below. More detailed information can be found elsewhere (Wagenet et al., 1989; Wagenet and Hutson 1989).

### Simulation of water flow in the soil matrix

In LEACHW water flow is calculated using a finite-difference solution of the Richards' equation.

$$\frac{\delta\theta}{\delta t} = \frac{\delta}{\delta z} \left[ K(\theta) \frac{\delta H}{\delta z} \right] - U(z,t) \quad [1]$$

Where  $\theta$  is volumetric water content ( $\text{m}^3.\text{m}^{-3}$ )  $t$  is time (day),  $K$  is hydraulic conductivity ( $\text{m}.\text{day}^{-1}$ ),  $H$  is hydraulic head (m), composed of matrix potential  $\psi$  and profile depth  $z$ ,  $U$  is a sink term representing water uptake by plants ( $\text{day}^{-1}$ ).

The original Campbell  $K$ - $\theta$ - $\psi$  equations to describe soil hydraulic properties (Campbell, 1974; Hutson and Cass, 1987), were replaced by Van Genuchten's closed form equations (Van Genuchten, 1980).

In this approach the relative saturation  $S_e$  is calculated according to:

$$S_e = [1 + |\alpha \psi|^n]^m \quad [2]$$

where  $\alpha$  is the reciprocal value of the air entry in the soil ( $\text{cm}^{-1}$ ), and  $n$  and  $m$  are dimensionless empirical constants. Mualem (1976) defined  $m$  as:

$$m = 1 - \frac{1}{n} \quad [3]$$

The volumetric soil water content  $\theta$  as a function of  $\psi$  can now be calculated with:

$$\theta = \theta_r + \frac{(\theta_s - \theta_r)}{S_e}, \quad \psi < 0 \quad [4a]$$

and,

$$\theta = \theta_s, \quad \psi \geq 0 \quad [4b]$$

where  $\theta_r$  and  $\theta_s$  refer to the residual and saturated water content ( $\text{m}^3.\text{m}^{-3}$ ) respectively. The  $K(\theta)$  relation, finally, is given by

$$K(\theta) = K_s S_e^\gamma [1 - (1 - S_e^{\frac{1}{m}})^m]^2 \quad [5]$$

where  $K_s$  equals the saturated hydraulic conductivity ( $\text{m}.\text{day}^{-1}$ ) and  $\gamma$  is a dimensionless fitting parameter.

To prevent numerical instabilities caused by infinite differential water capacities, the maximum saturation was limited to 0.99 percent of the saturated water content.

### Simulation of bypass flow

Since LEACHW originally does not consider bypass flow, the model was extended with the following modifications:

- A. For every rain or irrigation event (30 minutes interval), the amount of water that could not infiltrate in the soil surface during the time period available (amount divided by intensity of the rain event) was determined. This surplus is stored on the soil surface and when a certain threshold value for surface storage (MinSS) is exceeded, water starts to flow into the macropores. Not all macropores present are equally accessible, due to small differences in micro relief (Booltink et al., 1993). A maximum surface storage (MaxSS) was therefore defined. Above this level water flows directly into the macropores. Between MinSS and MaxSS excess water is proportionally divided between surface storage and bypass flow. Water remaining on the surface continues to infiltrate as soon as the rain stops.
- B. In the macropore domain, water transport is simulated using a tipping-bucket approach. Propagation of the water front in the macropores ( $Bp_{prop}$ ), i.e. tipping-bucket switching times, is calculated using a regression equation based on rain intensities ( $R_{inten}$ ) and measured morphological properties (Booltink et al., 1993).

$$Bp_{prop} = a * R_{inten} + c * G_{fac} + b \quad [6]$$

Parameters a, b, and c are empirical constants. The geometry factor ( $G_{fac}$ ) is defined as:

$$G_{fac} = \left[ \frac{Vs_l}{100} \right] (Ds3-1) \quad [7]$$

where  $Vs_l$  is the volume of methylene blue stains (% vol.) in the limiting soil layer and  $Ds3-1$  is the depth weighed fractal dimension of the stains. High values of  $Vs_l$ , which are an indication for either a large number of

small macropores, or a few big water conducting macropores, will lead to a reduction of  $Bp_{prop}$ . The fractal dimension on the other hand gives information on the geometry of water conducting macropores. A macropore system with a  $Ds3-1$  value of 1 consists of mainly vertical oriented cracks, a value of 2, on the other hand, indicates that horizontal cracks dominate the system. For more discussion on the parameters  $Vs$  and  $Ds3$  we refer to Hatano and Booltink (1990) and Booltink et al. (1993).

- C. When water flows into macropores it is absorbed into macropore walls. Lateral absorption of water in vertical continuous macropores is based on absorption described by a diffusivity equation (eq. 8a). Vertical absorption of water on horizontal pedfaces of structure elements is dominated by gravity forces, described by the Darcy equation (eq. 8b) (Booltink et al., 1993).

$$Q_{p_{hor}} = D(\theta) \frac{\delta\theta}{\delta x} \quad [8a]$$

$$Q_{p_{ver}} = K(\psi) \left[ \frac{\delta\psi}{\delta x} + 1 \right] \quad [8b]$$

where  $Q_{p_{hor}}$  and  $Q_{p_{ver}}$  represent the potential horizontal and vertical absorption flux ( $m \cdot day^{-1}$ ), respectively,  $D$  is soil water diffusivity in  $m^2 \cdot day^{-1}$  and  $x$  is distance to the centre of the structure element (m).  $\delta\psi$  and  $\delta\theta$  were calculated as a geometrical mean between saturation (macropore wall) and the actual value of respectively  $\psi$  and  $\theta$  in the adjacent soil matrix as simulated with the Richard's equation. The potential absorption fluxes were reduced for the area of soil in contact with bypass water as indicated by the occurrence of stains. Contact areas for horizontal and vertical absorption were determined by using dye tracers in laboratory experiments. This procedure was previously described by Booltink et al. (1993) and is based on stratification of methylene blue stained macropores into sets of horizontal and vertical

oriented macropores using the ratio between area and perimeter ( $Ar/Pe^2 < 0.015$ ) (Bouma et al., 1977).

The reduced, actual absorption fluxes were added as an additional sink term to Richard's equation.

The surplus of water, not absorbed during the residence time in a given compartement, is added to the next compartment and finally to the ground water.

- D. Originally LEACHM does not provide a special bottom boundary condition which can simulate dynamic ground water levels. Simulation of such a ground water level was realized by combining a freely draining profile with an impermeable soil layer at the bottom of the profile. Deep drainage towards ditches ( $Q_d$ ) was simulated using a third order polynomial

$$Q_d(h) = C_0 + C_1 h + C_2 h^2 + C_3 h^3 \quad [9]$$

where  $h$  is the pressure potential in the bottom compartment and the constants  $C_0$ ,  $C_1$ ,  $C_2$ , and  $C_3$  are fitting parameters. A similar procedure was followed to simulate discharge through tile-drains ( $Q_{td}$ ). Parameter  $h$  in eq. 9, in that case, represents the ground water level above a specified drain depth.

## SITE DESCRIPTION

### Soil survey

On the experimental farm "De Kandelaar" in Eastern Flevoland in The Netherlands a tile drained research site of approximately 100 x 300 m was selected. Tile drains in this site are 150 m long and placed at distance of 48 meter.

The soil was classified as a mixed, mesic Hydric Fluvaquent (Soil Survey Staff, 1975). A soil profile description is presented in Table 1. Macropores present were both, vertical and horizontal interpedal planar voids.

A soil survey was carried out following a nested sampling scheme (Webster, 1977) as described by Finke et al. (1992). The soil survey resulted in 72 profile

descriptions. Semivariograms (Journel and Huijbregts, 1978) were constructed for texture and thickness of distinguished functional layers.

**Table 1** *Soil profile description of the study site at the Kandelaar experimental farm.*

---

A <sub>p</sub>	0.00 - 0.30 m:	clay (42% clay) with a moderate, medium angular blocky structure and an abrupt wavy boundary
2C	0.30 - 0.70 m:	clay loam (40% clay), strong, very coarse prismatic structure
3C	0.70 - 1.03 m:	silty clay loam (30% clay), strong, very coarse prismatic structure
4BC <sub>6</sub>	1.03 - 1.20 m:	sand, single grain

---

Continuity of flow patterns was quantified by tracer experiments. To explore macropore continuity, at 6 plots within the experimental field, an iodide tracer experiment as developed by Van Ommen et al. (1988) was carried out. Macropore geometry and the quantification of vertical and horizontal contact areas between bypass flow water and macropore walls was quantified in laboratory experiments on large soil samples (0.20 m diameter and 0.20 m length) as reported by Booltink et al. (1993).

### Monitoring

In 6 research plots in the research site tensiometer profiles were installed at 0.05, 0.25, 0.35, 0.50, 0.80 and 1.00 m depth. Ground water piezometers were installed in every one of the 6 plots and on a line perpendicular to the tile drains. Deep ground water (4.5 - 5.0 m) was measured on 2 plots. A fortnightly monitoring scheme was maintained as much as possible during the year.

A CR10-datalogger (Campbell) was used for continuous monitoring drain discharge on one tile drain in the centre of the study site. Measuring resolution of the drain outflow meter was  $0.03 \times 10^{-3}$  m. Water samples were taken every  $0.06 \times 10^{-3}$  m of discharge, using a sequential sampler (ISCO). The drain water samples were analyzed for  $\text{NO}_3^-$ ,  $\text{NH}_4^+$  and  $\text{Cl}^-$  in the laboratory. The CR10-datalogger was also used for measuring rain intensity and amount, soil surface temperature and ground water level on one plot within the experimental field. A full description of the experimental lay out of the site is given elsewhere (Booltink, 1993).

The parameters Dra\_C, Dra\_D and Dra\_E in the third order polynomial (eq. 9) for drain discharge, were fitted on simultaneously measured ground water levels and drain discharge rates in the winter period 1989-1990 using multiple regression techniques (Statistical Package for Social Studies, SPSS (1991)).

### **Soil physical analyses**

At every one of the 6 plots in every distinguished soil horizon, samples were taken in large steel cylinders, 0.20 m long and 0.20 m diameter. These samples were analyzed in the laboratory using the following methods.

1. Suction crust infiltrometer: determination of the saturated conductivity and unsaturated conductivity near saturation (Booltink et al., 1991a).
2. One-step outflow method: for unsaturated conductivity- and retentivity curve (Parker et al., 1985).
3. Pressure extractors were used to determine water retentivity data at high suctions (Klute, 1986).

Determination of the Van Genuchten parameters, for describing the hydraulic functions (Van Genuchten, 1980), was performed on both retentivity and outflow data, as described by Bootink et al., 1991b. Basic water retention and hydraulic conductivity curves, to be used as input in the simulation model, were determined by averaging individual curves for every distinguished soil layer.

## **SIMULATION PROCEDURE**

### **Monte-Carlo analysis**

The adjusted LEACHW-model was tested at data from the Kandelaar experimental farm. The objective of this test was to: (i) obtain information on the performance of the model and, (ii) calibrate the model on measured time series of phreatic ground water levels. For this purpose a Monte-Carlo analysis was used. In this Monte-Carlo analysis (MCA) the uncertainty of model inputs is characterized in terms of distributions with or without mutual correlations among the various parameters.

From exploratory simulation runs the maximum compartment thickness was determined to be 0.02 m. The total profile depth was set to 1.5 m and consists, therefore, of 75 compartments.

During the exploratory runs it appeared that using the standard soil layers, as determined in the soil survey, bypass flow only occurred in a limited number of cases. An additional top soil layer of 0.02 m, which reflected surface resistance, caused by surface smearing during ploughing and small loose structure elements, was, therefore, added.

In table 2 the most relevant input parameters, as selected from the exploratory simulation runs, are briefly summarized:

- \* Vertical contact areas (Vercon\_up c.q. \_lo) represent the physical contact between bypass water and vertically oriented macropores for respectively top- and subsoil. Horizontal contact areas (Horcon\_up c.q. \_lo) represent the contact between bypass flow water and horizontal oriented macropores. Distributions were calculated on 15 samples.
- \*  $V_{s1}$  and  $D_{s3}$  are respectively the total volume of stained macropores and the 3-D fractal dimension of the stained macropores. These parameters were obtained in laboratory experiments as described by Booltink et al. 1993. Distributions were calculated on 15 samples.
- \* Minimum and maximum surface storage of water (threshold values before bypass flow occurs) are given by MinSS and MaxSS. Since no field measurements for these parameters were available, a uniform distribution with adequate minimum and maximum values, determined in the exploratory simulation runs, was selected. The value of MaxSS has to be added to MinSS.
- \* WCS\_1 to WCS\_4 depict the saturated water contents ( $\theta_s$ ) of the distinguished soil layers. WCS was determined on 24, 16, 16, and 8 samples for the respective layers 1, 2, 3, and 4.
- \* Similar to WCS, CON\_0 to CON\_4 represent the saturated hydraulic conductivities ( $K_s$ ) for the various soil layers. Distributions were calculated on the same amount of samples as WCS. For CON\_0 no measurements were made. Minimum and maximum values were determined during the exploratory model runs.
- \* Dra\_C to Dra\_E are the regression coefficients in the 3rd-order polynomial tile drainage characteristic ( $Q_{td}$ ). The coefficients were determined on 150 measured values for drain discharge and ground water level during the winter season 1989-1990.



Table 2 Overview of parameters used in Monte-Carlo analysis

Parameter	Distribution	Mean	Variance	Minimum	Maximum	Description	Dimension
Vercon_up	normal	0.174	0.004225	0.044	0.304	Vertical contact area 0.00-0.30 m depth	m <sup>2</sup> .m <sup>2</sup>
Vercon_lo	lognormal	0.0211	0.0145	0.001	0.07	Vertical contact area 0.30-1.03 m depth	m <sup>2</sup> .m <sup>2</sup>
Horcon_up	lognormal	0.0115	0.0017	0.001	0.10	Horizontal contact area 0.00-0.30 m depth	m <sup>2</sup> .m <sup>2</sup>
Horcon_lo	lognormal	0.0016	0.0019	0.001	0.04	Horizontal contact area 0.30-1.03 m depth	m <sup>2</sup> .m <sup>2</sup>
Vsl	lognormal	0.964	1.133	0.10	8.0	Volume of soil stained	%
Ds3l	normal	2.011	0.0177	1.75	2.26	Fractal dimension of stained area	-
B_tv	normal	1.718E-04	3.650E-10	1.302E-04	2.133E-04	Constant b in equation 6	-
A_tv	normal	-1.456E-07	1.399E-15	-2.271E-07	-6.410E-08	Constant a in equation 6	-
D_tv	normal	-7.661E-04	7.938E-07	-2.707E-03	1.175E-03	Constant c in equation 6	-
MinSS	uniform			5.000E-05	5.000E-04	Minimum surface storage	m
MaxSS	uniform			1.000E-05	3.000E-04	Maximum surface storage (to be added to MinSS)	m
WCS_1	normal	0.484	1.000E-04	0.46	0.50	Water content saturated 0.00-0.30 m depth	m <sup>3</sup> .m <sup>3</sup>
WCS_2	normal	0.623	1.000E-04	0.60	0.64	Water content saturated 0.30-0.70 m depth	m <sup>3</sup> .m <sup>3</sup>
WCS_3	normal	0.620	2.500E-03	0.50	0.72	Water content saturated 0.70-1.03 m depth	m <sup>3</sup> .m <sup>3</sup>
WCS_4	normal	0.320	1.000E-04	0.30	0.34	Water content saturated 1.03-1.50 m depth	m <sup>3</sup> .m <sup>3</sup>
CON_0	uniform			1.000E-04	0.02	Saturated hydraulic conductivity 0.00-0.02 m depth	m.day <sup>-1</sup>
CON_1	uniform			0.1	0.20	Saturated hydraulic conductivity 0.02-0.30 m depth	m.day <sup>-1</sup>
CON_2	normal	0.59	0.0160	0.050	1.25	Saturated hydraulic conductivity 0.30-0.70 m depth	m.day <sup>-1</sup>
CON_3	lognormal	0.22	0.0049	0.010	0.48	Saturated hydraulic conductivity 0.70-1.03 m depth	m.day <sup>-1</sup>
CON_4	normal	0.25	0.0125	0.050	0.40	Saturated hydraulic conductivity 1.03-1.50 m depth	m.day <sup>-1</sup>
Dra_C	normal	1.637E-01	6.204E-04	0.114	0.213	Constant C1 in drainage discharge function (eq. 9)	-
Dra_D	normal	-2.150E-03	1.887E-06	-4.870E-03	5.740E-04	Constant C2 in drainage discharge function (eq. 9)	-
Dra_E	normal	2.971E-05	3.232E-10	-5.932E-06	6.540E-05	Constant C3 in drainage discharge function (eq. 9)	-
Deep_D	normal	-3.100E-03	4.706E-06	-7.778E-03	1.586E-03	Constant C1 in deep drainage disch. function (eq. 9)	-
Deep_E	normal	1.618E-05	4.165E-11	2.234E-06	3.012E-05	Constant C2 in deep drainage disch. function (eq. 9)	-
Deep_F	normal	-9.194E-09	2.465E-17	-1.992E-08	1.532E-09	Constant C3 in deep drainage disch. function (eq. 9)	-
Deep_G	normal	-9.223E-02	3.043E-02	-0.469	0.285	Constant C0 in deep drainage disch. function (eq. 9)	-
Struc_0	uniform			0.010	0.120	Structure element size 0.00-0.02 m depth	m
Struc_1	uniform			0.040	0.120	Structure element size 0.02-0.30 m depth	m
Struc_2	uniform			0.200	0.400	Structure element size 0.30-0.70 m depth	m
Struc_3	uniform			0.150	0.300	Structure element size 0.70-1.03 m depth	m

\* for uniform distribution only minimum and maximum values are specified.

- \* Deep\_D to Deep\_G depict the regression coefficients for the deep drainage ( $Q_d$ ) towards ditches in eq. 9. The coefficients were calculated recursively on measured ground water levels and model simulation runs in the winter season 1989-1990.
- \* Struc\_0 to Struc\_3 represent the structure element size in the distinguished soil layers determined during the soil survey.

In cases of unclear distributions, or lack of data, uniform distributions with adequate minimum and maximum values, reflecting the actual uncertainty of the parameters, were selected.

The Monte-Carlo analysis was carried out using the newly developed software package UNCSAM 1.1 (Jansen et al., 1993a). This package was developed for uncertainty and sensitivity analysis on mathematical models. Sampling of the distributions was done using the Latin Hypercube Sampling (LHS) technique (McKay et al., 1979; Iman and Conover, 1980), which uses a stratified way of sampling from separate parameter distributions on basis of a subdivision in disjunct equiprobable intervals, resulting in an efficient and, therefore, relative small number of samples. When using LHS the parameter space is adequately represented with a number of samples ( $N$ ) between  $2p$  and  $5p$ , where  $p$  is the number of parameters to be sampled (Jansen et al., 1993a). In this study, with 31 parameters, the number of samples was 150.

Sampling distributions of mutually correlated parameters (e.g. drainage characteristics) will result in unrealistic combinations of parameters. To overcome this problem UNCSAM 1.1 provides the possibility for incorporating mutual correlations among parameters in the sampling procedure (Jansen et al., 1993a)

### Sensitivity analysis

Model simulation outputs were evaluated in a combined uncertainty and sensitivity analysis, using UNCSAM 1.1. In the sensitivity analysis the variations of the various parameters was tested against simulated water balance terms by means of a linear regression model (eq. 10).

$$y(k) = \beta_0 + \beta_1 x_1(k) + \dots + \beta_p x_p(k) + e(k) \quad k = 1, \dots, N \quad [10]$$

where  $\beta_0, \beta_1, \dots, \beta_p$  denote the ordinary regression coefficients, obtained by minimizing the sum of squares error ( $e(k)$ ). The values  $y(k)$  and  $x_1(k), \dots, x_p(k)$

represent the model output and input parameters respectively in the  $k$ -th model simulation.  $N$  denotes the total number of simulation runs.

In the uncertainty analysis attention was focused on structural model errors, so-called unstructured uncertainty (Keesman and Van Straten, 1989), i.e. uncompensated model error due to an inadequate model structure.

Total explained variance of the various model input parameters  $x_1, \dots, x_p$  on  $y(k)$  was used as a measure for structural model error.

Most significant model parameters were selected for further model calibration.

### **Model calibration**

Although model input parameters and their distributions reflect individual variability, not all combinations of these input parameters necessarily result in realistic simulation results. Further calibration is, therefore required. In this study a set-theoretic approach, developed by Jansen (1993) and Jansen et al. (1993b) was used. This **RO**tated **RA**ndom **SC**an (RORASC) procedure, based on previous work of Keesman and Van Straaten (1988, 1989) and Keesman (1989,1990) uses an iterative Monte-Carlo search procedure to reduce the parameter space by updating the currently available set of acceptable parameters. In this way one gradually and efficiently zooms in on the acceptable parameter set.

The RORASC procedure consists of three basic steps (Jansen, 1993):

1. ***Initialization.*** Before starting the iterative procedure, an initial set of parameters has to be determined, which serves as a starting point for the subsequent simulations. In this study the initial set of 150 model runs, as used for the sensitivity and uncertainty analysis, was selected.
2. ***Generation of new candidate samples.*** Simulated ground water levels for the winter season 1989/1990 were compared to measured time series for the same period. By visual inspection of the results, the simulation runs were divided in a population of acceptable and non-acceptable simulation results. The generation of a new set of parameters is achieved by transforming or rotating the original parameter space to focus on the current set of acceptable parameters. This transformation is based on the decomposition of the covariance matrix of the accepted parameters, as described in detail by Jansen (1993) and Jansen et al. (1993b). Subsequently a random-scan on basis of uniform random sampling in this

transformed space is performed which serves as a new set of candidate samples.

3. Simulation and acceptance. Model simulations are performed for the newly generated candidate samples and results are again divided into a population of acceptable and non-acceptable results. The file containing the total number of acceptable results is updated and the transformation and random-scan procedure are repeated iteratively until simulation results are satisfactory.

To obtain a reliable covariance matrix when using LHS in combination with RORASC a number of samples  $N > 10p$  is recommended, where  $p$  is the number of parameters to be sampled.

### Validation

A Monte-Carlo sampling was performed on the parameters obtained from the final set of acceptable simulation results, which was used as input for a validation session. Parameters showing insignificant sensitivity were fixed at a value obtained in the sensitivity analysis. The model validation was carried out using measured ground water levels and drain discharge from the winter season 1991-1992.

## RESULTS

### Data collection

Semivariograms constructed for soil texture and thickness of the distinguished functional layers all showed large nugget effects indicating that spatial correlation of the properties was weak. The lack of spatial correlation is mainly caused by the calm sedimentation regime in this part of a former sea which has led to a homogeneous deposition of soil material. Hence all variability was regarded as variation of a stochastic nature.

From the iodide experiments it appeared that the number of macropores sharply decreased around the boundary between plough layer and subsoil at about 0.30 m depth. Macropores present below the plough layer are permanent and originate from structural shrinkage processes during land reclamation. These

large macropores in the subsoil were continuous to the sandy subsoil at 1.0 m depth.

Since iodide is absorbed deep inside structure elements it cannot be used to derive contact areas between bypass flow water and macropore walls. Macropore geometry and contact areas were, therefore, determined on large soil columns. The procedure is extensively described by Booltink et al. (1993) and will not be further discussed here. The sharp decrease around the boundary between the plough layer and subsoil was confirmed by these experiments. Average contact areas for vertically and horizontally oriented macropores (respectively Vercon and Horcon in table 2) for top- and subsoil (respective subscripts  $_{up}$  and  $_{lo}$ ) show a decline of 85 to 90 percent for top- compared to subsoil.

During the first year of study, tensiometer profiles were monitored on a fortnightly time base. Data obtained from these measurements exhibited large scatter which resulted from the location of the tensiometer near macropores (fast reactions) or within structure elements (slow reactions) as previously reported by Booltink (1993). Tensiometer readings are for this reason a good indicator for whether or not bypass flow occurs. Such readings are unsuitable for use in a model calibration procedure.

Bypass flow is clearly demonstrated on measured time series of ground water levels e.g. on day number 19 and 57 in fig. 2a. Measured ground water levels exhibit a sharp rise of circa 0.4 m after rain events with high intensities. Instant drain discharge occurs when the ground water level is at a depth less than 0.82 m below soil surface. When drain discharge rates were plotted against measured ground water levels a hysteretic behaviour was sometimes visible. The regression parameters  $Dra_C$ ,  $Dra_D$  and  $Dra_E$ , describing the third order polynomial drain discharge characteristic, do not take into account this hysteretic behaviour. To correct for this inaccuracy the three parameters were incorporated in the Monte-Carlo analysis. The hysteresis of the drain discharge characteristic is probably caused by shrinkage and swelling of the soil around the tile drain. In table 3 average parameters from the Van Genuchten and Mualem equations (eq. 2-5) are presented. To differentiate between the saturated conductivity of the overall sample ( $K_s$ ) i.e. the maximum capacity for a sample to conduct water and the saturated hydraulic conductivity of the soil matrix ( $K_{(s)}$ ) (Bouma, 1982) the suction crust infiltrometer was used to determine the point in the conductivity curve where the soil matrix was just saturated. In the inverse

modelling procedure used, for the derivation of the hydraulic parameters, the parameters  $\alpha$ ,  $n$ ,  $\theta_s$ ,  $\theta_r$ , and  $\gamma$  were optimized within their physical boundaries.

**Table 3** *Averaged Van Genuchten and Mualem parameters as used in the simulation procedure.*

Profile depth (m)	$\alpha$ ( $\text{cm}^{-1}$ )	$n$ (-)	$\theta_s$ ( $\text{m}^3 \cdot \text{m}^{-3}$ )	$\theta_r$ ( $\text{m}^3 \cdot \text{m}^{-3}$ )	$\gamma$ (-)	$K_{(s)}$ ( $\text{m} \cdot \text{day}^{-1}$ )
0.00 - 0.30	0.00264	1.17184	0.484	0.001	-12.000	0.11
0.30 - 0.70	0.12238	1.08774	0.623	0.001	-22.985	0.59
0.70 - 1.03	0.01920	1.13178	0.620	0.050	-15.010	0.22
1.03 - 1.50	0.01320	1.33779	0.320	0.050	-7.361	0.25

When optimizing the various parameters it appeared that optimizations could be improved when also  $K_{(s)}$  was included.  $K_{(s)}$  was, therefore, optimized within the limits of measured  $K_{(s)}$  and  $K$  at a pressure head of approximately -1.0 kPa. To reduce the total amount of parameters in the Monte-Carlo procedure only the most important,  $K_{(s)}$  and  $\theta_s$ , were used.

**Sensitivity analysis**

The sensitivity analysis was carried out on the simulated mass balance terms for the winter season 1989-1990. Since not all parameter combinations show linear relations with the various mass balance terms, ordinary regression coefficients could not be used. Rank regression coefficients were used instead (ordinary regression coefficients were replaced by their rankings, where the smallest value gets ranking 1, the next one 2, etc.). This technique can be used to linearize nearly non-linear relations (Iman and Conover, 1982). In table 4 an overview of the parameters which had an influence on the simulated mass balance terms with a 95 % significancy (i.e.  $-2.0 > t\text{-statistic} > 2.0$ ) are presented. Next to the sensitivity of a parameter for a mass balance term, the contribution of that term to the total mass balance was also considered. These are given at the bottom of table 4, together with the total explained variance of the regression model (eq. 10) for the mass balance term.

Table 4

Parameters which contributed with 95% significance to the simulated cumulative mass balance terms using a linear regression model (eq.10). Total explained variance ( $R^2$ ) and the average simulated amount in the mass balance (Avg (mm)) is indicated, together with the standard deviation (Std (mm)).

Infiltration		Evaporation		Absorption		Bypass		Drain discharge		Leachate	
param	t-stat	param	t-stat	param	t-stat	param	t-stat	param	t-stat	param	t-stat
CON_1	16.82	CON_0	18.43	CON_0	-10.36	CON_1	-18.04	CON_0	-8.71	Deep_D	12.41
CON_0	13.76	CON_1	14.35	CON_1	-9.62	CON_0	-13.78	Deep_D	-7.28	Deep_E	9.91
CON_2	2.04	MinSS	2.59	Vercon_lo	9.11	CON_2	-2.02	CON_1	-6.79	Deep_G	9.51
		CON_2	2.05	Horcon_lo	5.66			Deep_E	-5.66	Deep_F	6.79
				D_trv	2.76			Deep_G	-5.36	CON_4	-5.33
				B_trv	2.69			WCS_3	-4.35	WCS_3	5.30
				A_trv	2.14			CON_4	3.99	CON_3	4.76
				Deep_G	2.04			Deep_F	3.73	Vercon_lo	2.52
								WCS_4	-2.01	CON_2	2.51
Total											
$R^2$	0.76		0.79		0.67		0.78		0.62		0.63
Avg	195.0		76.4		8.3		64.6		125.8		70.8
Std	32.7		4.8		11.2		25.2		11.6		10.4

Table 4 shows that the saturated hydraulic conductivity of layers 0 and 1 (CON\_0 and CON\_1) are dominating in most regression models. Cumulative absorption into macropore walls is also influenced by the horizontal and vertical

contact areas in the subsoil (Vercon\_lo and Horcon\_lo). Parameters regulating tortuous water transport in macropores, parameter D\_trv, B\_trv, and A\_trv, also have a significant impact on cumulative absorption into macropores walls. Considering the low contribution of only 8.3 mm to the total mass balance of 268 mm, this mass balance term does not play an important role in the overall simulation results. This can be explained by the relative small contact areas and the wet soil conditions during winter. In lighter textured soils with smaller structure elements or under dryer initial conditions, absorption will become more important as indicated by Booltink and Bouma (1993).

Leachate at the bottom of the soil profile is mainly influenced by the regression parameters of the deep drainage characteristic (Deep\_D, Deep\_E, Deep\_G and Deep\_F). Drain discharge is more dependent on parameters which control the transport of the water towards the drain than by the discharge-fitting parameters which regulate the actual discharge.

The total explained variances in table 4 indicate that mass balance terms could be well predicted with the various regression models, which implies that the aggregated model structure was able to adequately describe the processes considered.

### Model calibration

The underlined parameters in table 4 were selected for calibrating the simulation model. According to the criteria that for the RORASC procedure at least 10p simulations are required (where p is the number of parameters), 80 simulation runs were performed. Parameters not varied, were fixed at values obtained from the best simulation run in the first Monte-Carlo session. Calibration was performed on measured cumulative drain discharges during the winter season 1989-1990 and the measured time series of ground water levels in the same period. In the RORASC optimization procedure only three iterative steps had to be performed. The third step did not lead to significant better simulation results, indicating that the parameters had reached their limits. It also indicates that the initial parameter space was close to the calibrated one.

In fig. 1 the effect of the RORASC procedure is demonstrated on the surface storage parameter MinSS. This parameter can not be measured in experiments and was, therefore, ill-defined by means of a uniform distribution with maximum and minimum values (table 2). Due to consequently dividing the



simulation results in acceptable and non-acceptable results the original uniform distribution (C01 in fig. 1) slowly turns into a lognormal distribution (C02, C03). From fig. 1 it can also be seen that the third simulation run (C03) did not improve the parameter space of MinSS much further.

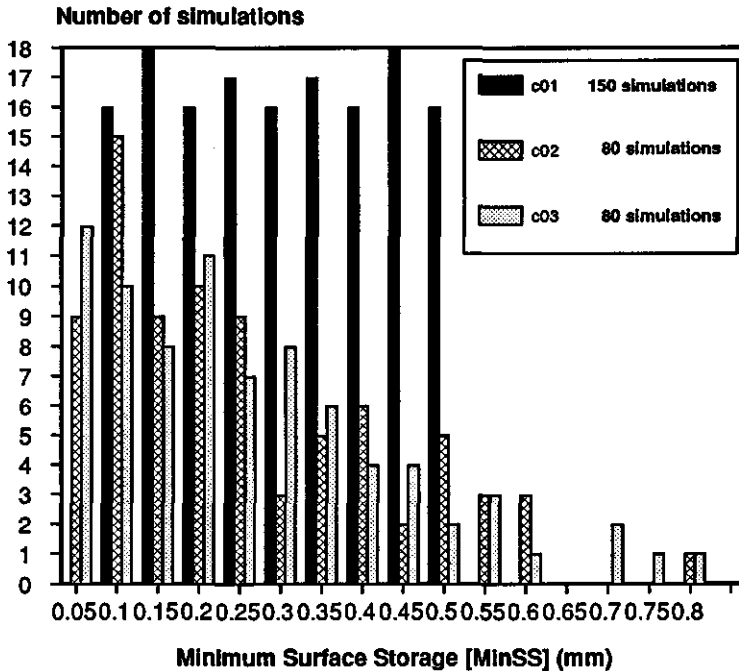
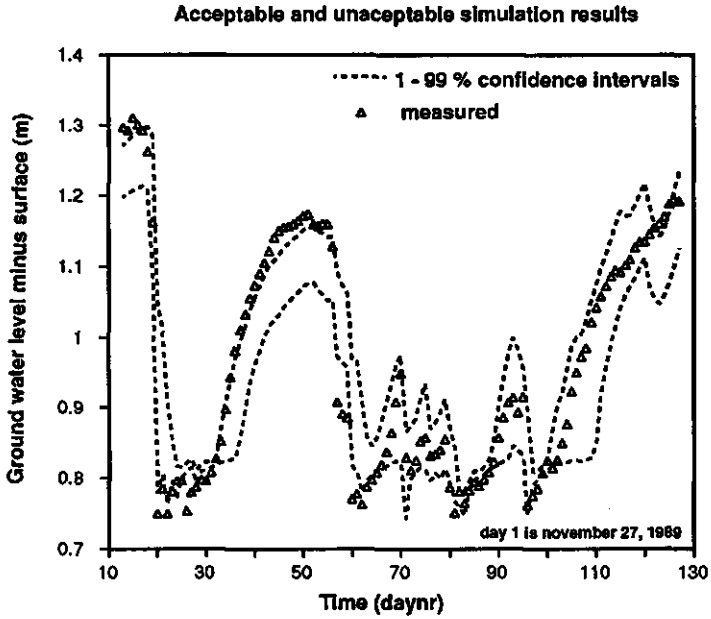


**Figure 1** The effect of the RORASC procedure on the original uniform distribution of surface storage parameter MinSS (C01). C02 and C03, respectively, show the transformation into a lognormal distribution. The number of simulations performed for the various steps has been included.

In fig. 2a and 2b measured ground water levels are presented with the 1-99% confidence intervals of the simulation results. The effect of the RORASC procedure is demonstrated by the smaller band between the upper and lower 1% confidence intervals which is especially obvious from day number 60 to 110. When interpreting these data one has to consider the difference in sensitivity for the ground water above and below the depth of the tile-drains (0.82 m minus surface).

2a



2b

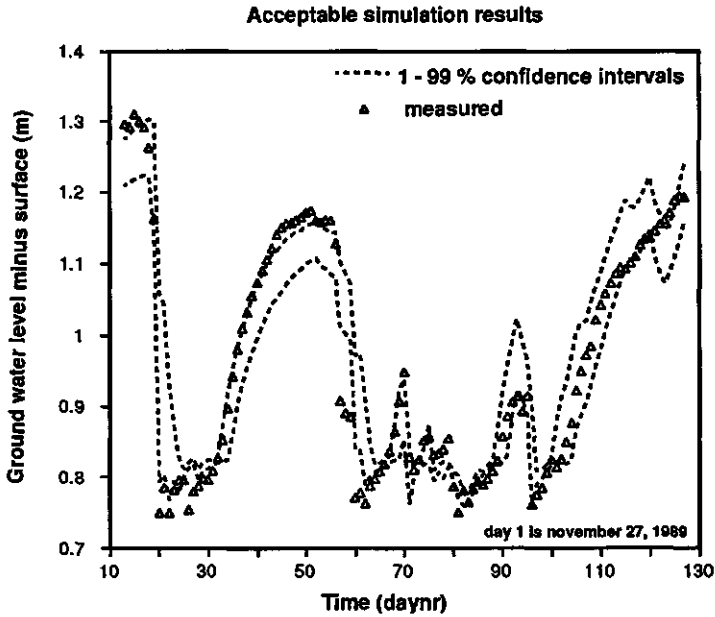


*Figure 2 Comparison of measured ground water levels for the winter season 1989-1990 with upper and lower 1% confidence intervals for all (acceptable and unacceptable) simulation results (2a) and for acceptable simulation results only (2b).*

While a simulated deviation of only a few centimeters below the tile-drain level will have a small effect on the water balance, an equal deviation will have a large effect on the drain discharge if the ground water level is above tile-drain depth, due to high drain discharge.

### Model validation

Using the input parameters as they were obtained in the third RORASC step, a Monte-Carlo simulation of 80 model runs was carried out to validate the model. In fig. 3 measured ground water levels in the winter season 1991-1992 are compared to the simulation results for the same period. The overall agreement between measured and simulated results is good.

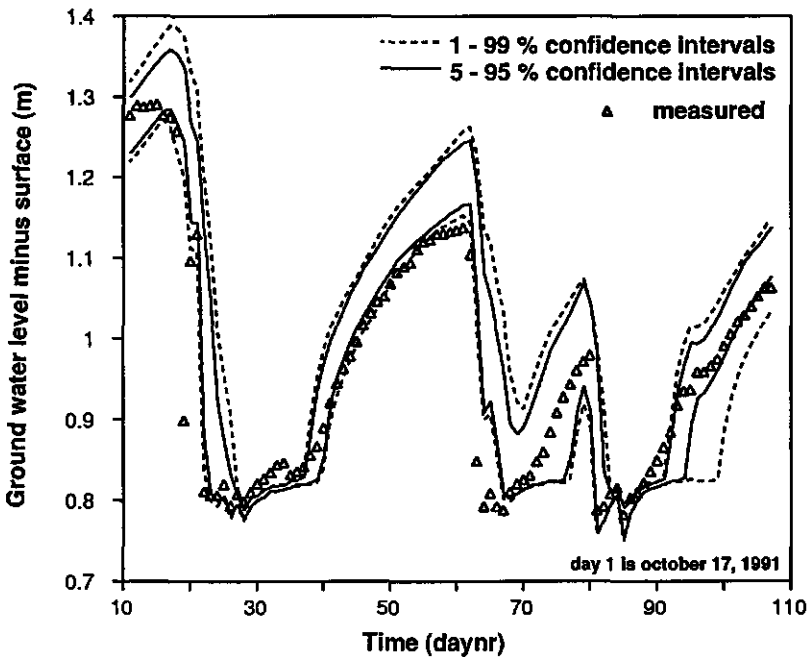


**Figure 3** *Validation results of simulated ground water levels for the winter season 1991-1992.*

Except for the bypass flow event around day number 65, all events were well simulated with the model. The model overestimates the ground water level in the period from day 45 to 60. This does, however, not necessarily lead to large mass balance errors, as discussed in the model calibration section.

The generally small difference between the 1 and 5% confidence intervals in fig. 3 indicates that the calibrated parameter space was within the limits and does, therefore, not lead to large simulation errors or outliers. Only around day number 95, a distinct difference between the 1 and 5% levels can be seen. In fig. 4 the 1 and 5% confidence intervals of the simulations are compared to the measured cumulative drain discharge.

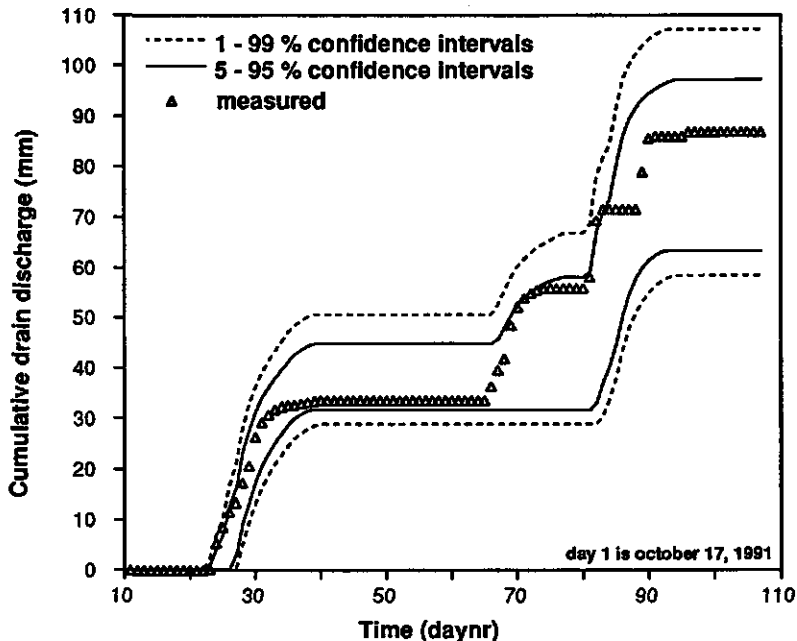


Figure 4 Validation results of simulated cumulative drain discharge for the winter season 1991-1992.

Although it seems that the model predicts the start of the drain discharge peaks a little late, the overall agreement is good. The average simulated cumulative drain discharge of 79.9 mm was close to the measured cumulative drain discharge of 86.9 mm.

In table 5 simulated terms of the mass balance are presented. Cumulative surface infiltration is the most important term in the water balance. Bypass flow is also a substantial term and was calculated to be 48.1 mm. Absorption along macropores in this winter period was, again, relatively small with 8.7 mm. The

mass balance error was small: for most simulations (60) the value was 0.6 mm with only a few outliers.

**Table 5** *Simulated cumulative average mass balance for the period 1991-1992. Delwat refers to profile water change over the simulation period and MBE to the mass balance error. STD is the standard deviation, SKN the skewness or 3th moment of the distribution and CV the coefficient of variation.*

	Infiltration	Evaporation	Drainage	Absorption	Bypass	Leachate	Delwat	MBE
Average (mm)	131.5	38.0	79.9	8.7	48.1	66.8	2.9	0.6
STD (mm)	37.5	3.9	11.5	11.7	27.9	10.9	1.2	0.4
SKN	-10.6	-23.9	5.3	3.9	11.9	-0.5	-0.1	0.0
CV (%)	28.5	10.4	14.4	134.7	58.1	16.3	41.6	58.7

The skewness and coefficient of variation of the mass balance terms in table 5 show that, except for the terms Leachate, profile water change (Delwat) and the mass balance error (MBE), distributions show an asymmetric tailing, towards positive values for a positive skewness and towards negative values for a negative skewness.

## CONCLUSIONS

The LEACHW model, extended with a module which describes tortuous water transport in macropores, is capable of simulating bypass flow under field conditions, as is illustrated by good agreement between the independent comparison of measured and simulated time series of ground water levels.

Water flow processes, simulated by the model, are well described as indicated by the explained variances obtained in the uncertainty analysis on the mass balance terms.

The pedotransfer function, based on measured soil structure characteristics is capable of predicting the propagation velocity of the water front inside macropores and, related to that, allows the calculation of water absorption along vertically and horizontally oriented macropores. In this study, water absorption

along macropore walls was only a small fraction of the total water balance. In soils with high contact areas between bypass water and macropore walls or dry initial conditions, this factor is bound to become more important. Well defined contact areas will become extremely important when, next to water transport in macropores, also reactive transport of solutes is simulated.

The simulation model does not take into account the effects of shrinkage and swelling of the soil matrix. The process of swelling and shrinkage in the clay soil being considered was, however, not very relevant. In the relatively loose-structured top soil smaller macropores never completely close, whereas in the subsoil macropores (cracks) were permanent as a result of ripening during land reclamation. The only effect which might have been caused by swelling and shrinkage was the slight hysteresis in the drain discharge curves.

From the conducted sensitivity analysis it appeared that the saturated hydraulic conductivity of the upper soil matrix ( $K_{(s)}$ ) was the most important parameter controlling bypass flow. Soil physical methods applied should, therefore, be able to quantify the effects of soil structure (e.g. crust infiltrometer, Booltink et al., 1991a). The high sensitivity for the saturated hydraulic conductivity also implies a high sensitivity for rain intensities. Since the measuring interval in the monitoring set up was 15 minutes, rain intensities are always a manifold of a 15 minutes. This results in smoothed values, especially for short rain events with high intensities. For this type of research it might, therefore, be better to work with continuously recording rain gauges.

Use of the rotated random scan procedure (RORASC) in combination with a Monte-Carlo simulation procedure provides a valuable tool for obtaining ill-defined model parameters and for restricting initially wide parameter spaces to more realistic values for the system considered. This makes interpretation of data in terms of confidence intervals more realistic.

## ACKNOWLEDGEMENTS

The author wishes to thank Prof. Dr. J. Bouma for critically reading the manuscript, P.D. Peters for the large number of soil physical analyses and Dr. P.H.M. Jansen of the RIVM for his assistance on the UNCSAM and RORASC software. This study was funded by the EC-research project STEP-0032-C.

## REFERENCES

- Beven, K., and R.T. Clark. 1986. On the variation of infiltration into a homogeneous soil matrix containing a population of macropores. *Water Resour. Res.* 18:1311-1325.
- Beven, K., and P.F. Germann. 1982. Macropores and water flow in soils. *Water Resour. Res.* 22:383-388.
- Booltink, H.W.G. 1993. Field monitoring of nitrate leaching and water flow in a structured clay soil. Submitted for publication in *Agriculture, Ecosystems and Environment*.
- Booltink, H.W.G. and J. Bouma. 1993. A sensitivity analysis on processes affecting bypass flow. *Hydrol. Proc.* 7:33-43.
- Booltink, H.W.G., J. Bouma, and D. Giménez. 1991a. A suction crust infiltrometer for measuring hydraulic conductivity of unsaturated soil near saturation. *Soil Sci. Soc. Am. J.* 55:566-568.
- Booltink, H.W.G., R. Hatano, J. Bouma. 1993. Measurement and simulation of bypass flow in a structured clay soil: a physico-morphological approach. *J. Hydrol.* (in press)
- Booltink, H.W.G., C. Kosmas, E. Spaans, and P.D. Peters. 1991b. Application of the one-step outflow method for determining hydraulic properties of soils. *Soil and ground water research report II: Nitrate in soils. Commission of the European Communities. Luxembourg.* p:116-127.
- Bouma, J. 1982. Measuring the hydraulic conductivity of soil horizons with continuous macropores. *Soil Sci. Soc. Am. J.* 46:438-441.
- Bouma, J. 1984. Using soil morphology to develop measurement methods and simulation techniques for water movement in heavy clay soils. In: J. Bouma and P.A.C. Raats (Eds.), *Proc. ISSS Symp. Water and solute movement in heavy clay soils, Wageningen, Netherlands, 27-31 august 1984. Publ. 37. Inst. for Land Reclamation and Improvement, Wageningen,* pp. 298-316.
- Bouma, J., A. Jongerius, O. Boersma, A. de Jager, and D. Schoonderbeek. 1977. The function of different types of macropores during saturated flow through four swelling soil horizons. *Soil Sci. Soc. Am. J.*, 41:945-950.
- Bronswijk, J.J.B. 1988. Modelling of waterbalance, cracking and subsidence of clay soils. *J. Hydrol.* 97:199-212.
- Campbell, G. 1974. A simple method for determining unsaturated conductivity from moisture retention data. *Soil Sci.* 117:311-314.

- Chen, C., and R.J. Wagenet. 1992. *Simulation of water and chemicals in macropore soils. Part I. Representation of the equivalent macropore influence and its effect on soil water flow.* *J. Hydrol.* 130:105-126.
- Edwards, W.M., R.R. van der Ploeg, and W. Ehles. 1979. *A numerical study of the effects of noncapillary-sized pores upon infiltration.* *Soil Sci. Soc. Am. J.* 43:851-856.
- Finke, P.F., J. Bouma, and A. Stein. 1992. *Measuring field variability of disturbed soils for simulation purposes.* *Soil Sci. Soc. Am. J.* 56:187-192.
- Germann, P.F. 1990. *Preferential flow and the generation of runoff. 1. Boundary flow theory.* *Water Resour. Res.* 26:3055-3063.
- Germann, P.F. 1985. *Kinematic wave approximation to infiltration into soils with sorbing macropores.* *Water resour. Res.* 21:990-996.
- Hatano, R., and T. Sakuma. 1991. *A plate model for solute transport through aggregated soil columns. I. theoretical descriptions.* *Geoderma.* 550:13-23.
- Hoogmoed, W.B., and J. Bouma. 1980. *A simulation model for predicting infiltration into a cracked clay soil.* *Soil Sci. Soc. Am. J.* 44:458-461.
- Hutson, J.L., and A. Cass. 1987. *A retentivity function for use in soil water simulation models.* *J. Soil Sci.* 38:487-498.
- Iman, R.L., W.J. Conover. 1980. *Small sample sensitivity analysis techniques for computer model, with an application to risk assessment. Communications in Statistics, Vol. A9, pp 1749-1842. Rejoinder to comments, ibid. pp. 1863-1974.*
- Iman, R.L., W.J. Conover. 1982. *A distribution free approach to inducing rank correlations among input variables. Communications in Statistics, Vol. B11, pp 311-334.*
- Jansen, P.H.M. 1993. *RORASC an SELACC: Software for performing the rotated-random-scanning calibration procedure. CWM memorandum, in preparation. RIVM, Bilthoven, The Netherlands.*
- Jansen, P.H.M., P.S.C. Heuberger, and R. Sanders. 1993a. *UNCSAM 1.1: a software package for sensitivity and uncertainty analysis; manual. RIVM report nr. 959101004, RIVM, Bilthoven, The Netherlands.*
- Jansen, P.H.M., P.S.C. Heuberger, and R. Sanders. 1993b. *Rotated-Random Scanning: a simple method for set valued model calibration. RIVM internal report, in preparation, RIVM, Bilthoven, The Netherlands.*
- Jarvis, N.J. 1991. *Macro a model of water movement and solute transport in macroporous soils. Dept. of Soil Sciences, Swedish Univ. of Agric. Sci., Uppsala, Sweden. pp 1-58.*
- Jarvis, N.J., and P.B. Leeds-Harrison. 1987a. *Modelling water movement in drained clay soil. I. Description of the model, sample output and sensitivity analysis. J. Soil Sci.* 38:487-498.
- Jarvis, N.J., and P.B. Leeds-Harrison. 1987b. *Modelling water movement in drained clay soil. II. Application of the model in Evensham series clay soil. J. Soil Sci.* 38:499-509.
- Journel, A.G., and C.J. Huijbregts. 1978. *Mining geostatistics. Academic Press, New York.*
- Keesman, K.J. 1989. *A set-membership approach to the identification and prediction of ill-defined systems: application to a water quality system. Ph.D. Thesis, Univ. of Twente, Enschede, The Netherlands,*
- Keesman, K.J. 1990. *Membership-set estimation using random scanning and principal component analysis. Mathematics and Computers in simulation.* 32:535-543.



- Keesman, K.J., and G. van Straaten. 1988. *Embedding of random scanning and principal component analysis in set-theoretic approach to parameter estimation*. Proc. 12th IMACS World Congress, Paris.
- Keesman, K.J., and G. van Straaten. 1989. *Identification and prediction propagation of uncertainty in models with bounded noise*. Intern. Journal of Control, 49:2259-2269.
- Klute, A. 1986. *Methods of soil analysis part 1. Physical and Mineralogical methods*. Second edition. Am. Soc. Agronomy, Monograph 9, Madison USA.
- McKay, M.D., Beckman R.J. and W.J. Conover. 1979. *A comparison of three methods for selecting values of input variables in the analysis of output from a computer code*. Technometrics. 28:211-217.
- Mualem, Y. 1976. *A new model for predicting the hydraulic conductivity of unsaturated porous media*. Water Resour. Res. 12:513-522.
- Parker, J.C., J.B. Kool, and M.Th. van Genuchten. 1985. *Determining soil hydraulic properties from one-step outflow experiments by parameter estimation: II Experimental studies*. Soil Sci. Soc. Am. J. 49:1354-1359.
- Soil Survey Staff. 1975. *Soil Taxonomy; a basic system of classification for making and interpreting soil surveys*. Agr. Handb. no. 436, SCS-USDA. Government Printing office, Washington DC.
- Statistical Package for Social Sciences, SPSS. 1991. *Base Manual*. SPSS Inc., 444 N. Michigan Avenue, Chicago, IL 60611, USA.
- Van Genuchten, M. Th. 1980. *A closed-form equation for predicting the hydraulic conductivity of unsaturated soils*. Soil Sci. Soc. Am. J. 44:892-898.
- Van Ommen, H.C., L.W. Dekker, R. Dijkema, J. Hulshof, and W.H. van der Molen. 1988. *A new technique for evaluating the presence of preferential flow paths in nonstructured soils*. Soil Sci. Soc. Am. J. 52:1193-1194.
- Wagenet, R.J., and J.L. Hutson. 1989. *Leaching Estimation and Chemistry Model: A process-based model of water and solute movement, transformations, plant uptake and chemical reactions in the unsaturated zone*. Continuum Water Resources Institute. Cornell University.
- Wagenet, R.J., J.L. Hutson, and J.W. Biggar. 1989. *Simulating the fate of a volatile pesticide in unsaturated soil: a case study with DBCP*. J. Environ. Qual. 18:78-84.
- Webster, R. 1977. *Quantitative and numerical methods in soil classification and survey*. Clarendon Press, Oxford.
- White, R.E. 1985. *The influence of macropores on the transport of dissolved and suspended matter through soil*. Adv. Soil Sci. 3:95-121.

## **CHAPTER 9**

### **GENERAL CONCLUSIONS**

## GENERAL CONCLUSIONS

1. In structured soils, water flow processes are strongly influenced by the occurrence of macropores. The suction crust infiltrometer is particularly suitable to measure the hydraulic conductivity near saturation and to express the effects of macropores on conductivity, because crusts, prepared according to the described procedure, ensure perfect contact with the soil.
2. Sensitivity analyses of models describing bypass flow indicate that in heavy textured soils the applied rain intensity and hydraulic conductivity of the soil matrix are important parameters controlling bypass flow. In lighter textured soils absorption processes, such as surface infiltration and absorption of water along macropore walls, are the controlling parameters.
3. Continuous macropores induce significant bypass flow in heavy clay soils. When modelling the fate of water in these macropores a stratification of water conducting macropores in terms of horizontal and vertical orientations is necessary, because infiltration is a function of macropore orientation.
4. The geometry of macropores has major impact on tortuous water transport. This tortuosity can be well described by a pedotransfer function based on measured morphological features such as volumes and fractal dimensions of methylene-blue stained macropores.
5. Absorption of water in structured soils with continuous macropores is more affected by their geometry, expressed in terms of fractal dimensions and volumes of stained macropores, than by their physical properties.
6. Field monitoring of bypass flow in a heavy clay soil shows that nitrate concentrations in drain discharge increase proportionally with the outflow rate during bypass flow events. This nitrate originates from the top soil,

- were there is good contact between bypass water and relatively small structure elements.
7. Soil solution sampling by suction cups is an unsuitable procedure for measuring nitrate concentrations in structured heavy clay soils.
  8. Good agreement between the independent comparison of measured and simulated time series of ground water levels and drain discharge indicates that bypass flow can be simulated on field scale using combined morphometric and soil physical properties in a dynamic water transport model.
  9. Use of the rotated random scan procedure in combination with a Monte-Carlo simulation approach provides a valuable tool for obtaining ill-defined model parameters and for restricting initially wide parameter spaces to more realistic values for the flow system being considered in a heavy clay soil with macropores. This makes interpretation of data in terms of confidence intervals more realistic.

## **Abstract**

Booltink, H.W.G., 1993. Morphometric methods for simulation of waterflow. Doctoral Thesis. Agricultural University Wageningen, The Netherlands.

Water flow in structured soils is strongly governed by the occurrence of macropores. In this study emphasis was given to combined research of morphology of water-conducting macropores and soil physical measurements on bypass flow. Main research objectives were to: (i) develop and improve soil physical methods in such a way that hydraulic effects of macropores in soils are accounted for, and (ii) quantify soil structure in such a way that bypass flow phenomena can be realistically represented in simulation models.

In chapter 2 a modified crust test is presented, to be used for measuring the unsaturated hydraulic conductivity near saturation. The test will be referred to as the suction crust infiltrometer. Since contact between soil and crust is perfect the suction crust infiltrometer is particularly suitable to express the effects of macropores on conductivity. Only one crust is used as fluxes through the crust occur at different heads, which makes the method less laborious and more convenient to use than the former crust test.

Chapter 3 combines physical measurements of soil water potentials (using small transducer equipped automated tensiometers) and bypass flow with morphological data obtained from staining patterns. Tensiometers in close contact with water-conducting macropores reacted very quickly during the start and at the end of a bypass flow event. Other tensiometers showed slow reactions indicating a location deep inside structure elements. The various tensiometer reactions were used as a point count to identify occurrence of soil physical processes such as internal catchment and bypass flow. Mass balances showed that 52 percent of the applied water left the soil cores through bypass flow while an estimated of 33 percent contributed to internal catchment.

In chapter 4 a sensitivity analysis on processes affecting bypass flow was carried out. A simulation model was used to determine the relative impact of different soil physical properties and boundary conditions on different soil types. For the light textured soils surface infiltration was the most important term in the water balance. For heavy textured soils drainage through macropores was the most important mass balance term. Lateral absorption was only a minor fraction in the total mass balances. Surface infiltration is a crucial parameter in bypass flow and is mainly dependent on rain intensity, initial pressure head and the conductivity of the soil matrix.

In chapter 5 an empirical equation was developed which relates total amount of measured outflow, derived from 5 bypass experiments, to fractal dimensions and volume fractions of methylene-blue stained macropores. The total amount of bypass flow was successfully regressed on measured time lag for initial breakthrough at the bottom of the soil column. This study indicates that morphology of flow paths is an important factor in the process of bypass flow. A physico-morphological approach for measuring and simulating bypass flow on 15 undisturbed soil columns was described in chapter 6. The impact of various physical boundary conditions on bypass flow was measured with a computer-controlled measuring device. Macropore geometry was characterized using fractal dimensions of methylene-blue stained macropores. Initial breakthrough at the bottom of the soil cores was predicted with a pedotransfer function based on fractal dimensions and methylene blue stained volumes. Measurements showed that geometry of water conducting macropores prevailed over soil physical properties with respect to water absorption along macropores walls. Soil physical and morphological data were used in a simulation model which predicted drainage at the bottom of the cores with significant precision. In chapter 7 bypass flow and nitrate leaching at the Kandelaar experimental farm was measured in drain outflow over a period of 4 years, using an automated monitoring set up. Bypass flow towards ground water exceeded sometimes 80 percent of precipitation. Simultaneously measured nitrate concentrations in drainage water increased during bypass flow, indicating that bypass flow is associated with an increased nitrate load to ground water. A catch crop grown directly after slurry application could reduce nitrate concentration in drainage water up to 75 percent. This study also showed the inability of suction cups in structured clay soils to provide representative samples for soil solutes. Chapter 8 describes the field scale modelling of bypass flow on the Kandelaar experimental farm. The LEACHW model was extended with a module that described bypass flow and tortuous water transport in macropores. This model was used in a Monte-Carlo analysis to calibrate the model parameters and to investigate the sensitivity of the various model parameters. Explained variances for the various terms in the water balance were always significant. Simulation of measured ground water levels and drain discharge from an independent year using the calibrated parameter set appeared successful.

# Samenvatting

## Morfometrische methoden voor de simulatie van waterstroming

Stroming van water in gestructureerde gronden wordt sterk beïnvloed door de aanwezigheid van macroporiën. In deze studie is de nadruk gelegd op het gecombineerde onderzoek naar morfologie van watervoerende macroporiën en bodemfysische metingen op het gebied van *bypass-stroming*. De belangrijkste onderzoeksdoeleinden waren: (i) het ontwikkelen en verbeteren van bodemfysische meetmethoden zodat de hydraulische effecten van macroporiën kunnen worden gemeten, en (ii) het kwantificeren van bodemstructuur zodat *bypass-stroming* realistisch in simulatie modellen kan worden weergegeven.

In hoofdstuk 2 wordt de vernieuwde korstmethode besproken. Deze methode wordt gebruikt voor het meten van de onverzadigde doorlatendheid nabij verzadiging. De korstmethode is gemodificeerd tot een korst-infiltrometer. Het perfecte contact van de korst met de bodem maakt de korst-infiltrometer bijzonder geschikt voor het meten van effecten van macroporiën op de doorlatendheid. Bij het gebruik van de korst-infiltrometer hoeft slechts één korst te worden gemaakt, wat de methode minder arbeidsintensief en makkelijker maakt vergeleken met de voormalige korstmethode.

Hoofdstuk 3 combineert fysische metingen van bodemvocht potentialen (door middel van kleine tensiometers uitgerust met drukopnemers) en *bypass-stroming* met morfologische gegevens verkregen van vlekken patronen. Tensiometers in de nabijheid van watervoerende macroporiën reageerden erg snel gedurende het begin en einde van het *bypass* experiment. Andere tensiometers gaven een zeer langzame reactie te zien wat aangeeft dat zij diep in structuur elementen waren gelocaliseerd. Om de verschillende bodemfysische processen te identificeren zijn de verschillende tensiometer reacties gebruikt als een punt-telling. Op grond van deze telling konden processen als *bypass-stroming* en interne infiltratie worden gekwantificeerd. Massa balansen gaven aan dat 52 procent van het toegediende water de bodemkolommen verliet als *bypass-stroming* en 33 procent bijdroeg aan interne infiltratie.

In hoofdstuk 4 is een gevoeligheids analyse uitgevoerd op processen die *bypass-stroming* beïnvloeden. Om het relatieve effect van verschillende bodemfysische eigenschappen en randvoorwaarden op verschillende bodemtypen te toetsen is een simulatie model gebruikt. Voor bodems met een lichte textuur was oppervlakte infiltratie de belangrijkste term in de waterbalans. Voor bodems met

een zwaardere textuur was stroming van water door macroporiën de belangrijkste massabalans term. Oppervlakte infiltratie is een cruciale parameter in *bypass-stroming*, die voornamelijk door neerslag intensiteit, initiële bodemvocht potentiaal en de doorlatendheid van de bodem matrix wordt bepaald.

In hoofdstuk 5 is een empirische relatie ontwikkeld die de totale hoeveelheid gemeten drainage, verkregen uit 5 *bypass* experimenten, relateert aan de fractale dimensies en volume fracties van methyleen blauw gekleurde macroporiën. De totale hoeveelheid drainage kon bovendien worden gerelateerd aan de gemeten vertraging van de doorbraak van drainage aan de onderkant van de grondkolom. Dit deelonderzoek geeft aan dat de morfologie van stromingspatronen een belangrijke factor is in het proces van *bypass-stroming*.

Een fysisch-morfologische benadering voor het meten en simuleren van *bypass-stroming* in 15 ongestoorde grondkolommen is beschreven in hoofdstuk 6. Het effect van verschillende fysische randvoorwaarden op *bypass-stroming* is gemeten met behulp van een computer gestuurde meetopstelling. De geometrie van macroporiën is gekarakteriseerd door middel van fractale dimensies van, door methyleen blauw gekleurde macroporiën. Initiële doorbraak van water aan de onderkant van de grondkolommen kon worden voorspeld met een bodem vertaalfunctie gebaseerd op fractale dimensies en methyleen blauw gekleurde volumina. In het proces van waterabsorptie in macroporiënwanden toonden metingen aan dat de invloed van bodemfysische eigenschappen ondergeschikt was aan de geometrie van watervoerende macroporiën. Bodemfysische en morfologische gegevens zijn vervolgens gebruikt in een simulatie model dat de drainage aan de onderkant van de grondkolommen met significante precisie kon voorspellen.

In hoofdstuk 7 wordt gerapporteerd over veldmetingen aan *bypass-stroming* en nitraat uitspoeling, uitgevoerd gedurende een periode van 4 jaar op de proefboerderij "De Kandelaar". Hiervoor is gebruik gemaakt van een geautomatiseerde meetopstelling. *Bypass-stroming* naar het grondwater was soms meer dan 80% van de hoeveelheid neerslag. Gelijktijdig gemeten nitraat concentraties in het drainage water namen toe gedurende een *bypass* gebeurtenis. Dit geeft aan dat *bypass-stroming* geassocieerd kan worden met een toenemende belasting van het grondwater met nitraat. Indien, direct na toediening van een bemesting, een vanggewas werd geteeld kon de nitraat concentratie in het drainage water met een factor van 75% worden gereduceerd. Verder bleek uit dit onderzoek dat bodemvocht bemonsteringscups ongeschikt zijn voor het



nemen van representatieve bodemvocht monsters in sterk gestructureerde kleigronden.

Hoofdstuk 8 beschrijft het modelleren van *bypass-stroming* op de proefboerderij "De Kandelaar". Het LEACHW-model is uitgebreid met een module die *bypass-stroming* en *tortuous* watertransport door macroporieren beschrijft. Dit model is gebruikt in een Monte-Carlo analyse om het model te calibreren en om de gevoeligheden van de verschillende modelparameters te onderzoeken. Verklaarde varianties voor de verschillende massabalans termen waren altijd significant. Het simulatie model is tenslotte gevalideerd op een gemeten tijdreeks van grondwaterstanden en drainafvoeren voor een onafhankelijk jaar.

## **Curriculum vitae**

Harry Booltink werd geboren op 12 december 1958 te Doesburg. In 1976 behaalde hij het MAVO diploma en in 1978 het diploma HAVO aan de Scholengemeenschap "Oost-Betuwe" te Bemmelen. Hierna begon hij een studie aan de Hogere Bosbouw en Cultuurtechnische School te Velp en behaalde in 1982 het diploma met als afstudeervakken Bodemkunde, Hydrologie en Informatica.

Van december 1982 tot juli 1983 vervulde hij zijn vervangende militaire diensplicht bij de Stichting Natuur en Milieu te Utrecht. Vanaf september 1983 is hij werkzaam aan de Landbouw Universiteit te Wageningen. Eerst voor een periode van 6 maanden bij de Vakgroep Waterhuishouding, daarna bij de Vakgroep Bodemkunde en Geologie. Binnen deze vakgroep heeft hij tot juni 1988 gewerkt voor de sectie Ecopedologie in het kader van het Zure Regen onderzoek onder leiding van Prof. Dr. ir. N. van Breemen. Van juni 1988 tot heden is hij werkzaam bij de sectie Bodeminventarisatie en Landevalutie onder leiding van Prof. Dr. ir. J. Bouma. Een belangrijk deel van zijn onderzoek vond plaats in het kader van het karakteriseren van bodemstructuur op perceelsniveau ten behoeve van de simulatie van nutriënten stromen.